CHALMERS

GROUTING THEORY AND GROUTING PRACTICE

Distribution of hydraulic properties and rock mass response
with regards to grouting aspects and seepage into tunnels

BJÖRN STILLE

B. Stille

THESIS FOR THE DEGREE OF LICENTIATE OF PHILOSOPHY

Grouting theory and grouting practice

Distribution of hydraulic properties and rock mass response with regards to grouting and aspects of seepage into tunnels

BJÖRN STILLE

Department of Civil and Environmental Engineering
Division of GeoEngineering
CHALMERS UNIVERSITY OF TECHNOLOGY
Gothenburg, Sweden 2016

B. Stille

Grouting theory and grouting practice

BJÖRN STILLE

Grouting theory and grouting practice
BJÖRN STILLE
Department of Civil and Environmental Engineering
Division of GeoEngineering
Chalmers University of Technology

ABSTRACT

The data, which is the basis for this thesis, comes from several case studies that have been performed with the aim to study the grouting process. For each case hundreds to thousands of grout holes have been studied. The cases show that the geological and the geohydrological conditions clearly influence the grout take and the grouting process. The single strongest influence on the grout results seem to be the density of zones. The study shows that the geohydrological conditions can be described statistically with a lognormal distribution. A simple methodology to curve fit the data is described as well as the option and method to scale the test results to relevant length. The grouting process is analysed with the real time grouting control method and the results show the applicability of the method. The analysis also shows some diagnostics possibilities to evaluate possible jacking.

The transmissivity distribution for the grout holes in the rock mass can be used to evaluate the grout results. An alternative way to analyse the water seepage is shown. The analysis shows that the results are reasonable and comparable to actual water seepage. The method is relatively easy to use.

The thesis shows that there is considerable variation in basic properties, models and the grouting process. The design and execution therefore needs to be adaptable to certify that a good result can be expected with regards to limiting water seepage and overall economy. The observational method is recommended.

Keywords: Case study, Grouting, Grout take, Dimensionality, Grout penetration, Distribution of transmissivity, Mean value and variation, Tunnel seepage, Observational method

B. Stille

LIST OF PUBLICATIONS

This thesis is based on the following publications:

I.   Stille B., Gustafson G. (2010). A review of the Namntall Tunnel project with regard to grouting performance. Tunnelling and Underground Space Technology. Vol. 25, pp. 346-356.

II.   Stille B., Stille H., Gustafson G., Kobayashi S. (2009). Experience with the real-time grouting control method. Geomechanics and Tunnelling. Vol 2, pp. 447-459.

III.   Stille B., Stille H. (to be submitted 2016). Distribution of rock mass hydraulic conductivity and its application to rock engineering problems.

DIVISION BETWEEN AUTHORS

Paper 1: The paper was written by B.Stille. The figure 3 (modified after Caine et al 1995) was suggested by Gustafson and figure 10 was performed after suggestion by Gustafson.

Paper 2: Section 1 was a joint effort by the authors B.Stille and H.Stille. Section 2 was almost entirely based on Gustafson and Stille 2005. Section 3 was based on Kobayashi's work, the figure 3-3 however was made by Gustafson. Section 4 was mainly written by B.Stille and the analysis was performed by B.Stille and Bruno. The conclusions in section 5 were mostly produced by Kobayashi, H.Stille and B.Stille. The text was compiled by B.Stille.

Paper 3: Most parts of the paper was written by B.Stille with the exception of the log normal distribution and the scaling of the lognormal distribution which was derived by H.Stille.

ACKNOWLEDGMENTS

B. Stille

TABLE OF CONTENTS

1 INTRODUCTION

1.1 Background

Grouting is performed to reduce water seepage through a rock mass, under a dam or into a tunnel. In the big picture, however, grouting limits the environmental impact caused by lowering the groundwater pressure or reducing damage to the object being constructed. As such, grouting is part of the construction and the process that starts much earlier and eventually ends with 'measuring' seepage or evaluating the grouting results.

The building process that involves the use of subsurface space starts with a societal need, regardless of whether it is related to infrastructure, energy or another area. Every such use will require an investigation of the influence on the groundwater situation or other issues related to seepage. These questions will eventually pass to the regulatory bodies for review and approval. One such body is the environmental court, which at an early stage will approve or regulate the permitted seepage or influence on the groundwater level depending on the situation and the phrasing of the application.

Societal needs and requirements will therefore regulate the construction process and the use of the subsurface space. The understanding therefore is that the grouting process starts, at least conceptually, at a very early stage with preliminary discussions about the needs and the many implications arising from the construction process, including water seepage, influence radius and so on. The level of detail is naturally lower at this stage and the estimates are more sweeping. Throughout the planning process the level of detail will increase up to delivery of the basic design (and possibly, but not usually in Sweden, during the detailed design stage). The basic design may be delivered at an earlier stage to ideally have the environmental court ruling available during the detailed design stage. However, the engineers or hydrogeologists may not be the same persons that carry out the grouting design or follow the grouting during the execution of the project. It is easy to understand the potential for miscommunication and conflicting interests, but the fact is that the data (e.g. from hydrogeological tests) and the interpretation of the data (e.g. by choosing different mean values) may be analysed differently, thus producing different results depending on the aim of the analysis.

The most detailed information on the ground conditions will be obtained during the construction phase. Unfortunately, the actual data, the hydrogeological distribution and the geological information related to these statistics, are often not collected or summarised for future reference. The organisation and/or contractual arrangements tend to limit the exchange of information between the environmental engineers and the design engineers and between the contractor and the client organisation.

This thesis provides information based on case studies dealing with the distribution of hydrogeological data, the mean values and the execution of the grouting. In addition, there is a discussion about the model used for analysing water seepage and the need for an open approach to controlling the grouting works by adopting an observational approach.

1.2   Aims

The aims of the thesis are fourfold

- Recommendations regarding the practical evaluation of parameters for the hydrogeological data (transmissivity) distribution.
- Recommendation regarding the choice of mean value and the influence of scale
- Show the applicability of the real-time grouting control method
- Provide an alternative approach for analysis of water seepage after grouting

The conclusions also include a discussion about the need to adopt an observational approach when considering the grouting process.

1.3   Scope of work

This thesis is based on information gathered from various projects in Scandinavia, mainly in crystalline rock such as metagreywacke, gneiss and granite. The thesis presents research based on grouting theory developed at Scandinavian universities and which is briefly summarised for the last few decades in section 2. The thesis in itself is a synthesis report bringing together different theories and their application (grouting) to provide a better understanding of the process. The thesis originated with a case study of the Namntall Tunnel, section 3, followed by the statistical analysis of mean values, including data from the City Line project, section 4, and the analysis using the real-time grouting control method in section 5. A slightly different approach to the analysis of water seepage is suggested in section 6 and the overall conclusion regarding the need for an observational approach to the grouting process is discussed in section 7.

2   DEVELOPMENT OF THEORETICAL GROUTING METHODOLOGY IN SWEDEN

Grouting theory spans almost three decades. The actual practice, however, has been carried out since the 1950s (or even earlier) with grouting of projects that included the Stockholm underground. The practice was often described by Morfeldt (1979) as a "dark art" and its methods were passed on verbally and through personal experience and experimentation. In this way, grouting methodology developed through 'wise men' and can be seen as a footprint of the general trends and analysis methods of the time.

In parallel, grouting theory evolved along four different paths:

1)   Hydrogeology
2)   Fracture(s)
3)   Grout properties, including testing methods
4)   Grout flow

Hydrogeology is in itself an older science, emanating from well theory and observations of aquifers, developed as a part of soil mechanics (pore pressure theory/effective stresses) and later for rock mass by Gustafsson and Alberts (1983) and others.

The description of the fracture was, at least in Scandinavia, made relatively late by, for example, Hakami (1995) identifying fracture characteristics such as contact areas, matedness, fracture width distribution and so on, see also Olsson (1998). The distribution of fractures and zones in the rock mass is part of the science of geology, although up to the mid-1990s it was not exactly usable for grouting theory purposes. The definition of zones by, for example, Caine et al. (1995), and the quite similar idea by Munier et al. (2003) at SKB, made it possible to explain some of the grouting problems experienced in, for example, the Namntall Tunnel, as demonstrated by Gustafson and Stille (2010).

The first doctoral thesis focusing on grouting was performed by Hässler (1991), who studied grout flow in channels and pipes, including a numerical tool for calculating grout penetration. Some of the ideas presented in Hässler's thesis were not completed more generally until Gustafson and Stille (2005) and Gustafson and Claesson (2005) presented their theory of grout spread later published as Gustafson et al (2013).

Hässler's thesis was followed by Håkansson (1993), who studied the rheology of cement-based grouts and developed methods for grout tests. Håkansson tested a number of grouts and in doing so demonstrated the importance of additives, thus possibly opening up a new era in cement suppliers' research and development programmes. Today, the yield limit and viscosity of cement-based grouts are no longer unheard of properties and additives have been developed that can adjust these properties to the desired values.

Research is still of course being carried out in these four main areas although some significant attempts have been made to bring the areas together. The realms of hydrogeology and fracture characteristics have been studied through work by Fransson (2001), Hernqvist (2011) and Zetterlund (2014) on characterising the rock mass, interpreting water pressure tests and analysing fracture transmissivities and hydraulic fracture widths.

Eriksson and Stille (2005) summarised the research with regard to certain aspects of grout flow, grout properties, grout effect and inflow analysis.

Gustafson et al. (2004) presented a paper analysing hydrogeological data (interval transmissivities) and fracture widths using a statistical model. The inflow calculation (based on the fracture distribution) and grouting effect by sealing some of the fractures brought together current ideas about geohydrology, fractures and grouting results. The ideas in the paper were further discussed in Gustafson (2009).

Gustafson and Stille (2005) demonstrated an analytical method to study grout flow based on grout rheology. In this paper, the diagnostic method used to identify dimensionality (planar or channel grout flow) combined grout rheology and ideas about fracture widths and implied that a design could be performed that included grout property and penetration length (grout hole distances) requirements. This paper was followed by several others, who studied the application of the theory to case records, including some suggested modifications to simplify use. The end product would be the Real-Time Grout Control Method (Kobayashi et al. 2007).

In his 'Hydrogeology for Rock Engineers' (2009), Gustafson summarises much of the research performed for the Swedish Nuclear Fuel and Waste Management Company. This book includes interpretation of various pre-investigation methods, groundwater flow in a rock mass, hydrogeological properties and groundwater modelling. Of particular interest for this thesis is the summary of statistical data for interpreting mean values.

The practical aspects of the grouting process were studied by Brantberger (2000) and Dalmalm (2004). Brantberger's study included a review of, for example, the GIN method, concluding that the method was developed for dam grouting and that the GIN design is based on a risk assessment/estimate of jacking in the rock mass. It may therefore not be relevant to grouting of tunnels in hard crystalline rock masses. Dalmalm (2004) made a detailed case study of the Southern Link project in his doctoral thesis as well as earlier work on, for example, the Arlanda Line, but had difficulty finding any significant relationship between the parameters in the Q-method and the grout take. Funehag's studies (e.g. Funehag and Gustafson 2004, Funehag 2007) include a silicate solution (silica sol) grout as well as practical aspects observed in the Hallandsås project and at the

Äspö Hard Rock Laboratory. However, the practical application of the theory has often suffered from a lack of large sets of 'real world' data. In the paper 'Review of the Namntall Tunnel project with regard to grouting performance' by Stille and Gustafson (2010), they studied and summarised around 6,000 water pressure tests and items of grout hole data. Following this paper and after verifying some of the observations at the Namntall Tunnel, two master's thesis reports were published – Bohlin and Urtel (2008) and Bruno (2009) – which studied the grouting process and performance in some of the Northern Link tunnels. These studies looked into both large-scale statistics and also revealed practical problems related to the grouting process in the field.

In the City Line project, the fracture width distribution theory (based on Gustafson and Fransson) and grout penetration theory (based on Gustafson and Claesson 2005 and Gustafson and Stille 2005) were used to calculate the required grouting time (Zetterlund and Eriksson, 2007). It was later shown by, for example, Holmberg et al. (2012) that although the required grouting time was based on not actual grout properties, the concept seemed correct and it was further developed in the project to take into account the actual grouting and the rock mass response (grout take, seepage etc.)

Not only has the research and development process at Scandinavian universities contributed to the emergence of a new perspective on grouting design, the materials industry has also followed the research and the requirements that have evolved over the years to create better and more finely grained cements of higher quality.

The steps in the grouting process related to research and development are shown in Figure 2-1.
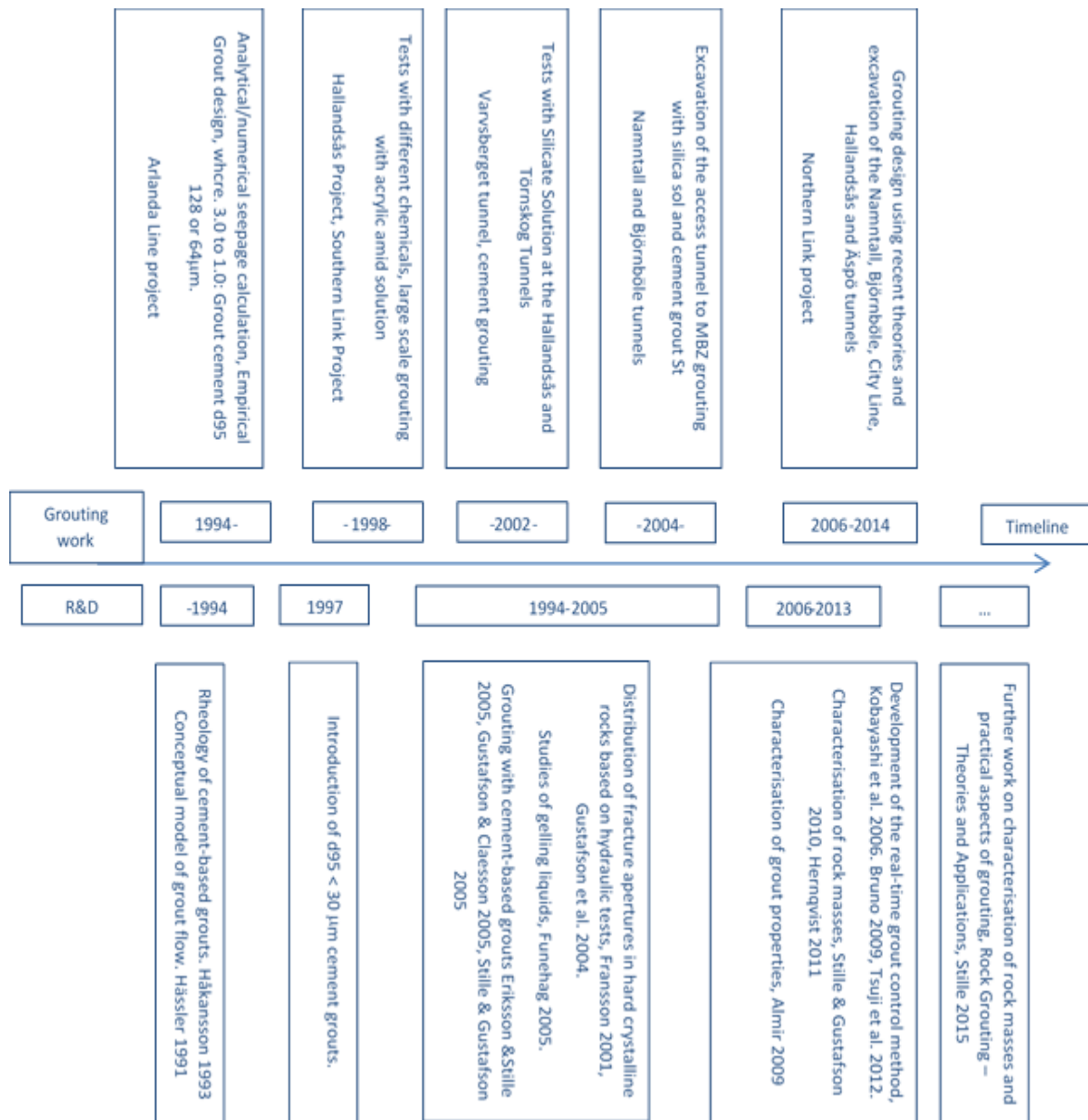
Figure 2-1. Research and development and a selection of the Swedish tunnelling projects discussed, modified after Sturk et al (2013).

3 A REVIEW OF THE NAMNTALL TUNNEL PROJECT WITH REGARD TO GROUTING PERFORMANCE, PAPER 1

3.1 Introduction

The six-kilometre Namntall Tunnel is part of the Bothnia Line project linking Örnsköldsvik and Kramfors. The tunnel was constructed as part of a design and build contract consisting of a single-track rail tunnel (65 m^2) and a parallel service tunnel (35 m^2). The client, Botniabanan AB (BBAB), was a partnership (90/10) between the Swedish Rail Administration and the municipal authorities in the area. The contract was awarded to Skanska Sverige AB as the main contractor for the civil engineering work. The total scope of the design and build contract included the six-kilometre Namntall Tunnel, several over ground parts and a five-kilometre second tunnel. The tunnels were excavated between 2004 and 2007 using the drill and blast method.

For the most part, the Namntall Tunnel, with a rock cover of 20-150 m, was excavated in greywacke and through a major intrusion of granite. The tunnels were excavated by drilling and blasting and using a normal grouting routine, including probe/grout hole drilling, water pressure tests (Moye, 1967), evaluation of grout class, cement grouting, drilling of control holes (water pressure tests) and supplementary drilling/grouting.

The paper is presented in publication I.

3.2 Geological history of the rock mass in the county of Ångermanland (Local orogenesis)

The geological history of the area can be said to have 'started' some 1,820-1,850 million years ago during the Swecokarelian mountain chain-folding process, Lundqvist et al. (1990). The greywacke bedrock was created during this process of intense tectonic events. Originally deposits of sedimentary material made up of sand and clay, the term greywacke is defined by its relatively large clay content (more than 15% in the matrix). In the Namntall area, several metamorphic stages in the greywacke have been observed, ranging from almost intact to a metamorphosed metagreywacke that is gneissic and even migmatised, resulting in, among other things, segregation of the mineral components into bands or strips.

The bedrock has been intensely folded, which is demonstrated by the steeply dipping foliation. The orientation/strike of the foliation is roughly NE-SW, indicating the probable direction of the local tectonic thrust NW-SE (perpendicular to the foliation) during this early phase of the orogenesis.
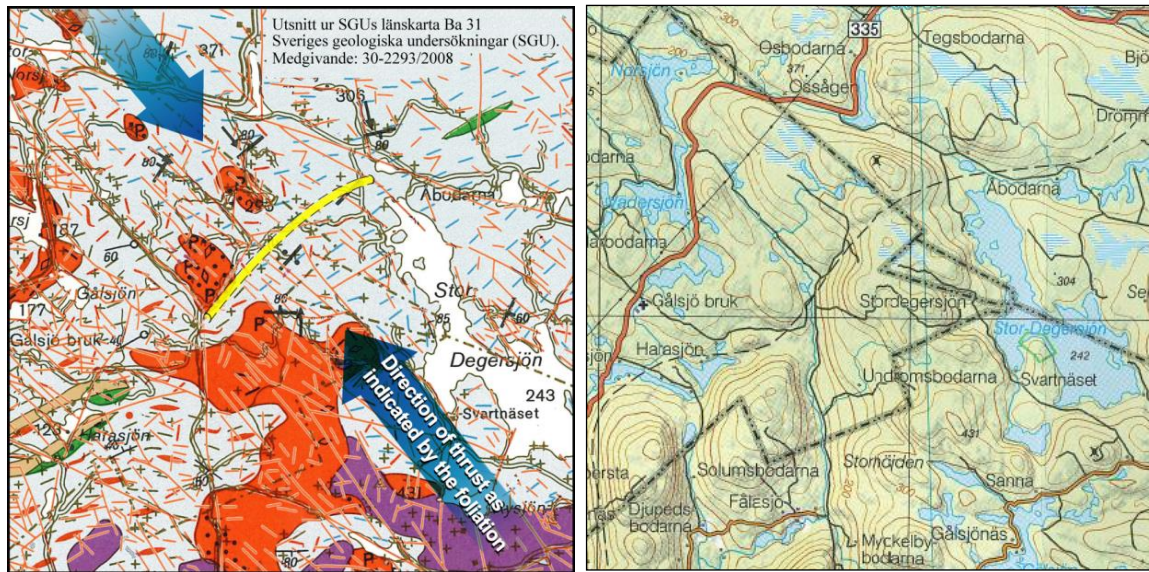
Figure 3-1. The topographical, geological and structural geological map of the Namntall area. The tunnel is marked in yellow, the foliation is indicated by the small blue lines and the lineaments are shown in brown. The bedrock consists of greywacke (grey) with intrusions of granite and pegmatites in red. The topographical map shows terrain features and the Bothnia Line railway, including the tunnel.

Since the mountain-folding process and the regional metamorphosis, the rock mass has been subjected to a number of faults, resulting in the local topography, Figure 3-1. The literature states that "valleys, the course of mires, steps in the terrain and straight lakeshores correlate to steep failure lines in the bedrock", Lundqvist et al. (1990). Furthermore, the erosion created by the moving direction (NNW – SSE) of the quaternary glacial ice has emphasised the weaker areas in the rock, especially where these coincide. It has also been observed that the deep failure lines also coincide with intrusive rocks such as granites, pegmatites and metabasites (which are considered to be the latest additions to the rock mass, originating some 1,200 million years ago). It has been observed that during the intrusions of metabasite dikes, the rock mass was subject to a considerable increase in fracturing, including the creation of horizontal crushed zones.

The large intrusion of granite between cross-sections 504+370 and 505+450, as well as numerous dikes, also support the theory that the area was subject to significant deep failure lines prior to the intrusion.

The general experience of the geological conditions during tunnelling led to a division of the geology into geological regimes or areas with similar characteristics. These are mainly related to water seepage, Figure 3-2, and the density of "zones", Figure 3-3, but as we shall see, they were also of consequence for the distribution of water pressure test results (grout class distribution) and grout take.

Discharge in the Namntall tunnel 2006-10-10 to 2006-12-29
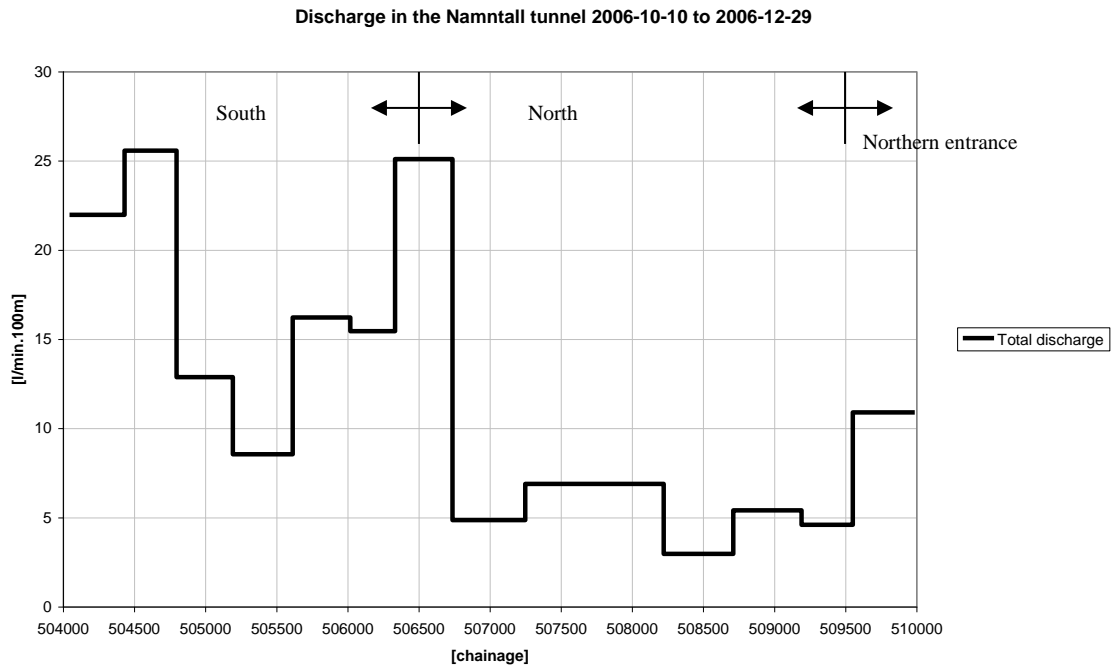
Figure 3-2. Total discharge in the Namntall Tunnel, including track and service tunnels. The measurement took place on October 10, 2006 and December 29, 2006.

Cumulative distribution of zones
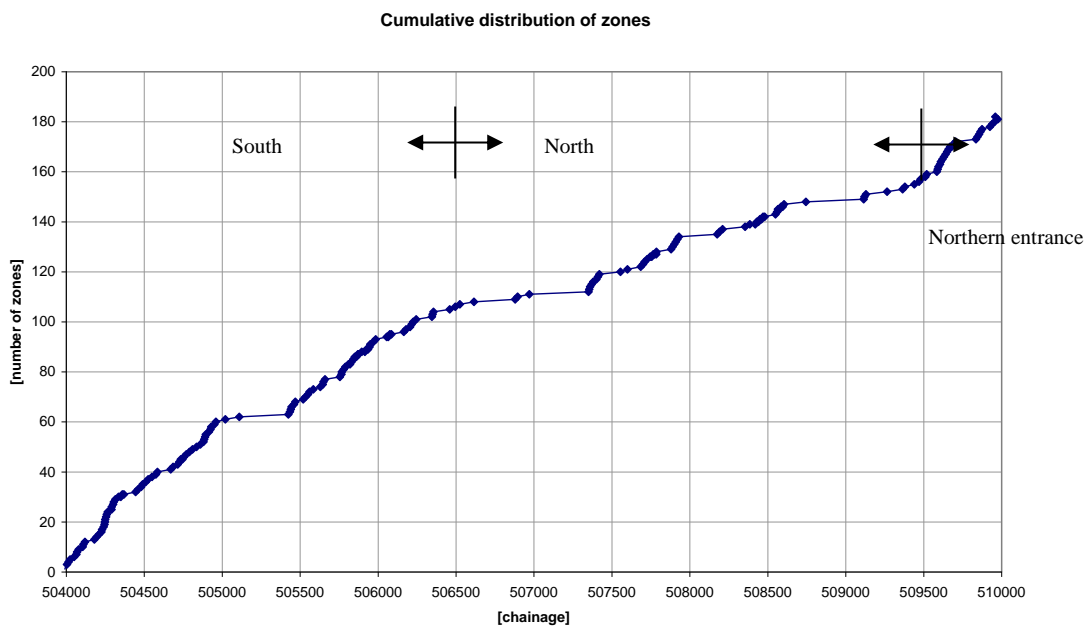
Figure 3-3. The cumulative distribution of zones across the tunnel length.

3.3 Zones and description of the nature of joints in the area

In this paper, *Zones* has been chosen as a designation to describe all areas that diverge from the surrounding host rock and which could be expected to have an impact on the water discharge. Zones include fracture zones (zones with a higher density of joints, e.g. 5-10 joints/m of a specific joint set), rock type contacts where the contact zone/area is more fractured, dikes that are either highly fractured or have a weathered or loosened contact area (a fractured, weathered dike is included whereas good pegmatites are not included) and shear zones.

The density/extent of zones is seen as an indication of where increased discharge could be expected. By adding the number of zones along the tunnel length (starting from the south) a cumulative distribution can be presented, Figure 2-3. The incline of the dotted line is indicative of the density of zones. A steep curve would therefore indicate a number of zones that lie close to each other. Figure 2-3 shows that the rock mass in the southern part of the tunnels has a high density of the zones (up to an approximate chainage of 506+500). The distribution of zones in the northern part of the tunnel (excluding the entrance area) shows a concentration of zones in certain areas but set some distance apart. The mean concentration of zones for the southern part is one zone every 23 m (2,500 m), for the northern part one zone every 62 m (3,000 m) and for the northern entrance part (500 m) one zone every 20 m.

Most of the zones have an estimated length of over 200 m. Most joints are 10-20 m in length although the length varies considerably. The foliation joints, for example, are in some areas very long, possibly over 100 m according to Lindström (2007).

The mapping performed by Stuge and Lindström (2007) shows that the joint systems in the area generally have two to three joint sets, often with one random joint set as defined in the Q-classification system (Barton, 2002). The spacing of the joints is generally 0.2-0.6 m, indicating fairly close spacing.

The filling in the joints varies along the tunnel although the joints are often coated with a thin, soft filling of clay, calcite or chlorite. In the areas with lower rock cover, the filling is generally thicker. In the area close to the southern tunnel entrance, some of the joints have a filling of swelling clays. For other parts of the tunnel, a partial clay coating has been noted, indicating difficult grouting conditions (Hässler, 2007).

3.4 Water pressure test results and grout classes

The hydrogeological conditions have been evaluated throughout the project by means of water pressure tests in the grout holes. The number of grout holes was generally between

10 and 20, arranged around the tunnel perimeter. The variations in number and length of the holes originated from the changes in grouting methodology that emerged from increased knowledge of the *in situ* hydrogeological conditions. After an initial period, 10 or 20 holes were generally drilled around the tunnel with a tested length of 21 or 23 m.

The water pressure tests were performed using digital water flow equipment with a measurement range of 2-38 l/min. The read-out range limited the water pressure test to between 0.2-4.0 Lugeon, l/min.m.MPa, (the values are for a test length of 20 m and 0.5 MPa overpressure). The water pressure test limits correspond to a hydraulic conductivity of $K = 3.7 \cdot 10^{-8}$ and $7.5 \cdot 10^{-7} \ m/s$).

The grout fans were classed as A, B or C fans after the highest water pressure test in each fan, Figure 3-4. The limits for the grout classes were based on the contractor's experience that a tight rock mass would produce a low water pressure test result (Grout class A: WPT < 0.5 Lugeon) whereas a conductive rock mass would have a significantly higher water pressure test result (grout class C: WPT > 2 Lugeon). Grout class B was defined as having a WPT of 0.5-2 Lugeon. For the most part the A fan included 10 grout holes, the B fan 20 grout holes and the C fan 20 grout holes plus additional control holes to verify the grout results.

The geological conditions along the length of the tunnel have been seen to vary considerably. A summary of the distribution of grout classes within each geological regime reveals some interesting statistics.
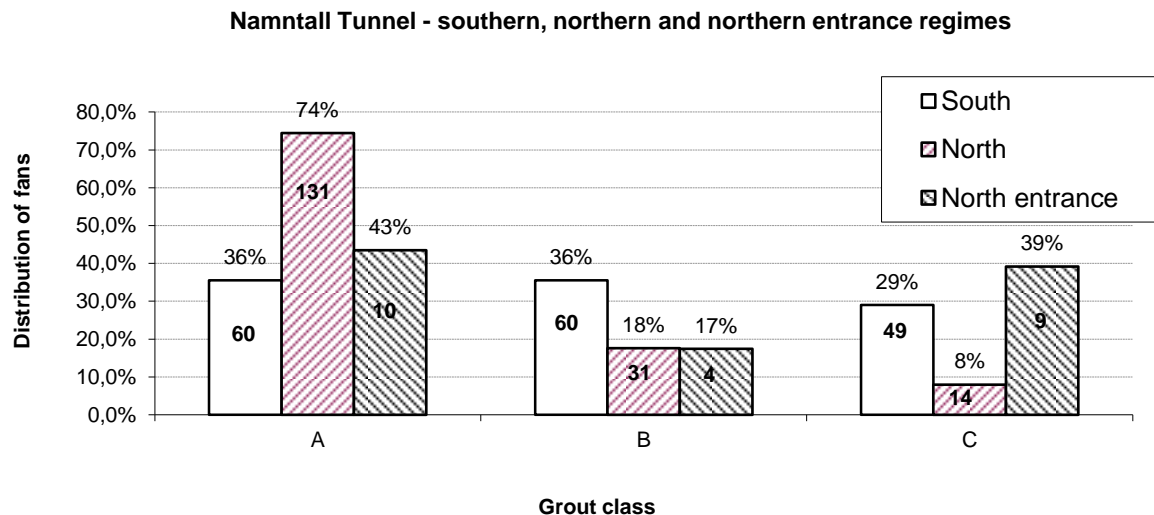
Figure 3-4. Distribution of grout classes for the south, north and north entrance regimes.

It is clear that the distribution of grout classes is influenced considerably the geological conditions. The water pressure test distribution for the southern part of the tunnel strongly indicates the grouting difficulty and the resulting water discharge, Figure 3-2. The difficulty obtaining a good grouting result is indicated here by the grout take in Figure 3-5. More specifically, the characteristics of the geological regimes can be expected to influence the grouting process and consequently the results of the grouting. A high concentration of zones and a combination of infilling and a high degree of jointing could be expected to be indicative of difficult grouting conditions. It is therefore reasonable to expect that for the southern part, where almost every grouting round crosses a zone, the grouting would be affected the most.
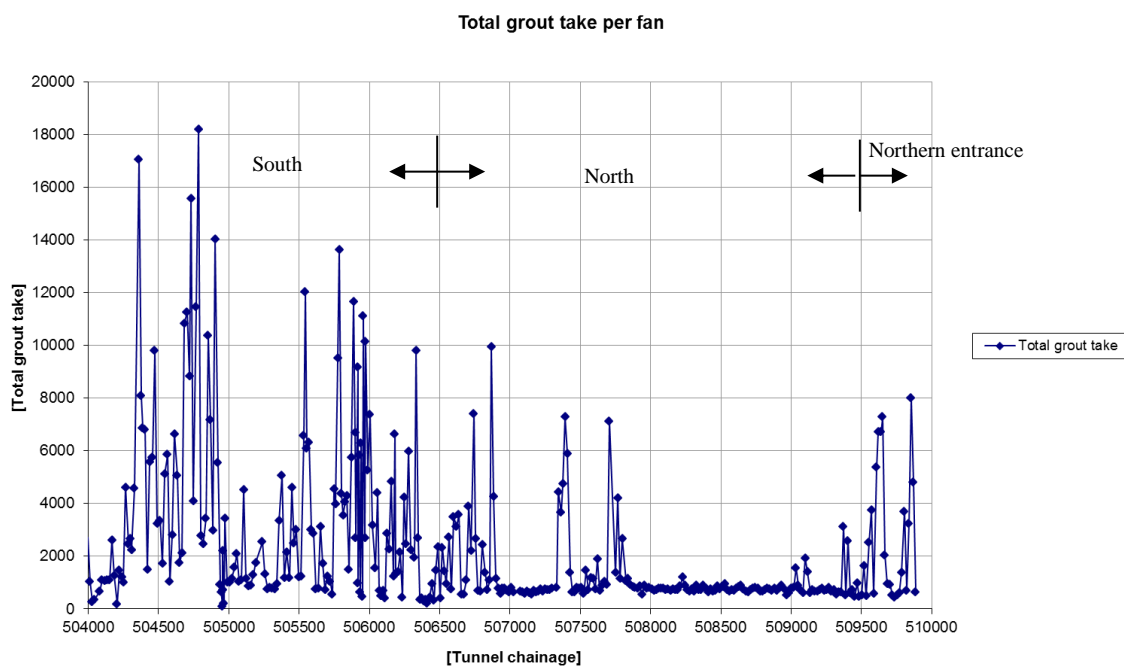
Figure 3-5. The total grout take for each fan, plotted against the location and tunnel chainage.

By arranging the grout data into the different grout classes, the distribution of grout take can be studied for each subgroup. The grout take per metre of borehole is studied to limit the influence of different hole lengths, number of holes etc. The data is presented in a histogram, where all three classes are represented, Figure 3-6. The Y-axis shows the percentage of holes and the X-axis shows the grout take. For example, around 13% of the grout class A holes have a grout take between 4 and 8 l/min. Furthermore, Figure 3-6 shows that there is an overall relationship between grout take and water loss in a fan. It also shows that there is a considerable number of holes in each fan that have a grout take approximately equal to the hole volume (3.2 l/m), although there is a significant difference between classes A and C.

12
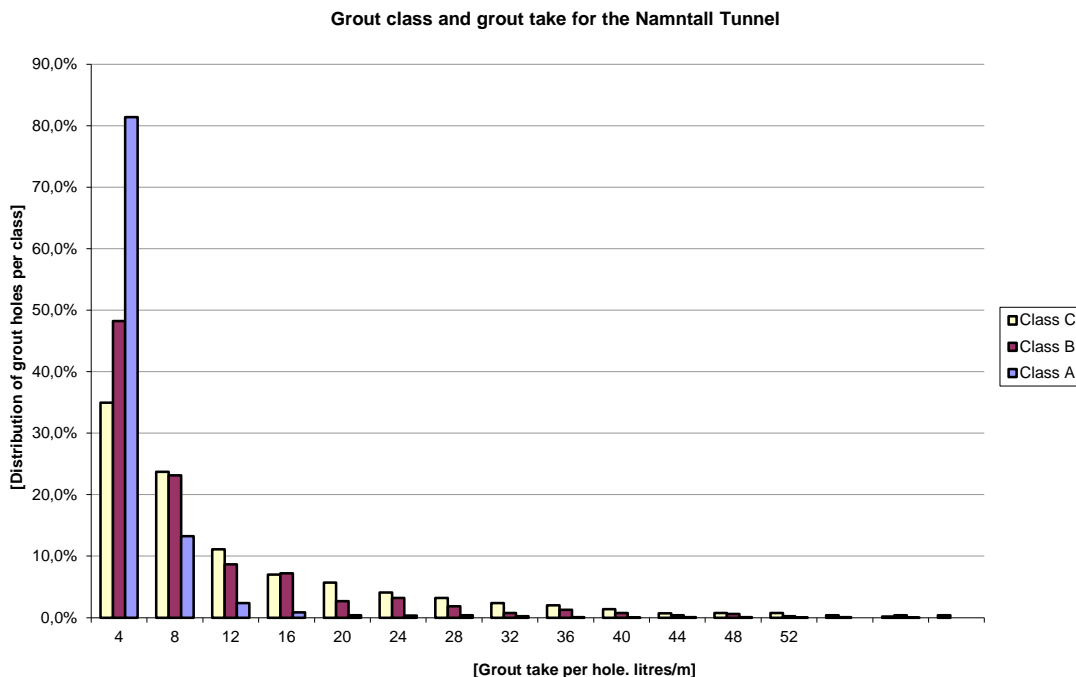
Figure 3-6. Histogram for the grout take for grout classes A, B and C. The figure shows the relationship between grout class and grout take distribution.

3.5 Summary

The grout take and the resulting water discharge indicate that a different approach to the grouting process could be suggested. Based on the large grout takes and the corresponding low grouting pressures that were common in grout class C rock, use of two grout rounds is recommended. It was also noted that the bottleneck in the grouting process was the grout mix capacities. The standard capacity for ordinary grout platforms was simply not sufficient to grout under higher pressure for a longer period of time in order to reach a stipulated penetration length for smaller fractures (calculated according to Gustafson and Stille, 2005).

The geological conditions that have the most prominent correlation with water pressure tests and grout take are the zone density. The properties of these zones (extent, water pressure test and grout data) indicate that the effective hydraulic conductivity may influence the general flow regime, studied further in *Paper 3: Distribution of rock mass hydraulic conductivity*.

There is a correlation between grout take and the largest water pressure test for each grout fan. Such a relationship could be used as a prognosis tool/classification method with regard to the extent of grouting and water seepage.

The geological conditions and the distribution of water pressure test results are indicative of the water seepage and grouting difficulty (grouting results). It is considerably more difficult to grout areas with zones and fractures that have clay/ partial clay filling. The evaluation of the grouting process/results is studied in *Paper 2: Experiences of the real-time grouting control method*). This should be considered when procuring tender documents and when describing geohydrological conditions.

4 EXPERIENCES OF THE REAL-TIME GROUTING CONTROL METHOD, PAPER 2

4.1 Introduction

The aim of this paper on the real-time grouting control method (RTGC) is to show how grouting theory can be used in practice through observations of grout flow and grouting time. Based on these 'real-time' data, predictions of grout penetration can be performed and the stop criteria can be adapted to the actual grouting process. The required penetration length needs to be defined at the design stage and is based on the hydraulic properties of the rock mass and a certain idea of grouting efficiency.

The real-time grouting control method concept involves calculating the grout penetration and controlling grouting in real-time by applying the development of the grout spread theories.

Grouting is completed when the grout penetration of the smallest fracture that needs to be sealed is above a certain minimum level (target value) or before the grout penetration for the largest fracture aperture reaches a certain maximum level (limiting value).

The spread of grout is governed by a number of complex relationships. This means that the issue of how or when the injection of grout should be stopped cannot be answered by simple rules of thumb. In recent decades there has been a substantial increase in the understanding of the mechanism behind the spreading of grout. Up until 1990, the understanding was more or less based on empirical knowledge as described by Houlsby, (1990). A deeper theoretical understanding of the mechanism, manifested by Lombardi (1985), Hässler et al. (1988), Gustafson and Stille (1996) and Eriksson et al. (2000), has had an impact on the development of both new stop criteria and new grouting materials.

Research in recent years has given us a better understanding of the water-bearing structures of the rock mass as well as analytical solutions of grout spread, see e.g. Gustafson and Claesson (originally submitted, 2005) later published as Gustafson et al (2013). In Hässler (1991), the concept of analysis of grout spread in real-time was discussed for the first time but was based on numerical calculations. The analytical solutions of the governing differential equations have made it possible to develop tools for analysing grout spread in real-time. The principle was first described in Gustafson and Stille (2005), and was further developed in Kobayashi and Stille (2007) and in Kobayashi et al. (2008).

The paper is presented in publication II.

4.2 Grouting control using RTGC

Grouting equipment has a computerised logging tool that continuously records different grouting parameters, such as grouting time, grouting pressure, grout flow and grouted volume. By following the grouting minute by minute it is possible to predict the course of the grout flow and the penetration and also analyse the risk of uplift and jacking.

The procedures for the real-time grouting control method system are shown in Figure 4-1.

```
┌─────────────────────────────────────────────┐
│  ┌───────────────────────────────────────┐  │
│  │           Required data input         │  │
│  └───────────────────────────────────────┘  │
└─────────────────────────────────────────────┘

Phase 1: Verification
┌─────────────────────────────────────────────┐
│  ┌───────────────────────────────────────┐  │
│  │  The dimensionality and grout         │  │
│  │  transmissivity (sum of grouted       │  │
│  │  fracture apertures) is estimated     │  │
│  │  based on recorded grout flow and     │  │
│  │  pressure during the first five to    │  │
│  │  ten minutes after hole-filling.      │  │
│  └───────────────────────────────────────┘  │
└─────────────────────────────────────────────┘

Phase 2: Prediction
┌─────────────────────────────────────────────┐
│  ┌───────────────────────────────────────┐  │
│  │  Prediction of grout flow and grout   │  │
│  │  penetration based on the estimated   │  │
│  │  dimensionality and grout             │  │
│  │  transmissivity (sum of grouted       │  │
│  │  fracture apertures) and the given    │  │
│  │  grouting pressure                    │  │
│  └───────────────────────────────────────┘  │
│  ┌───────────────────────────────────────┐  │
│  │  Estimation of the required grouting  │  │
│  │  time to fulfil penetration           │  │
│  │  requirements                         │  │
│  └───────────────────────────────────────┘  │
└─────────────────────────────────────────────┘

Phase 3: Control
┌─────────────────────────────────────────────┐
│  ┌───────────────────────────────────────┐  │
│  │  Controlling the grouting by          │  │
│  │  comparing the actual flow to the     │  │
│  │  predicted flow. Check the risk for   │  │
│  │  hydraulic jacking. Stop grouting.    │  │
│  └───────────────────────────────────────┘  │
└─────────────────────────────────────────────┘
```
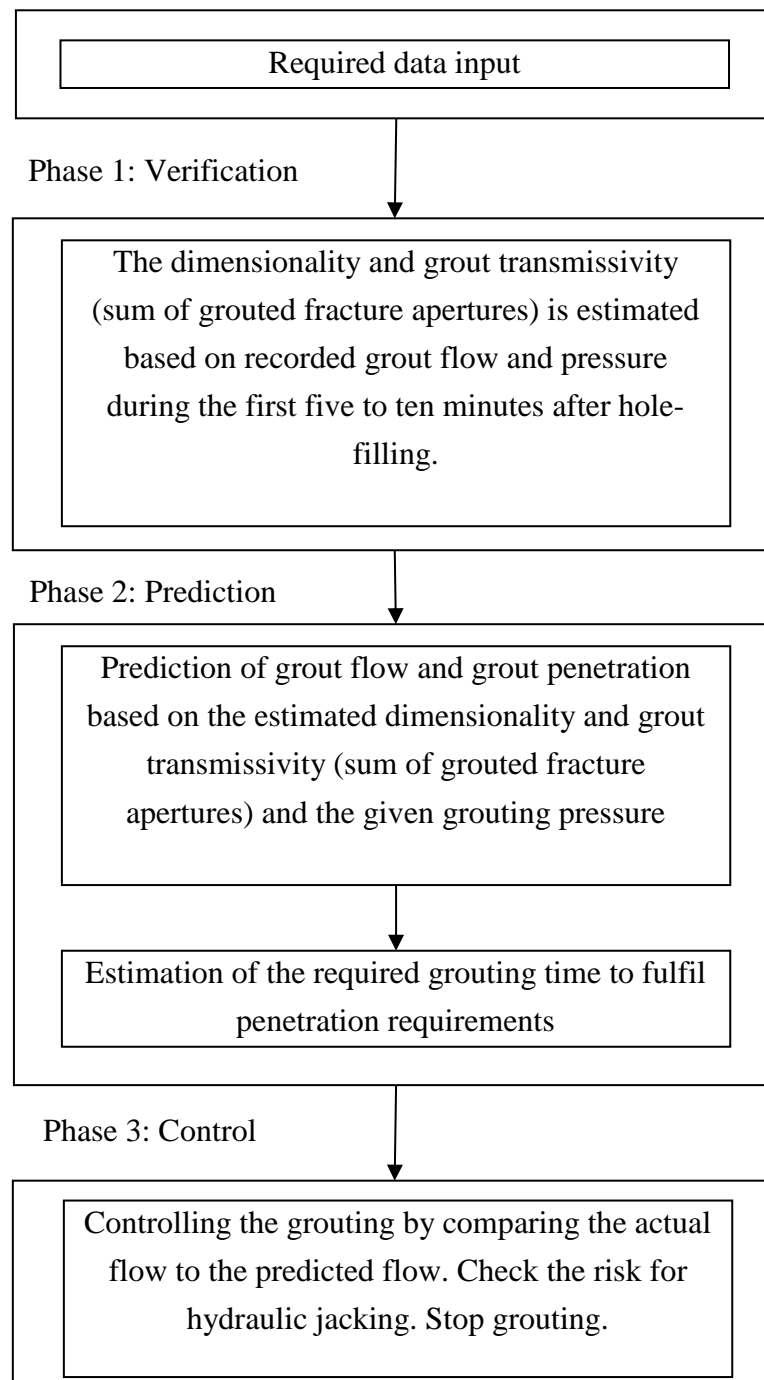
Figure 4-1. Grouting control procedures using the real-time grouting control method.

In the real-time grouting control method, the grout penetration is used as a stop criterion. The minimum penetration length and/or maximum penetration length will therefore be required as input data. Since the penetration length is proportional to the fracture aperture, the smallest aperture that needs to be sealed will be required as well as the aperture of the largest fracture.

In a hydrogeological description of the rock mass, the hydraulic fracture width is often used and can be calculated with the 'cubic law', see Snow (1965). However, experience shows that the physical or geometric fracture aperture (which can be calculated from the grout volume, grout flow and time) and the corresponding hydraulic fracture width often differ by about two times ($b_{physical} \approx 2b_{hyd}$), as shown by Tsuji et al. (2012).

Estimation of grout transmissivity (sum of grouted fracture apertures, $\sum wb^2$ or Σb^3)

The theoretical grout volume can be calculated for both the 1D and 2D cases. In both cases it must be borne in mind that grout may enter several fractures, shown by the term $\sum wb^2$ for the 1D case and $\sum b^3$ for the 2D case. Both terms are a function of the fracture aperture, b, and the channel width, w, for the 1D case. Taking the cubic root of $\sum b^3$ may therefore give a reasonable approximate value of the largest 'possible' aperture for the 2D case. Figure 4-2 (Äspö Hard Rock Laboratory Data, see for example Hernqvist et al 2008) shows a comparison of calculated and measured injected volumes after the borehole was filled with grout. The parameter $\sum b^3 = 5,5 \cdot 10^{-13} \text{ m}^3$ was determined by minimising the sum of squared differences between them. The assumption that the whole transmissivity corresponds to one fracture gives $b = 82$ μm. For the 1D case, the width of the channel must also be estimated.
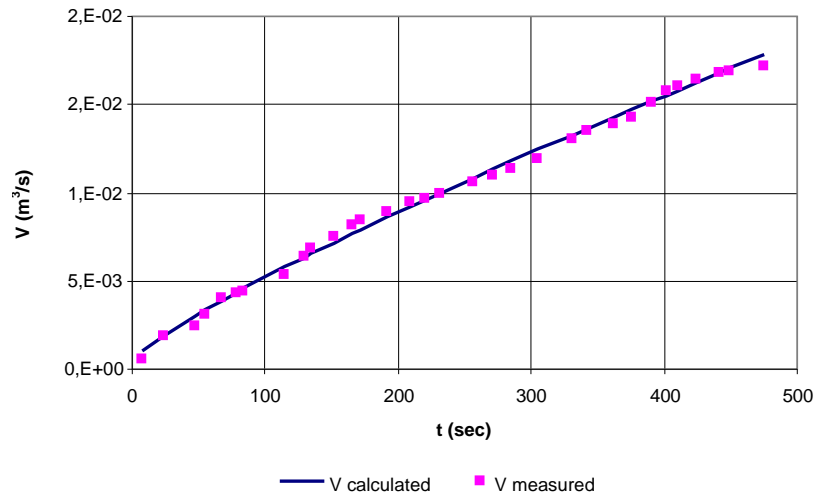
Figure 4-2. Comparison of calculated and measured grout volumes, $\sum b^3 = 5{,}5 \cdot 10^{-13}\ m^3$.

Calculation of the risk of hydraulic jacking and uplift

Grouting will induce stresses in the rock mass, which may cause block movements, hydraulic jacking or uplift. The risk of uncontrolled deformations depends on the pressure and volume and must be avoided (Lombardi and Deere, 1993). Studies carried out by Brantberger et al. (2000) showed that the risk of hydraulic uplift was analysed better by introducing grout penetration instead of volume. Since the penetration length will be calculated during the grouting process in the real-time grouting control method, it may be possible to check the risk of uplift in real-time. Comparison of predicted and measured grout flow, or estimation of grout transmissivity (fracture aperture), will also offer a direct opportunity to discover hydraulic jacking.

The term uplift in this context corresponds to the ultimate bearing capacity of rock mass. Hydraulic jacking may occur at a lower level (Gothäll and Stille, 2009). It is important to point out that there are also other cases, such as leakage of grout into the face or jacking of the face, that also need to be considered. Such risks can be controlled by reviewing the flow-pressure data. The largest risk of uplift is connected to the longest penetration. The penetration length for the largest fracture aperture should therefore be used in the calculations. In Brantberger et al. (2000), the permissible lifting force is calculated using an assumption of a circular open fracture. The uplift or risk of hydraulic jacking has been further developed by Rafi (2014) and the hydromechanical behaviour with regards to the fracture geometry was studied by Thörn (2015).

4.3 Experience from different case histories

The theory of grout penetration and grout flow has been investigated in four projects in order to demonstrate the applicability of the theory. The projects, case histories, are located in different parts of Sweden, in different geologies and at different depths. For each case, grout data have been recorded and the theory of dimensionality, the estimation of fracture apertures and the theoretical grout flow have been calculated. Some relevant samples are shown.

The case histories are from Äspö Hard Rock Laboratory at the 450 m level, the Northern Link road projects in Stockholm and the Bothnia Line rail project in central Sweden.

Short summaries of the project data are shown in Table 4-1.

Table 4-1. Case history summary.

Case history	Geology	Depth (data from)	Inleakage (after grouting)	Comments
Äspö HRL	Äspö diorite, very competent	450 m	<4.5 l/min.100 m	Swedish nuclear repository research centre. Very good quality data. Kobayashi et al. (2008).
Northern Link NL101	Granite, gneiss, competent	10-20 m	~2 l/min.100 m	Road tunnel system, Swedish Road Administration. Long (20 m) planar and smooth fractures. Bedding planes. Bohlin and Urtel (2008).
Northern Link NL34	Sedimentary gneiss, fractured	20 m	~4 l/min.100 m	Road tunnel system, Swedish Road Administration. Fractured rock. Zones. Bruno, (2009).
Bothnia Line (E3541) Namntall South	Metagreywacke, partly very fractured	80 m	~20 l/min.100 m	Rail-road tunnel system, Swedish Rail/Road Administrations. Very fractured in part. High frequency of zones. Stille and Andersson (2008).

Prediction of grout flow

After the flow dimensionality of the hole has been calculated, the sum of the fracture apertures and the theoretical flow can be calculated. The calculated flow in Figures 4-3 to 4-5 is related to the analysed dimensionalities. The calculation of the theoretical flow follows the pressure curve and the resulting theoretical flow curve can be compared to the actual recorded flow curve. In the figures, the nominal Q predicted is used as the theoretical flow.

Figure 4-3.Comparison between the measured flow and the predicted flow for hole 31, fan 6, 2D flow. The primary Y-axis show grout flow [l/min] and the secondary Y-axis show pressure [Pa].
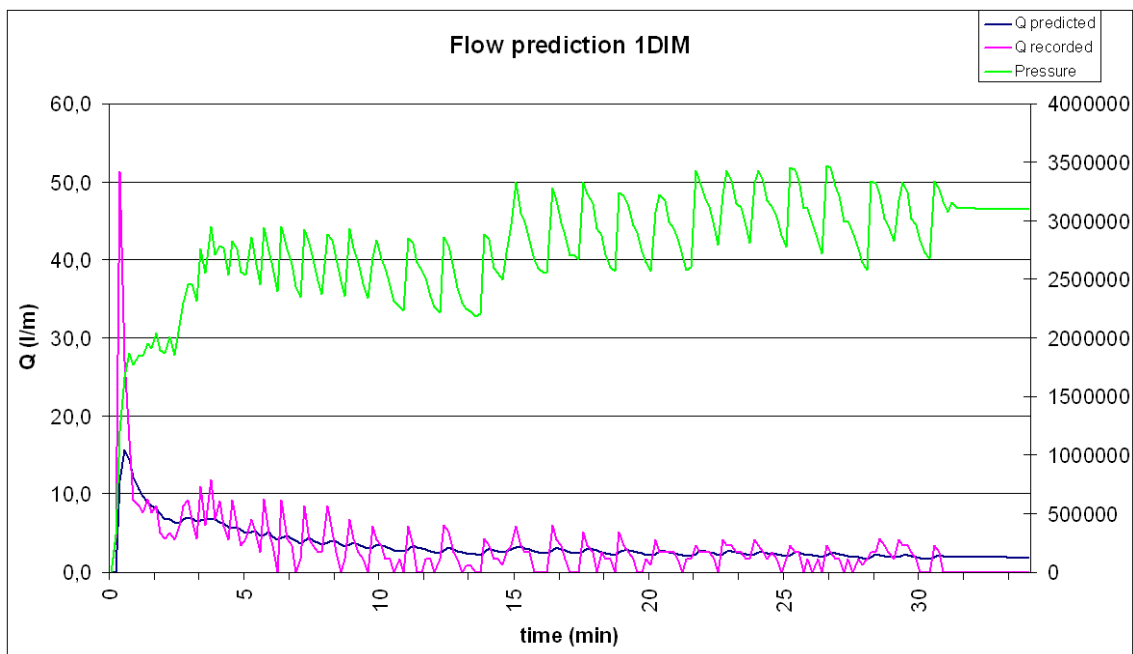
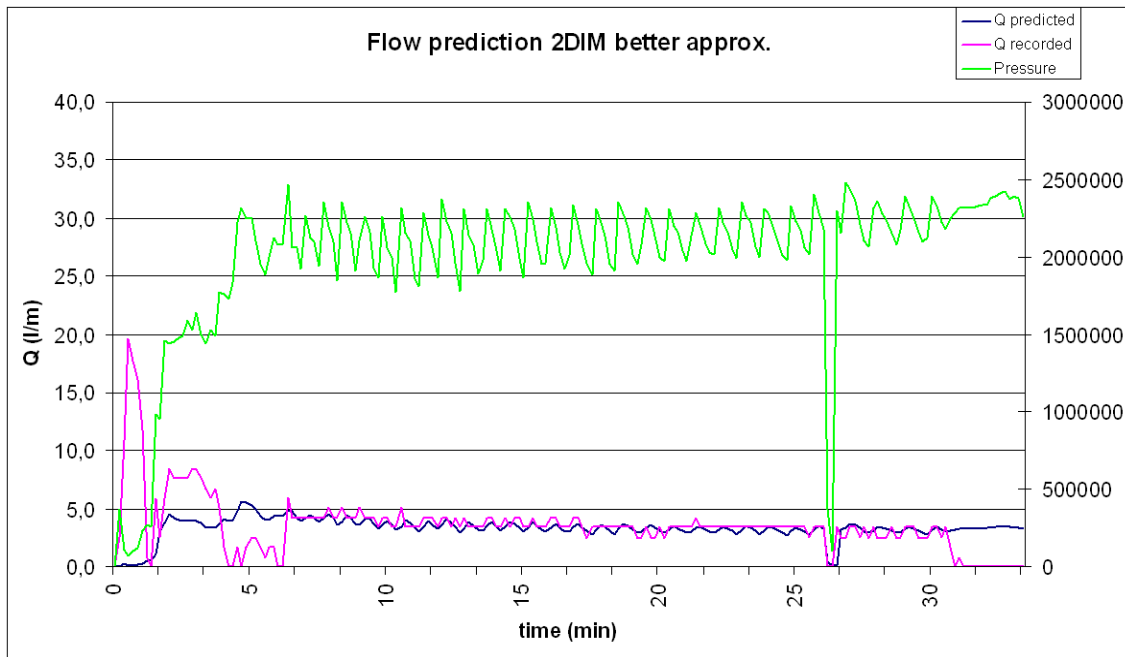*Figure 4-4. Comparison between the measured flow and the predicted flow for hole 1, fan 7, 1D flow. The primary Y-axis show grout flow [l/min] and the secondary Y-axis show pressure [Pa].*
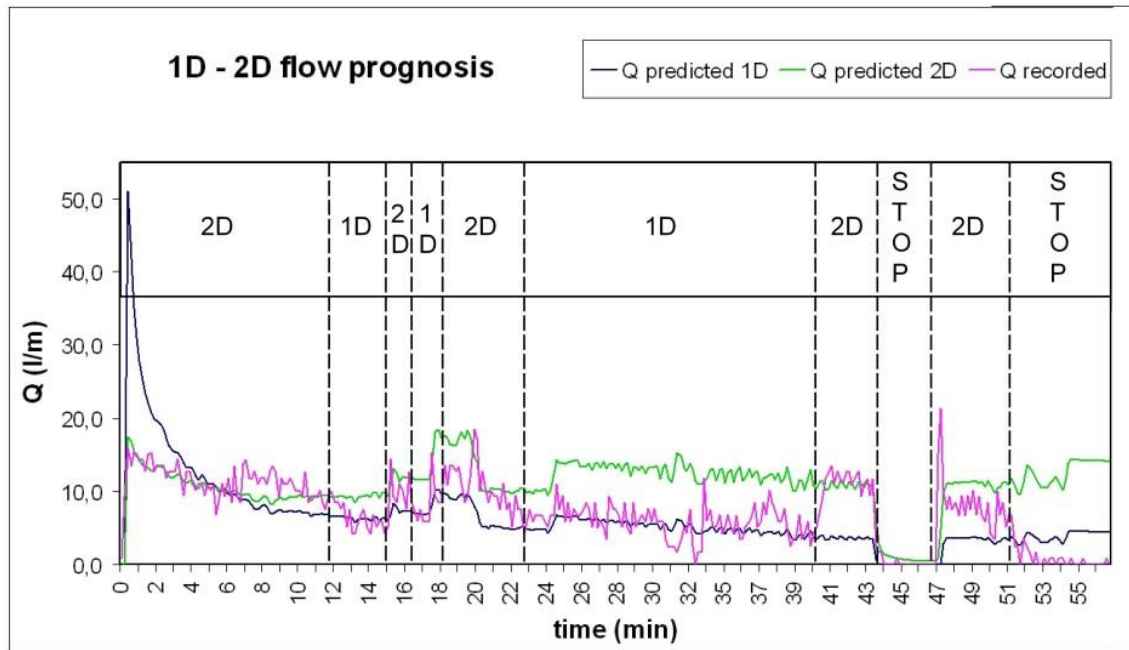
Figure 4-5. Comparison between the measured flow and the predicted flow for hole 22, tunnel 301 section 1547, varying flow. The primary Y-axis show grout flow [l/min].

As can be seen in Figure 4-5, which shows both 1D-predicted flow and 2D-predicted flow, the recorded grout flow follows the respective theoretical curves according to the varying dimensionality.

Jacking

Sometimes other anomalies were recorded during grouting. Some of these include uplift or jacking of the ground for shallow grouting operations, see Figure 4-6. Others seem to influence smaller areas of the rock mass, see Figure 4-7. A case from NL33-34 is shown in Figure 4-6, where after 26 minutes of grouting the pressure is increased, resulting in an immediate increase in flow. The flow then decreases and is followed by a continuous increase in flow until the grouting is aborted after about 40 minutes despite the fact that the pressure was reduced. In Figure 4-7, the grouting pressure increased slightly, producing a non-proportional increase in grout flow. As can be seen, after this initial increase the grout flow diminishes, indicating that the action in the rock mass is more local, including possible rock movements in the fracture zone opening one fracture and closing another.
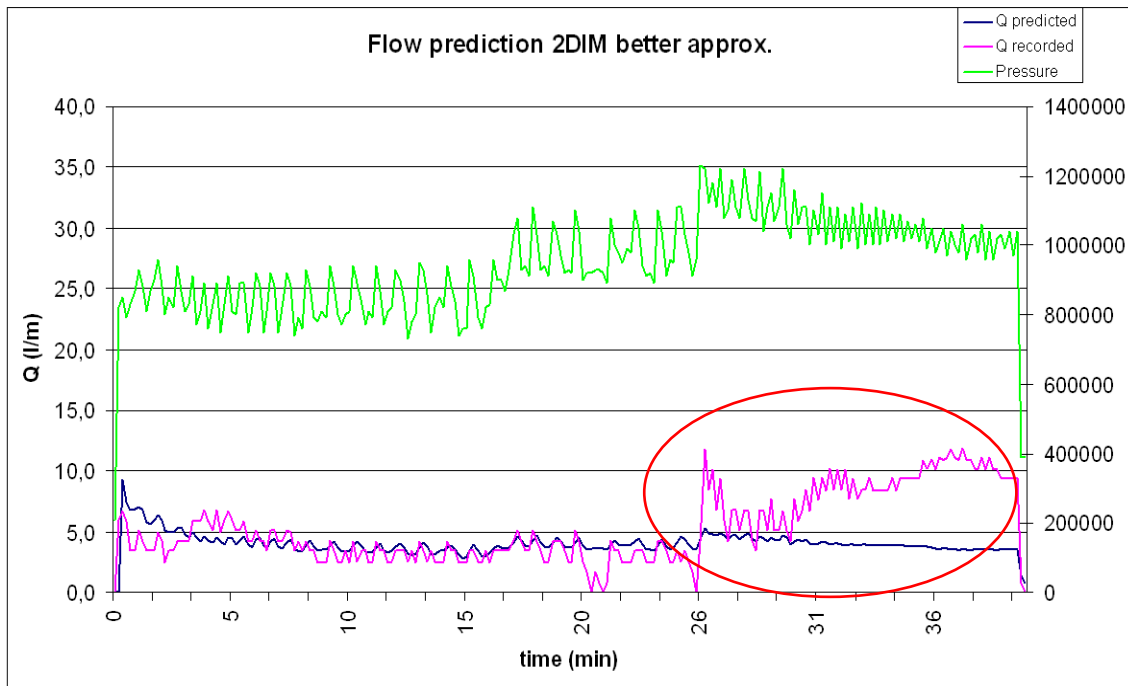
Figure 4-6. Possible uplift or jacking of the rock mass, hole 16, fan, 2D flow. The primary Y-axis show grout flow [l/min] and the secondary Y-axis show pressure [Pa].
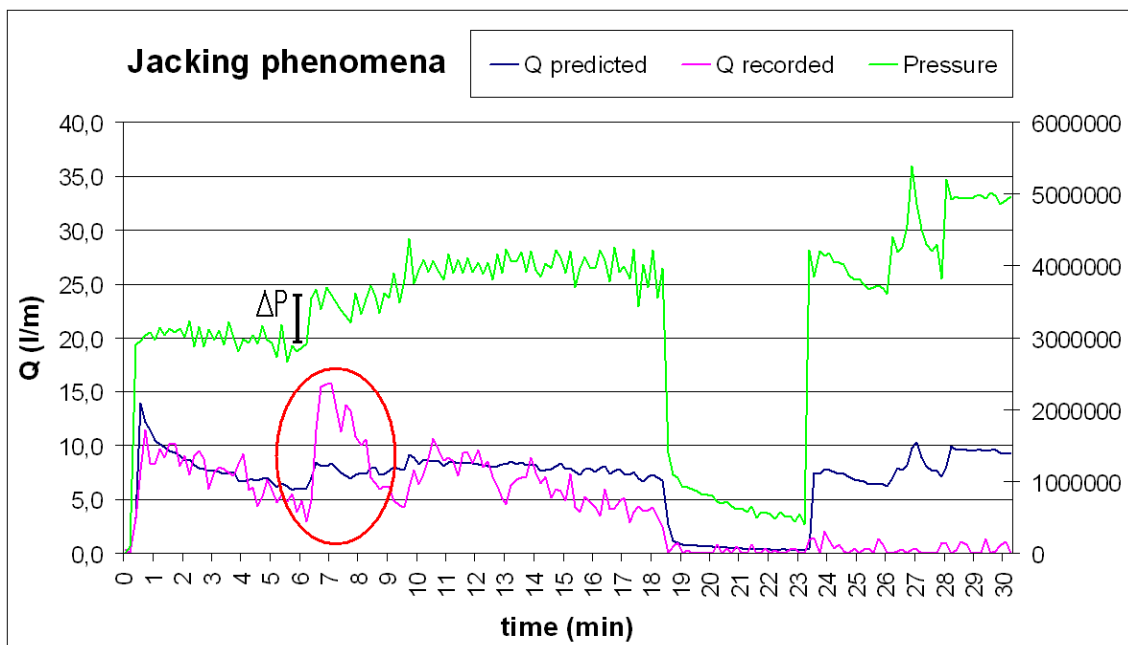

*Figure 4-7. Possible jacking influencing a local area of the rock mass, 2D flow. The primary Y-axis show grout flow [l/min] and the secondary Y-axis show pressure [Pa].*

4.4 Summary

The concept behind of a real-time grouting control method is to control the grouting in real-time by applying the grout spread theories. It is possible, by following the grouting minute by minute, to predict the course of the grout flow and analyse the risk of uplift and jacking.

This could be of particular interest for shallow surface grouting or grouting close to other subsurface areas where the possibility of detecting jacking or uplift of the rock mass could be of critical interest. The most significant action from the examples presented would have been the ability to abort grouting or lower the grouting pressures. These issues are also discussed in this paper.

Verification of the real-time grouting control method, with field data from four tunnel projects in Sweden, is presented in this paper. The calculated flow dimensionality, the calculated fracture apertures and the calculated grout flows were quite close to those measured. This indicates that the real-time grouting control method is applicable to real grouting design and control.

5 DISTRIBUTION OF ROCK MASS HYDRAULIC CONDUCTIVITY AND ITS APPLICATION TO ROCK ENGINEERING PROBLEMS, PAPER 3

5.1 Introduction

The most common sources of geohydrological information for Scandinavian tunnelling projects with regard to hydraulic properties come from water pressure tests in 3 to 9 m lengths. These are sometimes performed as double packer tests (the tested part of the borehole is closed off using two packers) but often as single packer tests (where one packer is used and the results are subtracted from the previous measurement to produce the result for a specific part of the borehole). During construction, and as part of the grouting work, water pressure tests are sometimes performed, as was the case with the Namntall Tunnel described by Stille and Gustafson (2010). The accuracy of such 'during construction' methods varies depending on the equipment and in the Namntall project it was concluded that results below 0.2 and over 4 Lugeons (litres/min.m.MPa) were unreliable (corresponding to a transmissivity of T = $7,4 \cdot 10^{-7}$ and $1,5 \cdot 10^{-5}\ m^2/s$).

The main focus here is the statistical distribution of the water pressure tests and the transmissivity calculated from those tests, the theory and method for scaling the distribution to the appropriate level, and the analysis of the probability that the rock mass has a mean hydraulic conductivity lower than a set value. Three important issues need to be considered.

1. The distribution of hydraulic conductivity in the rock mass.

2. The influence of the scale of the problem.

3. Water seepage flow regimes and appropriate mean values for the seepage calculations.

The Paper is presented in publication III.

5.2 Effective hydraulic conductivity and mean values

The transmissivities or hydraulic conductivities in a rock mass are neither uniform nor isotropic but vary considerably from rock volume to rock volume. The measurements show that the rock mass transmissivities can be described statistically and it is therefore of interest to study the distribution and the influence of the studied rock volume with regard to size and mean values, see also Holmén (1997). From an engineering point of view, the calculation of water inflow to a tunnel or under a dam should be done as accurately as possible to define the requirements for the grouting work but also with

regard to the environmental court rulings. This in turn requires either the use of relevant mean values or the entire statistically described distribution.

Gustafson (2009) indicates in the division of different scales that the statistical models for estimating the distribution of the hydraulic properties are different. For the 3-30 m scale, several fractures intersect the test section or the tunnel and fracture independence cannot be assumed. Instead, the interval transmissivities are a better description of the hydraulic properties of this scale. De Marsily (1986), for example, described the interval transmissivities as lognormally distributed.

Holmén (1997) defined the effective hydraulic conductivity of a rock volume as a representative mean value depending on the flow regime and the statistical distribution of the hydraulic conductivity. The flow regime in turn depends on the heterogeneity of the rock mass. The different flow regimes are shown in the attachment. The different mean values could also be used to estimate the upper and lower boundaries of the hydraulic conductivity where, for example, the arithmetic mean could be considered to be the upper boundary and the geometric mean the lower boundary. The influence of heterogeneous conditions (such as fracture zones) could influence and change the relevant model and thus the relevant mean for the engineering problem. It is clear that the better the description of the distribution, the more reliable the prognosis. The identification of a relevant statistical distribution for section transmissivities was performed by, for example, De Marsily (1986), identifying the lognormal distribution as relevant for most data.

5.3 Evaluation of lognormal distribution parameters of section transmissivity in different cases

The evaluation of lognormal distribution parameters has been performed for four cases (two cases are shown here, *Figures 5-1* and *5-2*). For these cases, the water pressure test results from the tunnelling operation are analysed and the lognormal distribution is fitted to the measured data. In all geotechnical investigations there are a number of uncertainties, such as measuring accuracy, measuring span and handling errors etc. related to the measured result. It is important to recognise that there are limits to the reliability of the measurements when it comes to interpreting the data.

The water pressure tests (WPT) presented in this analysis are performed in the grout holes over the whole length of the borehole for a limited period of time, 3-5 min, with a pressure of 0.5 MPa above the groundwater pressure. The transmissivities are calculated from the WPT tests and are presented as CDF's 'Grout hole test results' in the figures.

The transmissivity values from the water pressure tests are fitted to a lognormal distribution. The lognormal distribution has the property that the log values of the

stochastic variate (X) are normally distributed with $E(\ln X) = \lambda$ and variance $= \xi^2$. The case records are presented using the statistical values of the normal distribution of $\ln(X)$ and the mean transmissivity value, μ_T, and the standard deviation σ_T (*Figure 5-1* and *Figure 5-2*). The application of the lognormal distribution and the identification of the mean value and the standard deviation should be performed for the range of reliable data. The easiest way to perform such a curve fitting is to manually change the λ and the ξ values until a good fit is achieved.

The transmissivity results (over a section length of 20 m) and the transmissivity data are presented in the figures. The largest discrepancies are for both small and large values, as expected due to larger measurement errors.

Odenplan Station, City Line,
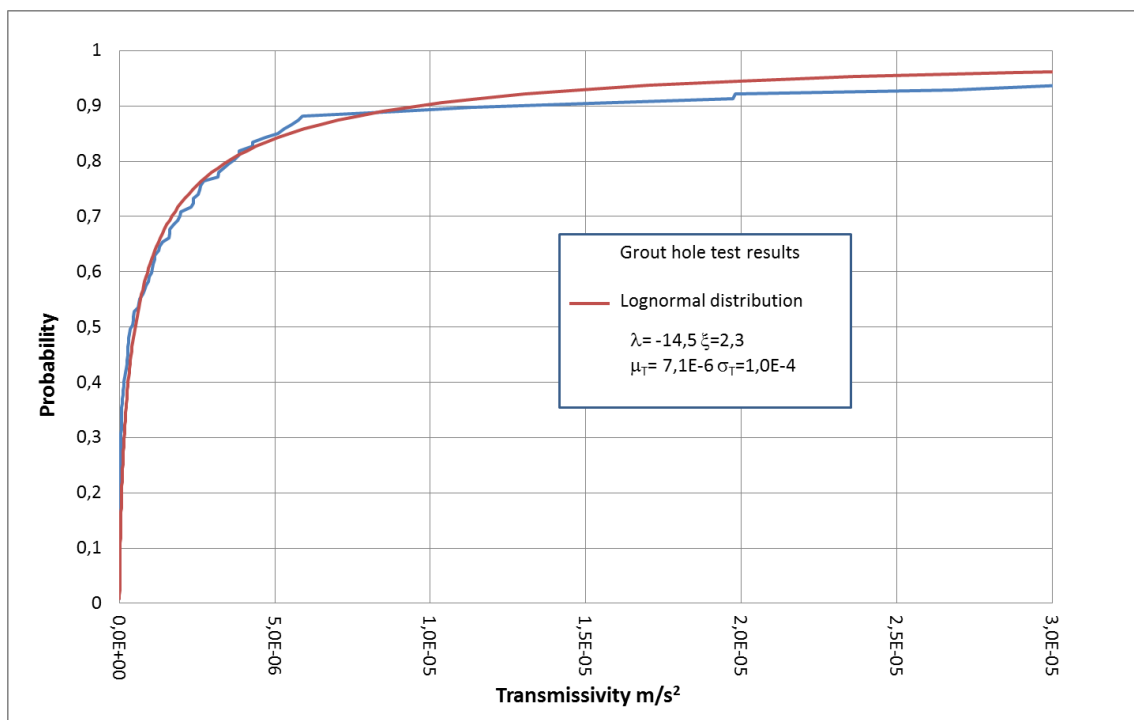
Figure 5-1. Transmissivity distribution for the Odenplan Station on the City Line.

Namntall Tunnel – South
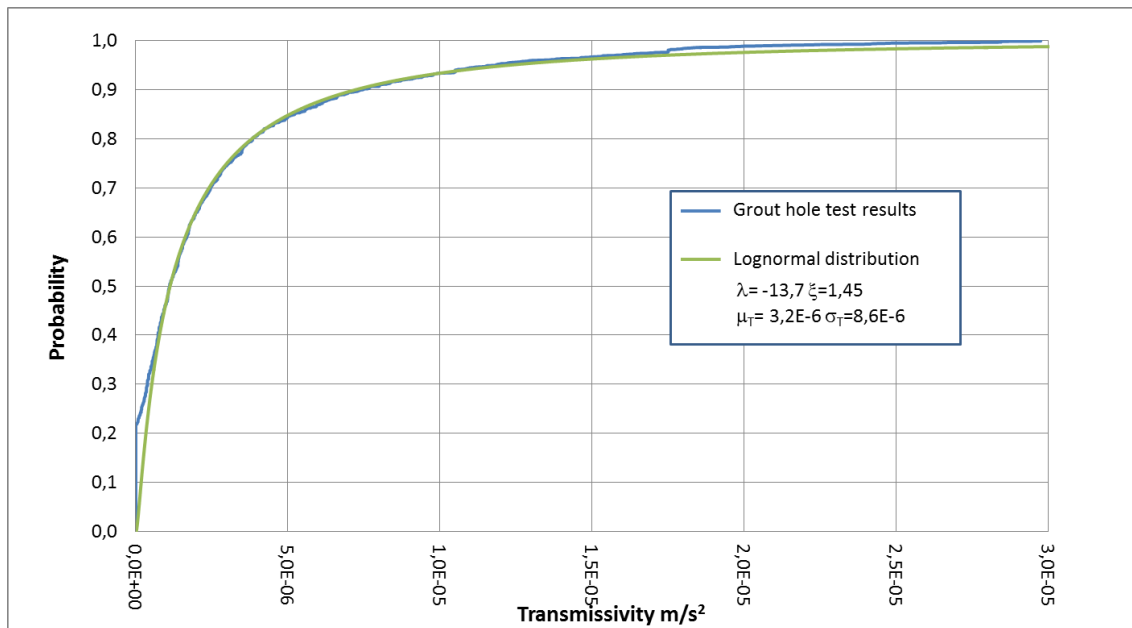
Figure 5-2. Transmissivity distribution for the southern part of the Namntall Tunnel.

The fit is very good, which confirms the use of the lognormal distribution to describe the variation in section transmissivity.

5.4 Influence of scale

The theory for the lognormal distribution is presented in the attachment. One of the properties of a lognormal distribution is that the mean values can be added for two lognormal distributions. This means that it is possible to scale the data to a size that is relevant for the engineering problem. If the transmissivity data is measured over a length, L_{base}, and the transmissivity is investigated for a length, L, then the mean values can be calculated from:

$$n = {L}/{L_{base}}$$

The arithmetic mean value and the standard deviation will then become:

$$T_a = \mu_{T,L} = n \cdot \mu_{L_{base}}$$

$$\sigma_{T,L} = \sqrt{n} \cdot \sigma_{L_{base}}$$

The geometric mean value of the transmissivity distribution can be calculated for different lengths, L, as:

$$T_g = \frac{\mu_{T,L}}{\sqrt{1 + \left(\frac{\sigma_{T,L}}{\mu_{T,L}}\right)^2}}$$

In this case the hydraulic conductivity is a useful value since it normalises the values of T and makes them comparable for different scales. The hydraulic conductivity can be described as K = T/L and the mean value is calculated as:

$$\mu_K = \frac{1}{L} \cdot \frac{L}{L_{base}} \mu_{T,L_{base}} = \frac{\mu_{T,L_{base}}}{L_{base}}$$

The arithmetic mean is evidently independent of an increase in scale. However, the standard deviation is dependent on the length, L, according to:

$$\sigma_K = \frac{1}{L} \cdot \sqrt{\frac{L}{L_{base}}} \cdot \sigma_{T,L_{base}} = \frac{\sigma_{T,L_{base}}}{\sqrt{L \cdot L_{base}}}$$

The geometric mean of the hydraulic conductivity for a length L can therefore be calculated using:

$$K_g = \frac{\mu_{K,L}}{\sqrt{1 + \left(\frac{\sigma_{K,L}}{\mu_{K,L}}\right)^2}}$$

According to the definition for a lognormal variate X, the variance of the normalised function is $\xi^2 = Var(lnX)$ and can be expressed for the length, L, as:

$$\xi^2 = ln\left(1 + \frac{\sigma_{T,L_{base}}^2}{\mu_{T,L_{base}}^2} \frac{L_{base}}{L}\right)$$

Using 'Matheron's conjecture', the relative hydraulic conductivity, K_D, can be described, depending on the flow dimension, as:

$$K_D = K_g \cdot e^{\left[\xi^2\left(\frac{1}{2} - \frac{1}{D}\right)\right]} \; where \; D = flow \; dimension$$

The statistics are based on the prerequisite that the data are statistically independent. The correlation distance for section transmissivity probably depends on the actual rock mass

characteristics. For fractures in a hard crystalline host rock, the correlation distance has been estimated by Butron (2012) at 2-8 m. The scale of fluctuation indicates that the measured data can be expected to be more or less independent.

For most problems in tunnelling situations, the length of a grouting fan is on an engineering applicable scale, although an extrapolation for the whole tunnel may be required to calculate tunnel seepage. The relationship between the statistical parameters and the hydraulic conductivity for different section lengths can be calculated by adding the transmissivities and dividing μ_T/L, which will produce the arithmetic mean, K_a. The arithmetic mean, K_a, is independent of scale while the standard deviation will decrease with scale. Since the geometric mean, K_g, depends on the standard deviation, the implication is that the geometric mean and K_{3d} will increase with scale and approach the arithmetic mean for very large scales.

The calculation presented in *Figure 5-3* is based on data from the Odenplan Station on the City Line, *Table 5-1*. The measured section intervals range from 3 m to around 20 m for these tunnels (water pressure tests before grouting). It can be shown that the arithmetic mean value for the 20 m sections is about equal to the 3 m sections. However, the standard deviation decreased from $9.7 \cdot 10^{-6}$ to $5 \cdot 10^{-6}$, which confirms the general finding that the geometric mean should increase with scale.

Table 5-1. Statistical data for the Odenplan Station on the City Line based on measured data for 3 and 20 m intervals.

Odenplan Station	3 m	20 m
σ [m/s]	$9.7 \cdot 10^{-6}$	$5 \cdot 10^{-6}$
ξ [-]	2.6	2.3
K_a [m/s]	$3.3 \cdot 10^{-7}$	$3.55 \cdot 10^{-7}$
K_g [m/s]	$1.1 \cdot 10^{-8}$	$2.5 \cdot 10^{-8}$

At the Odenplan Station on the City Line, the water pressure tests were carried out for both 3 m and 20 m sections in the same boreholes.
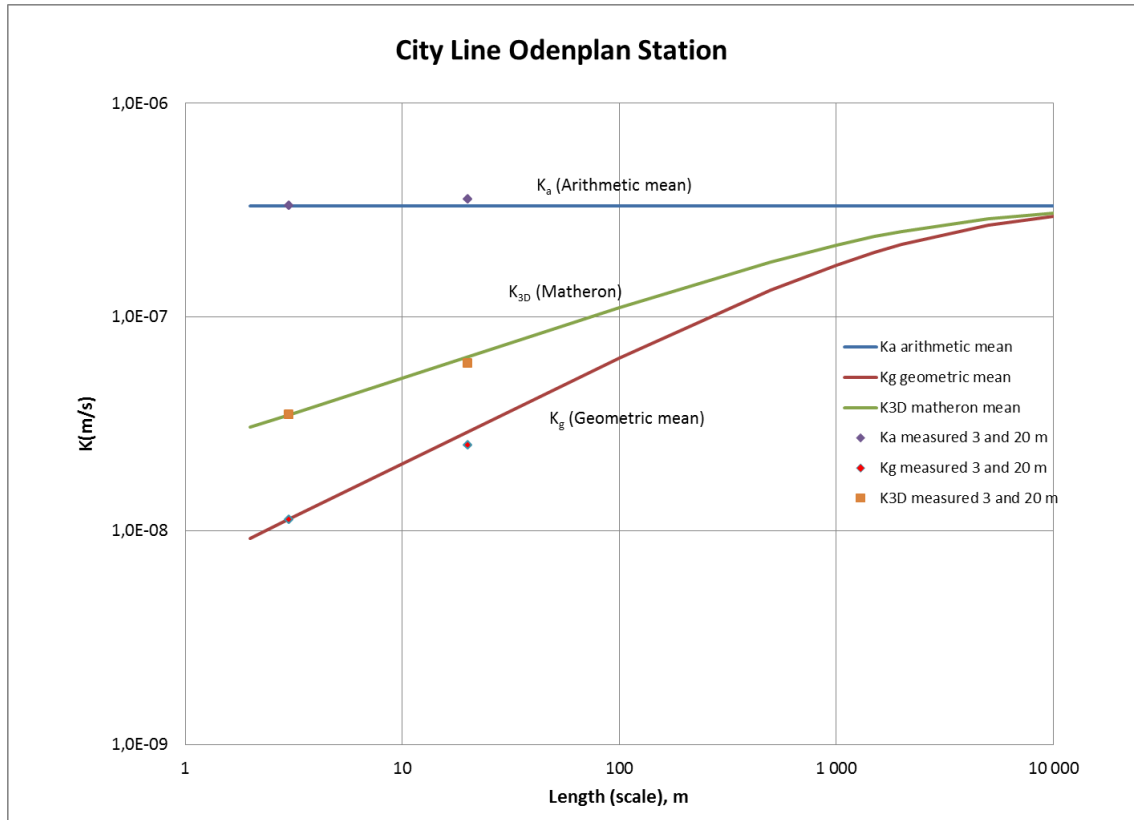
Figure 5-3. Mean values for the Odenplan station on the City Line.

By studying the density function for the different scales, some light is cast on the properties of the hydraulic conductivity distribution. The density function can be plotted to illustrate the variation in the likelihood of encountering a specific value, *Figure 5-4*. In the figure, the calculated density functions are presented for the intervals 20 m, 100 m, 500 m, 1,000 m and 5,000 m. These represent the scales from a grout hole section (20 m) to the whole tunnel.

31
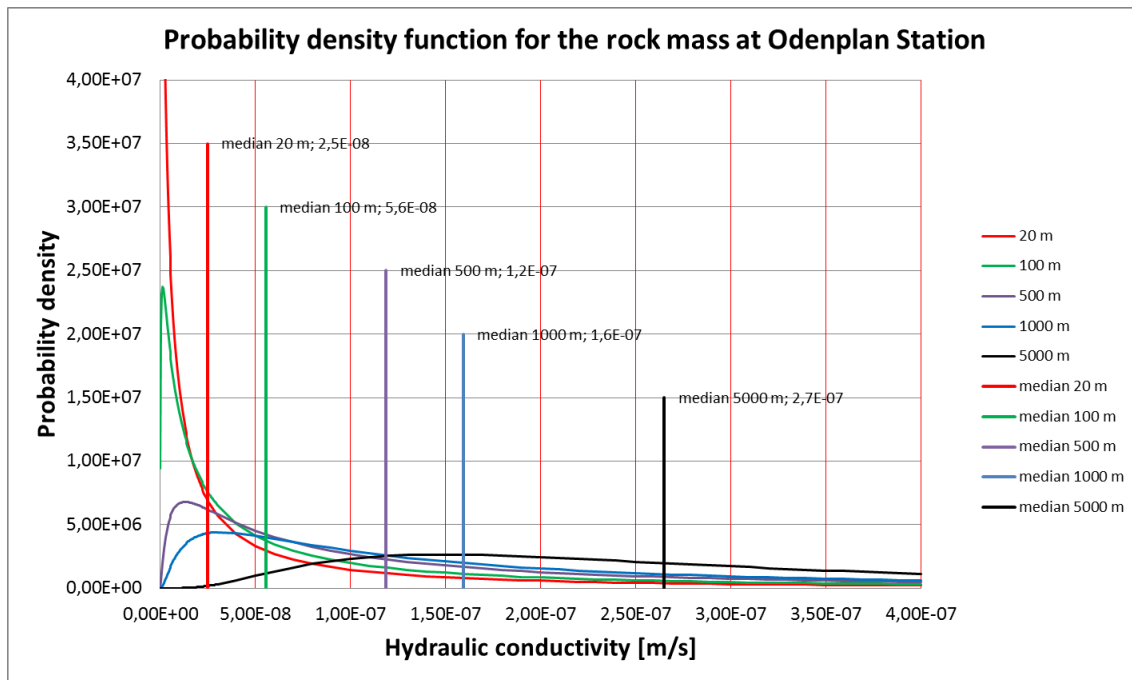
Figure 5-4. Probability density function for different scales (intervals) of hydraulic conductivity at the Odenplan Station.

The results are quite interesting in that they illustrate the variation and high probability that a very low value is encountered for the 20 m interval (median) whereas for the larger intervals the probability of achieving a certain value is more evenly distributed across the measured spectrum. The median represents the probability that for a stochastic tunnel or part of a tunnel, there is a 50% chance that the hydraulic conductivity is lower than or equal to the median.

It can be shown that for a lognormal distribution the probability that the variable X is smaller than b is

$$P(X < b) = \Phi\left(\frac{lnb - \lambda}{\xi}\right)$$

The probability that the hydraulic conductivity will be larger than a certain figure is a relevant question for the seepage analysis. The statistical data can be used to calculate this probability for the different scales. As an example, the probability that the hydraulic conductivity is smaller than the mean value and twice the mean value is calculated, *Table 5-2*.

Table 5-2. Data from the Odenplan Station and calculation of the probability that $K < K_{limit}$ (μ_K; $2\mu_K$) for different lengths.

Length	μ_K	σ_K	CV (σ/μ)	Median $\mu/\sqrt{1+(CV)^2}$	λ	ξ	Φ P($K<\mu_K$)	Φ P($K<2\mu_K$)
3	$3.55 \cdot 10^{-7}$	$1.3 \cdot 10^{-5}$	36.4	$9.8 \cdot 10^{-9}$	-18.45	2.68	0.91	0.95
20 m	$3.55 \cdot 10^{-7}$	$5.0 \cdot 10^{-6}$	14.1	$2.5 \cdot 10^{-8}$	-17.50	2.3	0.88	0.93
100 m	$3.55 \cdot 10^{-7}$	$2.2 \cdot 10^{-6}$	6.3	$5.6 \cdot 10^{-8}$	-16.70	1.92	0.83	0.91
500 m	$3.55 \cdot 10^{-7}$	$1.0 \cdot 10^{-6}$	2.8	$1.2 \cdot 10^{-7}$	-15.95	1.48	0.77	0.89
1000 m	$3.55 \cdot 10^{-7}$	$7.1 \cdot 10^{-7}$	2.0	$1.6 \cdot 10^{-7}$	-15.65	1.27	0.74	0.88
5000 m	$3.55 \cdot 10^{-7}$	$3.2 \cdot 10^{-7}$	0.9	$2.7 \cdot 10^{-7}$	-15.14	0.76	0.65	0.9

5.5 Summary

For an ungrouted tunnel it is suggested that the effective hydraulic conductivity is represented by a mean value ranging from the 3D mean (model d) to the arithmetic mean (model b) with a scale (block size) that depends on the depth of the tunnel but not less than 20 m. In the case of a grouted tunnel, the grouting will significantly change the hydraulic conductivity close to the tunnel and the pressure gradient will act across the grouted zone. The water flow for the grouted tunnel will be parallel (model b) and the effective hydraulic conductivity would be represented by the arithmetic mean (model b) after grouting. It is recommended that the scale is equal to the grout hole length, i.e. around 20 m.

The mean values can be analysed and scaled according to the presented theory. The lognormal distribution seems to fit the transmissivity data. It is important to take the accuracy of the measuring system into consideration when evaluating the data. In this study there seems to be an interval of $7.4 \cdot 10^{-7}$ to $1.5 \cdot 10^{-5}$ m²/s, which is more reliable. When analysing the scale effects, an increase in scale reduces the variance and the geometric mean increases. For tunnels over 500 m in length, the difference between the mean and arithmetic mean values seems to be relatively small. Considering the general trend in the statistical data, it would seem reasonable that arithmetic mean values should

be used for calculating seepage into most tunnels longer than 100 to 1,000 m. However, the requirement is that the data is from the same hydrogeological domain. The variation in data should be considered, especially for cases with a limited number of tests. By applying the statistical data, the variation can be used to describe a likely interval of mean hydraulic conductivity that can be used as an upper and lower boundary for calculating seepage.

The geometric mean values represent the 50% value of the rock mass hydraulic conductivities. This means that there is a 50% chance that the actual mean value is higher than the geometric mean. In the case of the arithmetic mean value, the chance that the actual mean is higher than the arithmetic mean would be about 10%. There seems to be little difference between the probability that the mean value is higher than the arithmetic mean or twice this value. This is a function of the relative low probability to encounter the higher values in the distribution.

The probability that the hydraulic conductivity is predicted accurately is relatively low – 50-90% depending on the mean values that are used. This calls for a design approach that can be adjusted for actual conditions equivalent to an observational method where the inflow and the grouting work are followed up. It is recommended that the initial part of the tunnel is followed more closely since any changes to the design or grouting operation have a greater impact at an early stage.

6 ANALYSIS OF WATER SEEPAGE AFTER GROUTING, SUGGESTED MODEL

6.1 Introduction

The accuracy of predicting seepage is of considerable interest since this is part of environmental court rulings, the seepage requirements and the procurement process. Consequently, the seepage calculation influences not only the requirements but also the grouting process and the total project cost.

The conceptual models for calculating seepage into a grouted tunnel are illustrated in *Figure 6-1*. In principle, these are either a homogeneous model where the mean hydraulic conductivity, K_0, of the rock mass is assumed to be valid over the tunnel or actual domain, or a fracture model where each fracture contributes individually to the seepage.
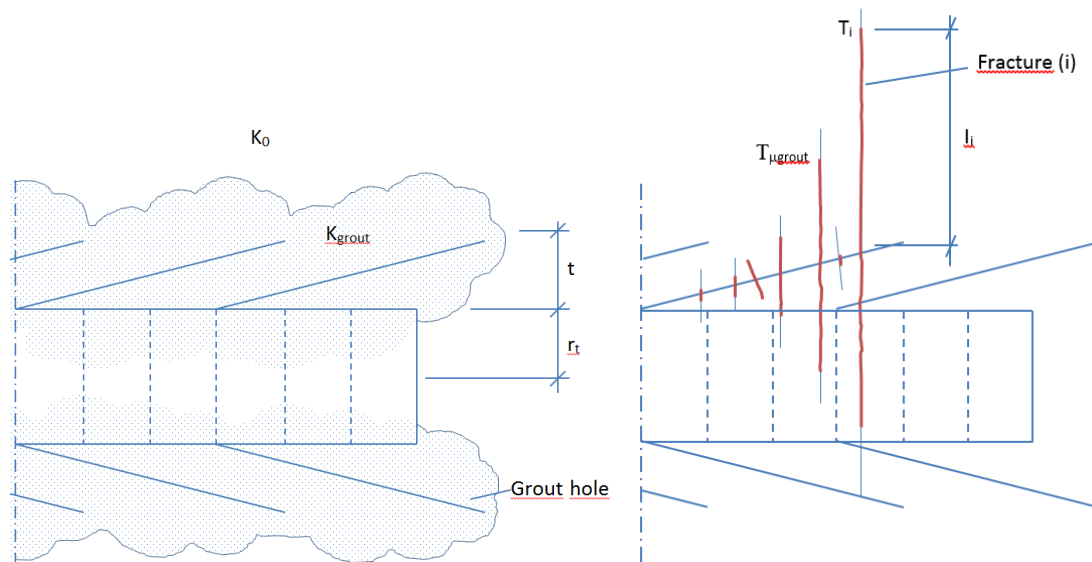
Figure 6-1. Illustration of two conceptual models (homogenous and fracture) for estimating tunnel seepage.

In hard crystalline rocks the rock mass is naturally neither homogeneous nor porous and water seeps through fractures in the rock. The fractures are not independent and may be connected especially for fracture zones. During grouting, the grout penetrates some of the fractures. However, the penetration length for the smaller fracture apertures will be very short or even almost zero and for larger fracture apertures the penetration length will be very long, *Figure 6-2*. This variation in penetration length and grouting result indicates that the models for analysing seepage may be discussed and modified to accommodate a better understanding of the fracture/grout penetration relationship.

6.2 Grout penetration and grouting results

Several previous back calculations have been performed to analyse the achieved grouting result, K_{grout}, based on the homogeneous model, see e.g. Hernqvist (2011) or Tsuji et al (2012). However, some practical issues related to the grouting work need to be considered when evaluating the grouting result. During grouting, the grout penetrates the fractures down to a certain fracture aperture depending largely on the grout mix and the grain size distribution, Draganovic (2009). Furthermore, the grout penetrates a certain distance into the rock mass depending on the fracture apertures, grout properties, grouting pressure etc., Gustafson and Stille (2005).

The grout filtration tests (EN 14497) of the cement grout from the cases mostly show a b_{min} of about 50 μm and a b_{crit} of about 80 μm, which indicate that no grout penetrates the 50 μm physical fracture and that filtration limits the penetration up to an 80 μm physical fracture. See Eriksson and Stille (2005) for a discussion of the filtration test.

It is shown that for Namntall North (Stille and Gustafson, 2010), the Bangård Tunnel (Tsuji et al 2012) and the Odenplan Station (Stille et al 2014), the grout take for about 50 - 70% of the holes is about equal to the hole volume (< 1 l/m). The grout flow stop criteria in most of these cases indicate a grouting time of 1-5 min after the hole has been filled.

For a grouting pressure of 20 bar, the theoretical penetration length, according to Gustafson and Stille (2005), can be calculated as 0.6 m and 1.3 m for a 50 μm fracture and for the 80 μm fracture 1.0 m and 2.2 m with a grouting time of 1-5 min, *Figure 6-2*. The figure shows that the penetration length is proportional to the fracture aperture, although no filtration is considered for the small fractures, which means that the actual penetration length is probably shorter. The calculation is performed with grout properties typical for most of the grout used in the presented cases with the yield limit and viscosity values shown in the figure.
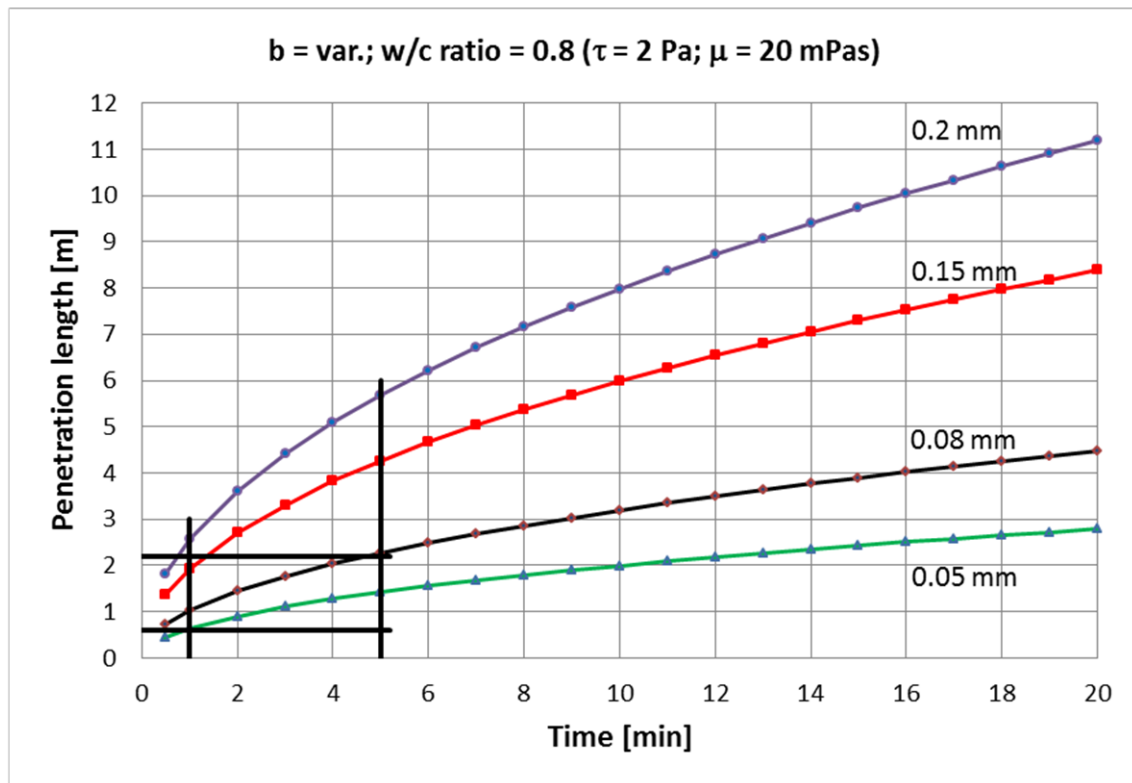
Figure 6-2. Calculated penetration length, according to Gustafson and Stille (2005) for short grouting times. Each curve represent the penetration length for a specific fracture aperture. The straight lines indicate 1 and 5 min grouting time and the penetration length for 0.05 mm and 0.08 mm fracture aperture. The grout pressure is 20 bars.

At Namntall North and South the end point distance of the grout holes were equal to or larger than 4 m and for the City Link Bangård Tunnel and Station Oden the end point distance of the grout holes were about 2.5 m. It seems clear that for fracture apertures smaller than about 80 μm, the penetration length is too small to consider the fractures as fully grouted if stopped within 5 min of grouting time as is the case for many of the grout holes with small grout takes.

The grout flow can be calculated, using the same theory, for each fracture, *Figure 6-3*. It is shown that the grout flows for the smaller fractures are very small as is exemplified for the 0.08 mm fracture. The calculated grout flow for this fracture is about 0.3 l/min. This is especially interesting when discussing the grout results in relation to grout take, the number of fractures and the grout flow stop criteria, exemplified for Station Odenplan as 5 l/5min or 1 l/min. For a grout take of <1 l/m and a grout time of 5 min this would indicate a grout flow of <0.2 l/min.m and consequently a fracture aperture <0.08 mm/m. If only one fracture in the hole contributed to the grout take the size of this fracture would theoretically be 125 μm (grout flow = 1 l/min).
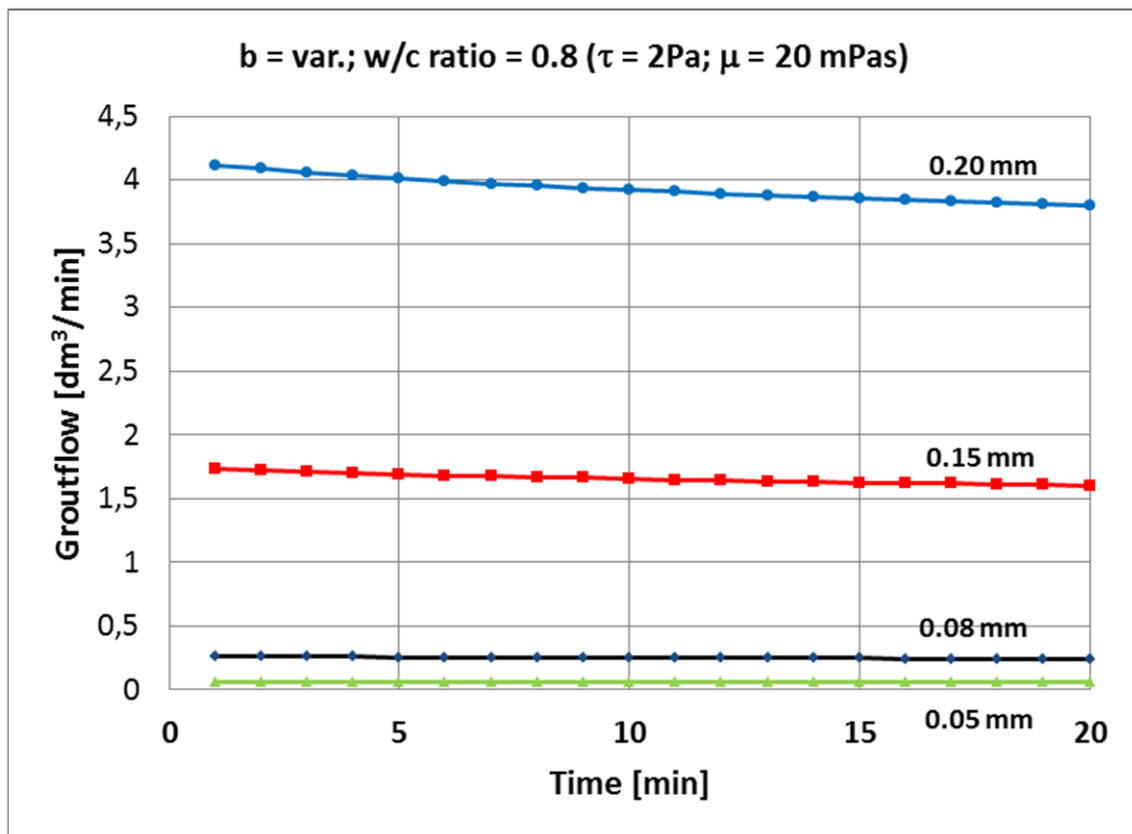
Figure 6-3. Calculated grout flow, according to Gustafson and Stille (2005). Each curve represent the grout flow for a specific fracture aperture. The grout pressure is 20 bars.

Considering the number of fractures that each grout hole crosses is seems likely that for most holes the fracture aperture is quite small. However, it should also be noted that the grout flow meter has quite poor accuracy. The total grouted volume is commonly seen as a more accurate value.

The theory and the cases in this thesis lead to the following line of reasoning:

- The larger fractures may for the Namntall North, the City Link Bangård Tunnel and the City Link Station Odenplan be considered sealed.

- Fractures with small apertures have theoretically small grout take.

- Grout holes with small grout take have short grout time due to the grout flow stop criteria.

- Grout holes with short grouting time (and consequently small apertures) have theoretically short penetration lengths.

- About 50 - 70% of the grout holes have little grout take.

- The general spacing of the fractures show that there generally may about 1 to 5 fractures/m intersecting the grout hole. Each fracture contribute to the total grout take.

- By combining the case histories, the grout flow stop criteria, the number of fractures and the theoretical grout flow calculation it seem likely that for the majority of the grout holes the largest fracture taking grout is smaller than about 80μm.

After considering the execution of the grouting, it is reasonable to conclude that for these cases about 50 - 70% of the rock mass can be considered more or less ungrouted which is important for the conceptual model of calculating water seepage. The remaining 30 - 50% of the holes shows a variety of grouting times and varying grouting pressures. Considering that the rock mass is made up of a number of different-sized fractures it follows that the transmissivity of a section of rock mass that has been grouted must be lower than a certain value indicated by the penetrability of the grout. It is also reasonable to assume that the grouting results (expressed as transmissivity of a section of the rock mass after grouting) cannot be equal for a 'poorer' rock mass with more fractures, as is the case for Namntall South compared to a 'good' rock mass as for Namntall North, Stille and Andersson (2007).

6.3 Transmissivity after grouting

Depending on the scale and flow mode, the arithmetic mean hydraulic conductivity may be representative for water seepage into a tunnel whereas the 3D mean hydraulic conductivity may be representative for the rock mass in general if a distribution is considered for representative block sizes. Each grout hole penetrates a relatively short and inhomogeneous part of the rock mass. The results after grouting should be considered for a length (scale) equal to the grout holes. This is in accordance with the general decision criteria during the execution of the works and the evaluation method in the design.

For a fracture model, the interval transmissivity, T_i, in each hole is a sum of the individual fracture transmissivities, T_f.

$$T_i = \sum_1^n T_f$$

If the grout penetrates and seals the fractures down to a certain fracture aperture, then the interval transmissivity of the grouted section of rock mass, T_{igr}, can be described as

$$T_{igr} = \sum_{1}^{n} T_f - \sum_{x}^{n} T_{grouted\ fracture}$$

Where n is the number of fractures in the interval and x represent the number of the smallest grouted fracture (in order) for the interval and $T_{groutedfracture}$ represent the transmissivity of the grouted fracture. This method for estimating the residual transmissivity after grouting is similar to the one described by Gustafson et al. (2004) for the fractures in the rock mass. As described, it is the borehole interval transmissivities that are measured and described statistically not individual fractures. It follows that a reduction in transmissivity for each interval is a more approachable variable as a function of the grouting results compared to an analyses based on each fracture transmissivity, even though the rationale for such a reduction can be described according to the equations above. Such a reduction in interval transmissivity after grouting is illustrated for the lognormal distribution in *Figure 6-4*. In this case, a lower grouting limit or cut off is stipulated as $8.2*10^{-7}$ m^2/s, corresponding to the transmissivity of a single fracture of 0.1 mm (which is an engineering estimate of the transmissivity sum of all ungrouted, seeping fractures in the interval) via the 'cubic law', Snow (1965).
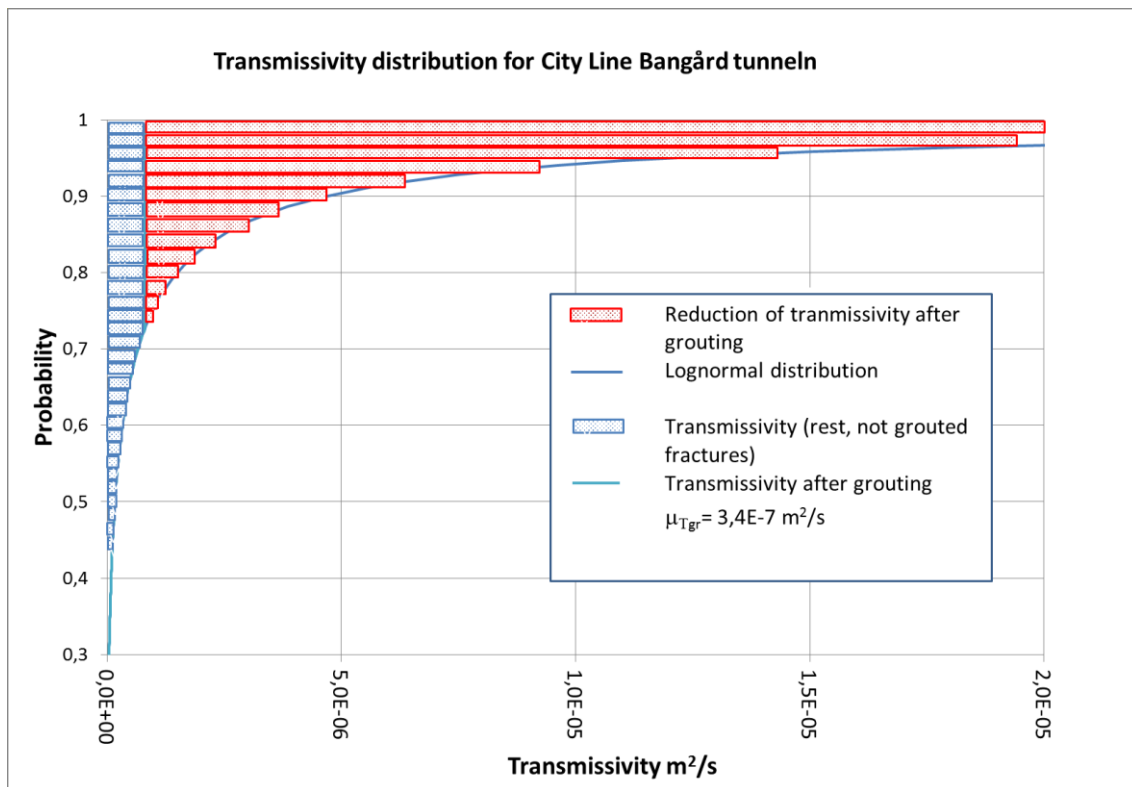
Figure 6-4. Interval transmissivity distribution and reduction in transmissivities after grouting. The mean transmissivity after grouting is denoted, μ_{Tgr}. The cut-off is $8.2*10^{-7}$ m^2/s.

The lower grout limit or boundary representing the transmissivity after grouting will depend on a number of factors, such as the number of fractures, the fracture transmissivity distribution, the grout penetrability and the grouting process. The grout results may not give such a low mean transmissivity after grouting if the rock mass is highly fractured and conductive. For an investigation into fracture/borehole transmissivity, see the Hernqvist et al (2014) study, which shows, especially for measurements over larger intervals, that there are several fractures that significantly contribute to the transmissivity of the measured interval. Factors such as for example connected holes, limits to the grout mix capacity, grout leaking face or unexpected low pressures (due to jacking or other technical reasons) will influence the results. For Namntall South the end results was often influenced by such factors. It is therefore considered that the limit (or cut-off) would be higher than for the other cases. An engineering estimate could be that this limit would be 3x to 8x the cut-off transmissivity of the relatively tight rock mass in the other cases corresponding to a single fracture aperture of 0.15 to 0.2 mm evaluated according to the 'cubic law', Snow (1965). The grout limit (cut-off) depends on the transmissivity sum of the remaining ungrouted fractures, which is probably higher than the grout penetrability property, b_{crit}.

6.4 Analysis of water seepage

The presented approach to analysing limits to transmissivity and seepage through the grouted tunnel is a conceptually different approach to the more standard way of estimating the effect of grouting in the general equation. We can see that the factor K_{grout}/K_{eff} originates from the assumption that water flows through a homogeneous grouted zone, K_{grout}, outside which the rock mass is represented by the original mean hydraulic conductivity, K_{eff} or K_0. For this assumption the seepage can be calculated with the common equation:

$$q_{inj} = \frac{2\pi K_{grout} \cdot H}{\left(1 - \frac{K_{grout}}{K_{eff}}\right) ln\left(\frac{D + 2t}{D}\right) + \frac{K_{grout}}{K_{eff}}\left[ln\left(\frac{4H}{D}\right) + \xi\right]}$$

By applying the assumption that a grouted fracture is sealed and that the remaining fractures in the interval constitute the remaining or residual transmissivity, as ungrouted fractures, a new mean hydraulic conductivity can be calculated, $K_{grout} = \mu_{Tgr}/L$. Observe that the mean transmissivity must be divided with the length, L, for which the interval transmissivity was evaluated. Conceptually, the water flows through the ungrouted smaller fractures. This also means that there is a normal water pressure gradient driving the water flow compared to the general idea that the water pressure acts over (across) the grouted zone. This is further strengthened by the conclusion from section 6.2 that a

majority of grout holes can be considered as more or less ungrouted. For this assumption the grouted fractures have been removed from the distribution affecting both the mean transmissivity and the variation. In effect the resulting hydraulic conductivity of the rock mass, K_{eff} or K_0, becomes K_{grout}. The assumption that the fractures are ungrouted also implies that the expression can be simplified according to the equation for an ungrouted rock mass albeit with a different hydraulic conductivity:

$$q_{inj} = \frac{2\pi\mu_{Tgr}/L \cdot H}{\ln\left(\frac{2H}{r_t}\right) + \xi}$$

For both equations the H represent a constant groundwater pressure height which is a boundary condition for the solution see for example Gustafson and Alberts (1983).

6.5 Calculation of water seepage/Case comparison

The seepage has been calculated for the cases presented above. For Namntall North, the Bangård Tunnel and the Odenplan Station in predominantly good rock, it was assumed that the level of achieved tightness after grouting can be represented by an interval transmissivity equal to the transmissivity of a hydraulic fracture width of 0.1 mm. This assumes that the actual grout penetrability is better than 0.1 mm and that the sum of the remaining fractures is not higher than the corresponding transmissivity value. The ground conditions for the Namntall South Tunnel with regard, for example, to zone and fracture density, were described by Stille and Gustafson (2010). It was shown that these conditions differed significantly from the northern part of the Namntall North Tunnel. Furthermore, it was shown that the grouting work encountered significant difficulties due to the adverse ground conditions but also due to the capacity of the grout mixer. It is reasonable to expect that the resulting transmissivity after grouting would differ from the grout result in rock types similar to the Namntall North and City Line tunnels. For this case the cut-off transmissivity was set to 2.8E-6 m^2/s. The rock mass with a transmissivity beneath these levels will be unaffected by grouting. The transmissivity after grouting, the 'residual transmissivity', indicates the effectiveness of grouting. In

Table 6-1 the calculated residual transmissivity, K_{grout}, is presented together with the distance to the phreatic surface, H, K_0, and the calculated seepage using the normal and suggested modified method using the arithmetic mean. The seepage is calculated for the tunnel radius, $r_t = 5$ m, the thickness of the grouted zone, $t = 5$ m, and the assumed 'skin' factor, $\xi = 5$.

Table 6-1 Seepage calculations compared to measured data.

Case	H [m]	K_0 [m/s]	K_{grout} [m/s]	Calculated seepage standard eq. [l/min.100m]	Calculated seepage modified eq. [l/min.100m]	Measured seepage [l/min.100m]
Namntall South	50	$1.6*10^{-7}$	$7.0*10^{-8}$	34.0	16.4	10-25*
Namntall North	135	$5.0*10^{-8}$	$1.5*10^{-8}$	24.3	8.5	5-7*
City Line, Bangård Tunnel	27	$1.4*10^{-7}$	$1.7*10^{-8}$	10.7	2.2	1-3**
City Line, Odenplan Station	20	$2.3*10^{-7}$	$2.4*10^{-8}$	13.0	2.5	2***

*Stille and Gustafson 2010 **Tsuji et al. 2012 ***City Line, Odenplan Station project 2013

The results of the seepage calculation (modified equation) seem to correspond better with the measured seepage for the Namntall North and South Tunnels, the City Line Bangård Tunnel and the Odenplan Station.

6.6 Summary

The seepage calculation could be performed using a concept of adapting the interval transmissivity distribution of the rock mass in relation to the grouting result. Conceptually, the grouting result is based on the idea that grouted fractures are sealed and removed from the distribution. Partly grouted fractures are not considered to be grouted and water may flow through these fractures. The grouted transmissivity distribution can be calculated and since this part of the rock mass is considered ungrouted, the grouted arithmetic mean value can be used for the rock mass in the same way as for an ungrouted tunnel. The calculations in section 5.5 show better conformity with measured seepage values using this method. In hard crystalline rock of generally good quality, the lower grouting limit seems to be equivalent to $8.2*10^{-7}$ m^2/s for a 20 m grout hole. It should be noted that this is a limit for the part of the holes that reveal higher transmissivity. The mean for the whole grouted distribution is lower when the whole population is considered. For poorer rock, the grouting result can be difficult to estimate and for these conditions it is appropriate to follow up the initial tunnelling operation with regard to water seepage into the tunnel (observational method).

7 DISCUSSION AND CONCLUSION

7.1 Mean values and their use

The mean value of the rock mass hydraulic conductivity is used for early hydrogeological predictions of water seepage but also, for example, to estimate the influence areas of groundwater drawdown, possible settlements due to changes in the pore pressure distribution in clay layers and so forth. Individual major fracture/weakness zones are often modelled using a higher mean hydraulic conductivity to study the influence of more systematic variations in the rock mass. However, the spatial variations within such an individual zone are not described using the data presented in this thesis even though water pressure tests performed for individual grout fans may represent the zone passing the tunnel alignment. If zones are modelled to identify the extent of the influence area and possible drawdown, great care should be taken when reducing the distribution data of the rock mass to identify new mean values for the rock mass in general. It should always be borne in mind that the rock mass is not its mean value. The mean value may be representative from one or more perspectives but there is considerable variation.

The mean values can be analysed and scaled according to the presented theory. The lognormal distribution fits the transmissivity data. It is important to take the accuracy of the measuring system into consideration when evaluating the data. When analysing the scale effects, an increase in scale reduces the variance and the geometric mean increases. For tunnels over 500 m in length, the difference between the geometric mean values and the arithmetic mean values seems to be relatively small. Considering the general trend in the statistical data, it seems reasonable that arithmetic mean values should be used for calculating seepage into most tunnels longer than 100-1,000 m. However, the requirement is that the data is from the same hydrogeological domain. The variation in data should be taken into account, especially for cases with a limited number of tests. By applying the statistical data, the variation can be used to describe a likely interval of mean hydraulic conductivity that can be used as an upper and lower boundary for calculating seepage.

Statistically, the probability that the rock mass effective hydraulic conductivity is smaller than the arithmetic mean value would be about 90% for a scale of 20 m (the approximate length of a grout hole) for a tunnel in the City Line Odenplan Station geological domain. The probability for an effective hydraulic conductivity value smaller than 2x the arithmetic mean value is also about 90% and seems independent of the scale. This is a function of low probability to encounter the larger values in the distribution.

As can be seen, the probability that the hydraulic conductivity is accurately predicted is relatively low, 50-90% depending on which mean values are used. The geometric mean or the median value represents the 50% probability that a stochastic value for the rock

mass is lower than the geometric mean. However, this is only true for the actual scale from which the geometric mean was taken. When looking at the 1,000 m scale from the City Line Odenplan Station data, the geometric mean for this scale will represent the 50% probability of having this value for any 1,000 m tunnel in similar geological conditions. It should be noted that this value is five times as large as the geometric mean for a 20 m section. The probability of having such a low value for a longer tunnel is evidently small.

It seems reasonable from a design perspective that the boundaries of the mean hydraulic conductivity values are the arithmetic mean (upper boundary) and the geometric mean of the tunnel (lower boundary). In other words, it is probable that the rock mass hydraulic conductivity is smaller than the arithmetic mean value and from a design point of view it does not seem suitable to use a value lower than the geometric mean. It should be noted that the scale in this case is the tunnel or geological domain length.

For the grouting results, the expected mean hydraulic conductivity after grouting should be the arithmetic mean although the expected grouting result should be related to the anticipated geological conditions. The experience from projects in similar geologies will be very valuable in this respect when evaluating probable grouting results.

The general conclusions with regard to rock mass transmissivity are:

- The lognormal distribution fits the transmissivity data.

- The accuracy of the measuring system must be considered when evaluating the transmissivity data

- An increase in scale reduces variation and increases the geometric mean of the transmissivity

- The presented theory for the lognormal distribution can be used to calculate different scales.

7.2 The observational method as a design approach

The rock engineering problems in this thesis are related to the water flow into a tunnel or under a dam. The variation and the heterogeneity of the rock mass and the hydrogeological properties have been clearly shown, as well as the measuring and model uncertainties that are connected to the design. It is therefore not surprising to recommend the observational method for the design. In general, the observational method consists of three steps: prediction, observation and adaptation. The method requires a stringent approach and certain rules should be followed if it is used as a design method. The principle of the observational method was presented by Peck (1969) and was further discussed by Holmberg and Stille (2007). Sometimes the observational method is confused with a 'design as you go' attitude, but the method requires a much more

structured and transparent way of working. It is necessary that the decision points are clear and that the observed behaviour is relevant for the interpretation/verification of the design prerequisites.

The basis for the method is to work with a design that's defining probable behaviour and likely limits, including prepared mitigations, thus avoiding an overly conservative design. By structuring the problem, the relevant steps can be highlighted and the results can be presented transparently, as is the case in steps 0-7 below. Equally important is to observe the resulting behaviour and verify the assumptions in the design during the construction phase. The water pressure tests before (and sometimes after) grouting and the water seepage for a length of tunnel after grouting are two such measureable parameters that should be followed very closely during the initial construction phase since any changes to the design or grouting have a greater impact at an early stage. Although observations should be carried out throughout the project, the frequency can usually be reduced over time.

The general design procedure, preconstruction, is described sequentially to reach the objective of predicting water seepage and required sealing effect (sufficient level of grouting). As is usual for engineering problems, some updates may be required after going through an initial estimate before finalising the approach.

0. Definition of the engineering problem

1. Tests for rock mass interval transmissivity, T_i, over the tested length, l_i.

2. Calculation of statistical parameters for the transmissivity distribution, mean value, μ, and standard deviation, σ.

3. Define the objective scale length, L, of the analysis "20 – ≈1000 m": the lower limit correspond to the length of the grout fan, whereas the upper limit of the scale length is the size of the geological domain or the tunnel length.

4. Rescale data from test length $T(l_i)$, to $T(L)$ and subsequently $K(l_i)$, to $K(L)$.

5.   A. Estimate of mean hydraulic conductivity; upper and lower boundaries.

   B. Estimate of hydraulic conductivity after grouting.

6.   A. Calculation of water seepage

   B. Calculation of water seepage after grouting

7. Decision of design approach taking into account the uncertainties in the tests, mean values and the grouting results, with regard to the objective scales (L), grout fan or tunnel (domain).

8. Follow up during construction, possible grout procedure adaptation with predefined measures or actions.

As can be seen, there are several choices that need to be made. These should be motivated and described in the design. In the spirit of the observational method, these choices should be shown to be representative of the geological domain and represent a probable outcome or property. An adjustment to the water pressure test results due to an increase in measuring/analysis error can be discussed, where the hypothesis is that the ΣT_i (3 m) is larger than the ΣT_i (20 m) and that the error is reduced with increased L. However, more research needs to be performed to verify this assumption.

7.3 The grouting process

The grouting process shows several interesting conditions that influence the idea of grouting result and performance. In hard crystalline rock the rock mass is often relatively tight and about 50 - 70% of the holes are grouted with a grout take (volume) of about the hole filling (grout hole volume). The stop criteria used for these holes is usually the 'grout flow criterion'. Theoretically, this indicates that about 50 - 70% of the rock mass around a tunnel is more or less considered to be ungrouted. On the other hand, since the porosity or the fracture void of the rock mass, again for hard crystalline rock, is very small the grout spread will for a relatively small amount of grout be quite large. For 100 l of grout in a physical aperture of 0.2 mm, the grouted area would be about 500 m^2. The relationship between the physical aperture and the hydraulic aperture is also a very interesting topic that requires further study. Considering the experience from the City Line for example, where the physical aperture was shown to be about twice the hydraulic aperture. Since the water seepage is related to the hydraulic aperture it seems reasonable that the grout result is related to the hydraulic aperture. It also seems reasonable that the penetrability of the grout and therefore the grouting result should be related to the physical aperture. For the individual fractures the hydraulic aperture would be smaller than the physical aperture. This indicates that the expected size of the smallest grouted fracture could be about half its corresponding hydraulic fracture aperture.

Andersson and Stille (2007) and Bruno (2009) showed that one of the more detrimental issues for the grouting result is the connected holes. It was clearly shown by Bruno that the sequential grouting procedure with long grouting times produced smaller and smaller grout takes. It was concluded that this was related to changes in grout properties where non-flowing grout 'settles' within 2 h. It is clear that grouting of holes should be

completed within about 15 minutes and that connected holes, if possible, should be grouted within 45 minutes for this type of grout. The connected holes aspect indicates that the smaller fractures (and possibly some larger ones) may not be considered to be grouted. This is especially true for a more fractured rock mass where there may be a need for a second grouting round.

Each grout hole crosses a number of fractures, some water-bearing and some not. The grout can only penetrate fractures of a certain size and there will always be fractures that remain more or less ungrouted. The fractures that are not grouted will be part of the 'residual' transmissivity after grouting. The sum of the residual transmissivity will be a function of the smallest grouted fracture.

Examples from the Namntall Tunnel and the Northern Link show that elastic jacking frequently occurs and that this may, in some cases, influence the final seepage or grouting result. It might be possible, by following the grouting minute by minute, to predict the course of the grout flow and also analyse the risk of uplift and jacking. This could be of particular interest for shallow surface grouting or grouting close to other subsurface areas where the possibility of detecting jacking or uplift of the rock mass could be of critical interest. The most significant action from the presented examples would have been the ability to abort grouting or lower the grouting pressure.

Another condition that influences the grouting performance is the grout mixing capacity, which was observed during the excavation of the Namntall Tunnel in 2004-2006. It was observed that in reality the grout mix capacity was about 20 l/min for each of the two pumps and that the design grouting pressures often could not be reached for this reason. Lower grouting pressures naturally result in shorter grout penetration lengths or longer grouting times, which is especially poor for conditions with many connected holes.

Grouting is to a large degree a special skill and experience is required to handle the rig decisions rationally. In the report 'Field tests with multi-hole grouting ' by Stille et al 2014 it was clearly shown that this was the case. Recurring issues, such as poor planning and poor communication, were often the case when inexperienced personnel handled the equipment compared to the relatively efficient grouting procedure with experienced personnel.

The case studies show that it is generally easier to achieve a better grouting result in good quality rock mass compared to poor rock. Furthermore, there are practical aspects with regard to the grouting process that need to be considered, such as equipment types and capacities, temperature, organisational competencies and contractual arrangements, which may influence the grouting result.

The general conclusions with regard to the grouting process are

- The grouted fracture aperture will be about twice the hydraulic aperture.

- For the presented cases in generally good quality crystalline hard rock, about 50 - 70% of the rock mass can be considered ungrouted from a water seepage calculation perspective.

- Connected holes influence the grouting performance, resulting in areas that are not grouted or only partly grouted. After the third or fourth connected hole that is sequentially grouted, the holes are almost lost (small grout take, short grouting time and a resulting short fracture penetration).

- Mixing capacities may limit the grouting performance, especially in areas with higher seepage and with many connected holes.

- Elastic (and ultimate) jacking should be avoided.

- Two (or more) grout fans may be required to seal more seeping areas.

- For most grouting fans, one person at the face can only handle two hoses effectively. For more seeping areas, up to four hoses can be handled with grouting times of around 15-20 minutes per hole.

- An efficient grouting procedure requires experienced personnel and may limit the problems related to connected holes and grouting capacity problems.

7.4 Future research

This thesis sheds some light on the grouting process and the difficulties encountered both theoretically and practically. It shows that there is a need for an observation of the process if we are to successfully reduce the seepage to an acceptable level. Many of the specific issues related to the grouting operation should also be studied further to verify the findings and also to document good treatment practices. There is also a need to study more large sets of data with the objective to find prognosis tools and methods to describe the rock mass out of a geohydrological perspective. Some ideas for future research are summarised here:

- Development of geohydrological prognosis methods including statistical description of rock mass geohydrological domains and statistically described definitions of domain boundaries.
- Further development of the statistical analysis for the lognormal distribution of transmissivity with regards to independency and special consideration for transmissivity of zones and flow regime/relevant mean value.
- Development of statistical/mathematical method to evaluate lognormal distribution for truncated data sets.

- Pressure distribution during grouting, influence of grout penetration with regards to different boundary conditions. Influence on analysis methodology with regards to pressure loss in outer (grout equipment) and inner (rock mass) system.
- Further development of the analysis of water seepage considering various boundary conditions.
- Development of stop criteria through analysis of large data sets with regards to grout take and geohydrological conditions e.g. water pressure tests, also considering changes to stop criteria.
- Description and analysis of specific field conditions such as connection (links) between holes, leakage to the face, face stability and jacking.
- Statistical analysis and geological description of the same field conditions.
- Best practice in difficult grouting conditions.
- Post grouting practice and diagnostic analysis.
- Development of a model for analysing aging of grout under field conditions including grout in agitator and grout in a fracture.

REFERENCES

Alberts C. Gustafson G., 1983: *Undermarksbyggande i svagt berg: 4 Vattenproblem och tätningsåtgärder.* BeFo 106. Stiftelsen Bergteknisk Forskning.

Axelsson M. Eriksson M. Wilén P., 2007: *Dimensionering av typinjektering – koncept 1.* design document 9563-13-025-001 for Citybanan in Swedish.

Barton N., 2002. *Some new Q-value correlation to assist in site characterisation and tunnel design.* International Journal of Rock mechanics & Mining Sciences, Vol. 39, pp 185-216.

Bieniawski Z.T., 1989: *Engineering rock mass classifications.* Wiley, New York.

Bohlin M. Urtel K., 2008: *Utvärdering av injekteringsutförande – Fallstudie av NL101 och Hornsberg.* Stockholm, Master Thesis, Division of Soil and Rock Mechanics, Royal Institute of Technology.

Botniabanan AB, 2003. Adapted from the tender documents rev.E, project E3541 Offersjön-Bjällstaån.

Brantberger M. Stille H. Eriksson M., 2000: *Controlling the grout spread in tunnel grouting – Analyses and developments of the GIN-method.* Tunneling and Underground Space Technology, Vol 15, No. 4, pp 343-352.

Brantberger M., 2000: *Metodik vid förinjektering i uppsprucket hårt berg.* Licentiate Thesis, Division of Soil and Rock Mechanics, Royal Institute of Technology Stockholm.

Bruno A., 2009: *Grouting operation monitoring and analysis of the "Real-Time Grouting Control" method.* Master Thesis at KTH and Politechnico di Torino.

Caine J.S. Evans J.P. Forster C.B., 1996: *Fault zone architecture and permeability structure.* Geology, No. 11, pp 1025-1028.

De Marsily G., 1986: *Quantitative Hydrogeology: Ground Water Hydrology for Engineers.* Academic Press. Inc. San Diego, USA.

Dalmalm T., 2004: *Choice of grouting method for jointed hard rock based on sealing time predictions.* Ph.D. thesis, Royal Institute of Technology, Stockholm.

Draganovic A., 2009: *Bleeding and Filtration of Cement-Based Grout.* Trita-JOB PHD ISSN: 1650-9501; 1015, PhD Thesis, Division of Soil and Rock Mechanics, Royal Institute of Technology.

Eriksson M. Stille H. Andersson J., 2000: *Numerical calculations for prediction of grout spread with account for filtration and varying aperture.* Tunnelling and Underground Space Technology, Vol 15, No. 4, pp 353-364.

Eriksson M. Stille H., 2005: *Cementinjektering i hårt berg (Grouting with cement based grout in hard jointed rock).* SveBeFo, Stockholm, Sweden.

Fransson Å., 2001: *Characterisation of fractured rock for grouting using hydrogeological methods.* PhD thesis, Chalmers University of Technology, Department of Geology, Gothenburg.

Funehag J. Gustafson G., 2004: *Injekteringsförsök med Cembinder U22 i Hallandsås.* Publication 2004:1, Division of GeoEngineering, Chalmers University of Technology, Gothenburg.

Funehag J., 2007: *Grouting of fractured rock with silica sol — Grouting design based on penetration length.* Ph.D. thesis, Chalmers University of Technology, Division of GeoEngineering. Gothenburg.

Gothäll R. Stille H., 2009. *Fracture dilation during grouting.* Tunnelling and Underground Space Technology, Vol. 24, pp 126-135.

Gustafson G. Stille H., 1996. *Prediction of groutability from grout properties and hydro geological data.* Tunnelling and Underground Space Technology 11(3), pp 325-332.

Gustafson G. Franson Å. Funehag J. Axelsson M., 2004: *Ett nytt angreppssätt for berg-beskrivning och analysprocess för injektering.* (in Swedish). Väg- och Vattenbyggaren 4, 2004.

Gustafson G. Claesson J. Fransson Å., 2013: *Steering Parameters for Rock Grouting.* Journal of Applied Mathematics, vol. 2013 pp. article ID 269594.

Gustafson G. Stille H., 2005: *Stop criteria for cement grouting.* Felsbau 23(3), pp 62-68.

Gustafson G., 2009: *Hydrogeologi för bergbyggare.* in Swedish, Formas, ISBN 978-91-540-6029-0.

Hakami E., 1995: *Aperture distribution of rock fractures.* Doctoral Thesis, Division of Engineering Geology Department of Civil and Environmental Engineering, Royal Institute of Technology.

Hernqvist L. Fransson Å. Gustafson G. Emmelin A. Eriksson M. Stille H., 2008. *Analyses of the grouting results for a section of the APSE tunnel at Äspö Hard Rock Laboratory.* Journal of Rock Mechanics and Mining Sciences.

Hernqvist L., 2011: *Tunnel Grouting: Engineering Methods for Characterization of Fracture Systems in Hard Rock and Implications for Tunnel Inflow.* Institutionen för bygg- och miljöteknik, Chalmers University of Technology, Göteborg.

Hernqvist L. Einarsson V. Höglund A., 2014: *Does one fracture dominate the borehole transmissivity?* Conference paper, Swedish Rock Engineering Research foundation, BeFo.

Holmberg M. Stille H., 2007: *Observationsmetodens grunder och dess tillämpning på design av konstruktioner i berg.* (in Swedish). SveBeFo Report 80.

Holmén J., 1997: *On the flow of groundwater in closed tunnels – generic hydrogeological modelling of nuclear waste repository, SFL 3-5.* Doctoral thesis, Uppsala University.

Houlsby A.C., 1990: *Construction and design of cement grouting.* ISBN 0-471-51629-5, John Wiley & Sons, Inc., USA.

Håkansson U., 1993: *Rheology of fresh cement-based grout.* Ph.D. thesis, Royal Institute of Technology (KTH), Division of Soil and Rock Mechanics, Stockholm.

Hässler L. Stille H. Håkansson U., 1988: *Simulation of grouting in jointed rock.* Proc. 6th International Congress on Rock Mechanics, Vol. 2, pp 943-946, Montreal.

Hässler L., 1991: *Grouting of rock –Simulation and classification.* PhD Thesis, Division of Soil and Rock Mechanics, Royal Institute of Technology, Stockholm.

Hässler L., 2007: Personal communication, Golder Associates AB.

Kobayashi S. Stille H., 2007. *Design for rock grouting based on analysis of grout penetration. Verification using Äspö HRL data and parameter analysis.* R-07-13, Swedish Nuclear Fuel and Waste Management Company, Stockholm.

Kobayashi S. Stille H. Gustafson G. Stille B., 2008: *Real- Time grouting Control Method, Development and application using Äspö HRL data.* R-08-133, Swedish Nuclear Fuel and Waste Management Company, Stockholm.

Lombardi G. Deere D., 1993: *Grouting design and control using the GIN principle.* Water Power and Dam Construction, June 1993, pp 15-22.

Lindström L., 2007: Site geologist, Personal communication. Vattenfall Power Consultants AB.

Lundqvist T. Gee D. Kumpalainen R. Karis L. Kresten P., 1990: *Beskrivning till berggrundskartan över Västernorrlands län.* pp 18 – 44, pp. 322 – 327.

Morfeldt C-O., 1979: *Är injektering i berg en svartkonst?* Bergmekanikdagen 1979, BeFo, Stockholm.

Moye D.G., 1967: *Diamond Drilling for Foundation Exploration.* Civil Engineering Transactions, April, pp 95-100.

Munier R. Stenberg L. Stanfors R. Milnes A.G. Hermanson J. Triumf C-A., 2003: *Geological Site Descriptive Model. A strategy for the model development during site investigations.* R-03-07. Swedish Nuclear Fuel and Waste Management Company, Stockholm.

Olsson R., 1998: *Mechanical and Hydromechanical Behaviour of Hard Rock joints, A laboratory study.* Ph. D. Thesis, Chalmers University of Technology. Göteborg.

Peck R.B., 1969: *Advantages and limitations of the observational method in applied soil mechanics: 9th Rankine lecture.* Géotechnique, 19 (2), pp. 171-187.

Rafi J.Y., 2014: *Study of Pumping Pressure and Stop Criteria in Grouting of Rock Fractures.* TRITA-JOB PHD ISSN: 1650-9501; 1020, PhD Thesis, KTH Royal Institute of Technology.

Rhén I. Bäckblom G. Gustafson G. Stanfors R. Wikberg P., 1997: *Äspö HRL - Geoscientific evaluation 1997/2. Results from pre-investigations and detailed site characterization. Summary report.* SKB TR-97-03, Svensk Kärnbränslehantering AB.

Snow U. T., 1965: *A Parallel Plate Model of Fractured Permeable Media.* Ph.D. thesis, University of California, Berkeley.

Stille B, Anderson F., 2008: *Injektering – tillämpning av injekteringsforskning i fält. Pre-grouting – application of grouting research in the field.* SveBeFo rapport 79, Stockholm.

Stille B. Batres R. Forslund C., 2014: *Fältförsök med multihålsinjektering, Field tests with multi-hole grouting*, in Swedish. BeFo rapport 140, Stockholm.

Stille H., 2015. *Rock Grouting – Theories and Applications.* BeFo, Stockholm.

Tsuji M. Holmberg M. Stille B. Rafi J Y. Stille H., 2012: *Optimization of the grouting procedure with RTGC method. Data from a trial grouting at city line project in Stockholm.* SKB R-12-16, Svensk Kärnbränslehantering AB.

Thörn J., 2015: *The Impact of Fracture Geometry on the Hydromechanical Behaviour of Crystalline Rock.* Ph. D. Thesis, Chalmers University of Technology. Göteborg.

Zetterlund M., 2014: *Value of Information Analysis in Rock Engineering Investigations*. Institutionen för bygg- och miljöteknik, Chalmers University of Technology, Göteborg ISBN: 978-91-7597-023-3.

Publication I

Stille B., Gustafson G. (2010). A review of the Namntall Tunnel project with regard to grouting performance. Tunnelling and Underground Space Technology. Vol. 25, pp. 346-356.

Publication II

Stille B., Stille H., Gustafson G., Kobayashi S. (2009). Experience with the real-time grouting control method. Geomechanics and Tunnelling. Vol 2, pp. 447-459.

Publication III

Stille B., Stille H. (to be submitted 2016). Distribution of rock mass hydraulic conductivity and its application to rock engineering problems.

A review of the Namntall Tunnel project with regard to grouting performance

Björn Stille *, Gunnar Gustafson

Division of GeoEngineering, Chalmers University of Technology, SE-412 96 Göteborg, Sweden

ABSTRACT

The 6 km tunnel under the Namntall hill is a part of the Botniabanan railway project in northern Sweden. The tunnels were excavated by means of drilling and blasting and with, for Scandinavian conditions, a normal grouting routine. The grouting is performed to reduce water ingress into the tunnel to the level defined in the contract. When the water ingress requirements proved difficult to meet, it was obvious that the geological and the hydrogeological conditions in the tunnel would dictate the work processes. A distinctive change in rock conditions influenced both grouting performance and seepage into the tunnel. The rock conditions and the grouting were quantified throughout the project and these are summarized in this paper. It can be concluded that the strongest correlation is between the water ingress, the hydrogeological conditions and the density of the zones and the conditions in and around these zones. The paper suggests a different approach to hydrogeological prognosis and the grouting process, such as distribution of grouting classes, increased mixer capacities and regular use of two grouting rounds.

© 2010 Elsevier Ltd. All rights reserved.

1. Introduction

1.1. Background

The 6 km Namntall Tunnel is a part of the Botniabanan project linking Örnsköldsvik and Kramfors. The tunnel was constructed as part of a Design-build contract consisting of a single-track rail tunnel (65 m^2) and a parallel service tunnel (35 m^2). The client, Botniabanan AB (BBAB), is a partnership (90/10) between Banverket (Swedish Rail Administration) and the municipal authorities in the area. The contract was awarded to Skanska Sverige AB as the main contractor for the civil engineering work. The total scope of the Design-build contract included the 6 km Namntall Tunnel, several over ground parts and a 5 km second tunnel. The tunnels were excavated using the drill and blast method between 2004 and 2007.

For the most part the Namntall Tunnel, with a rock cover of between 20 and 150 m, was excavated in a greywacke and through a major intrusion of granite, Fig. 1. The tunnels were excavated by means of drilling and blasting and with, for Scandinavian conditions, a normal grouting routine, including probe drilling, water pressure tests (Moye, 1967) performed by pressurizing the whole probe/grout hole and measuring the outflow of water for a period of time, evaluation of the water pressure test class (grouting class), drilling of grout holes, cement grouting, drilling of control holes (water pressure tests) and supplementary drilling/grouting. A schematic illustration of the grout fan layout is shown in Fig. 2. The grouting is performed to reduce the water ingress into the tunnel as defined in the contract (temporarily 20 l/min 100 m and in the permanent situation 12 l/min 100 m). Originally, the permissible ingress was stipulated in an environmental court ruling based on, amongst other things, a hydrogeological prognosis (taken from the tender documents, based on the exploratory drillings, Botniabanan AB 2003).

1.2. Hypothesis

This case study of the Namntall Tunnel focuses on the correlation between certain geological and hydrogeological data and grout performance (grout take). More specifically, the density of fractures, "zones", joint filling, water pressure test measurements and grout take are examined. The analyses are performed using large-scale statistical data that make links and comparisons more reliable, limiting the influence of variations in individual data.

For this case study the following hypotheses are formulated:

- Geological factors, such as rock type, density of zones, fracture frequency or block size and *in situ* stress, could explain the large-scale distribution of water pressure test results in the rock mass.
- The greatest water pressure test value in a grout fan can be used to classify the rock mass and a statistical link to grout take can be established.
- The degree of difficulty of the grouting can be defined by means of geological factors such as fracture filling, density and zone characteristics.

* Corresponding author. Tel.: +46 70 6330851; fax: +46 31 7722107.
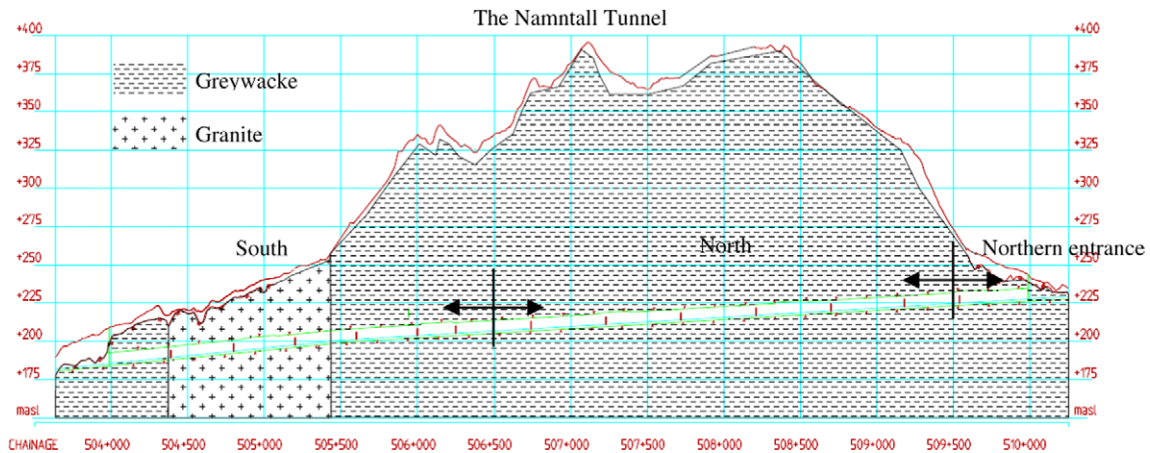*E-mail address:* bjorn.stille@vattenfall.com (B. Stille).

Fig. 1. Longitudinal section of the Namntall Tunnel illustrating the rock cover above the tunnel and the main rock types (Adapted from Botniabanan AB, 2003).
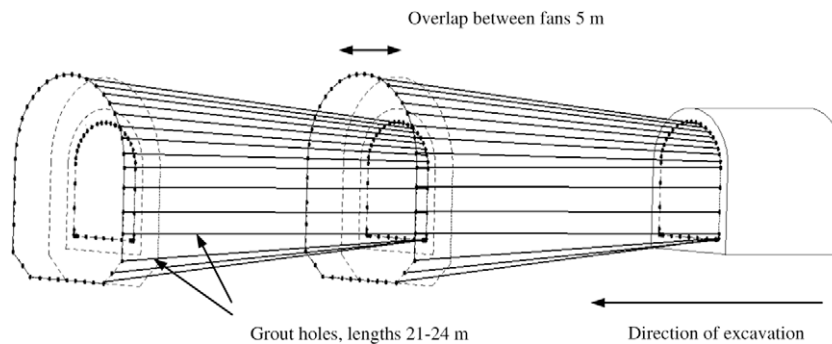

Fig. 2. Schematic illustration of two grout fans. Grouting class A had 10 holes whereas the B and C classes had 20 holes arranged around the tunnel periphery. (Adapted from Butrón 2009).

1.3. Outline of the paper

Paragraph 2 focuses on the geological and hydrogeological conditions in the Namtall Tunnel. It includes the local geological history and a definition of the investigated parameters. The quantification of the data is presented in figures (diagrams) showing the overall tunnel conditions. The investigated data include: "zones", fracture density (block size), joint filling and water pressure test measurements.

Paragraph 3 studies the total grout take along the tunnel, the distribution of grout take for different water pressure test classes and the total grout take related to the largest measured water pressure test. The data are presented as diagrams showing the conditions along the tunnel and statistically in the form of a histogram and a scatter plot.

Paragraph 4 concludes the paper and shows the resulting inleakage along the tunnel after grouting.

2. Geological and hydrogeological conditions

2.1. The geological history of the rock mass in the county of Ångermanland (local orogenesis)

The geological history of the area can be said to have "started" some 1820–1850 million years ago during the Sweco-Karelian mountain chain folding process. The greywacke bedrock was created during this process of intense tectonic events. Originally deposits of sedimentary material comprising of sand and clay, the term greywacke is defined through a relatively large clay content (more than 15% in the matrix). In the Namntall area several metamorphic stages in the greywacke have been observed, ranging from almost intact to a metamorphosed metagraywacke that is gneissic and even migmatized resulting in, among other things, segregation of the mineral components into bands or stripes.

A characteristic of the greywacke is the existence of skarn lenses (metamorphic carbonate congregations) and in some areas it is also rich in graphite and sulphides (Lundqvist et al., 1990).

The bedrock has been intensely folded, which is demonstrated by the steeply dipping foliation. The orientation/strike of the foliation is roughly NE-SW, indicating the probable direction of the local tectonic thrust NW-SE (perpendicular to the foliation) during this early phase of the orogenesis, Fig. 3.

Since the mountain folding process and the regional metamorphosis the rock mass has been subjected to a number of faults, resulting in the local topography. The literature states that "valleys, the course of mires, steps in the terrain and straight lakeshores correlate to steep failure lines in the bedrock" (Lundqvist et al. 1990). Furthermore, the erosion created by the moving direction (NNW–SSE) of the quaternary glacial ice has emphasized the weaker areas in the rock, especially where these coincide. It has also been observed that the deep failure lines also coincide with intrusive rocks such as granites, pegmatites and metabasites (which are considered to be the latest additions to the rock mass, originating some 1200 million years ago). It has been observed that during the intrusions of metabasite dikes the rock mass was subject to a considerable increase in fracturing, including the creation of horizontal crushed zones.

The large intrusion of granite between cross-sections 504 + 370 and 505 + 450 as well as numerous dikes, also supports the theory
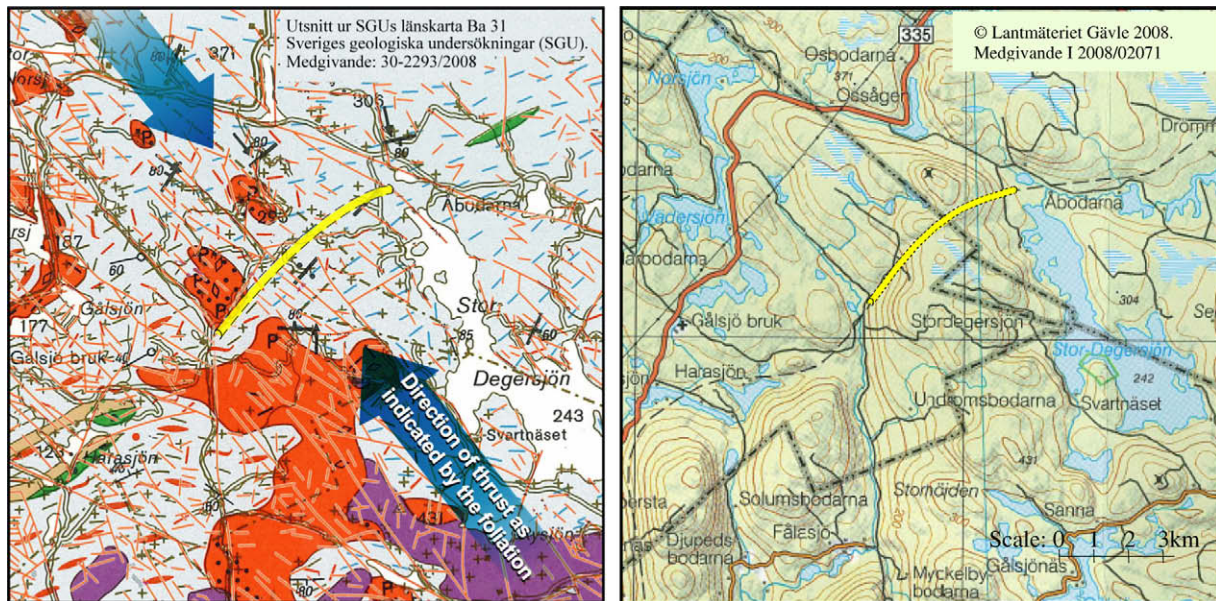
Fig. 3. The topographical, geological and structural geological map of the Namntall area. The tunnel is printed in yellow, the foliation is indicated by the small blue lines and the lineaments are shown in brown. The bedrock consists of greywacke (grey) with intrusions of granite and pegmatites in red. The topographical map shows terrain features and the Botniabanan railway line, including the tunnel.

that the area was subject to significant deep failure lines prior to the intrusion.

2.2. Definition of "zones" and description of the nature of joints in the area

Several models exist to define "zones", focusing primarily on fault zones. Caine et al. (1996) present a conceptual model to classify the conductivity structures in fault zones, Fig. 4. A similar approach to defining the architecture of deformation zones is adopted by Munier et al. (2003). Both approaches define the zone as a core area (fault core) with a transition zone (damage zone) to the undisturbed host rock (protolith). The brackets indicate the nomenclature used by Caine et al. (1996).

"Zones" in this paper, have been chosen as a designation to describe all areas that diverge from the surrounding host rock and which could be expected to have an impact on the water discharge. "Zones" include fracture zones (zones with a higher density of joints e.g. 5–10 joints/m of a specific joint set), rock type contacts where the contact zone/area is more fractured, dikes that are either highly fractured or have a weathered or loosened contact area (a fractured weathered dike is included whereas good pegmatites are not included) and shear zones.

The definition of the conductivity structures in the zones could be based on the Caine et al. (1996) model as: "Localized conduit (e.g. localized shear zones, absent to small damage zones), distributed conduit (e.g. slip or shear along distributed fractures, associated fracture network), localized barrier (e.g. localized slip within a cataclastic zone), combined conduit-barrier". In the Namntall Tunnel most zones are considered to fit into any of these categories although unevenly distributed along the tunnel.

Most of the zones have an estimated length of over 200 m. The lengths of most joints is about 10–20 m. However, the length varies considerably and, for example, the foliation joints are in some areas very long, possibly over 100 m according to Lindström (2008).

The mapping performed by Stuge and Lindström (2007) shows that the joint systems in the area generally have two to three joint sets, often with one random joint set as defined in the Q-classification system (Barton, 2002). The spacing of the joints is generally between 0.2 and 0.6 m, indicating fairly close spacing. The joints form blocks varying in size along the tunnel. Generally, the ratio is 1:2 between the smallest and the largest of the joint set spacings, indicating a rectangular block shape.

The filling in the joints varies along the tunnel although the joints are often coated with a thin, soft filling of clay, calcite or chlorite. In the areas with lower rock cover the filling is generally thicker. In the area close to the southern tunnel entrance some of the joints have a filling of swelling clays. For other parts of the tunnel a partial clay coating has been noted, indicating difficult grouting conditions (Hässler, 2007).

2.3. Quantification of the geological conditions

Geological mapping was performed after each blast of generally 4–5 m in the tunnels, Fig. 5. The parameters in the Q-system (Barton, 2002) were mapped as well as joint sets (including orientation and joint spacing)/fracture zones/rock type/joint filling etc. The volumetric joint count (Palmström, 1995) was also mapped giving an estimate of the average joint density.

2.3.1. Zones

The density/extent of zones is seen as an indication of where increased discharge could be expected. By adding the number of zones along the tunnel length (starting from the south) a cumulative distribution can be presented, Fig. 6. The incline of the dotted line is indicative of the density of zones, a steep curve would therefore indicate a number of zones that lie close to each other. Fig. 6 show that the rock mass in the southern part of the tunnels has a high density of zones (up to approx. chainage 506 + 500). The distribution of zones in the northern part of the tunnel (excluding the entrance area) shows a concentration of zones in certain areas but set some distance apart. The average concentration of zones for the southern part is one zone every 23 m (2500 m), for the northern part one zone every 62 m (3000 m) and for the northern entrance part (500 m) one zone every 20 m.
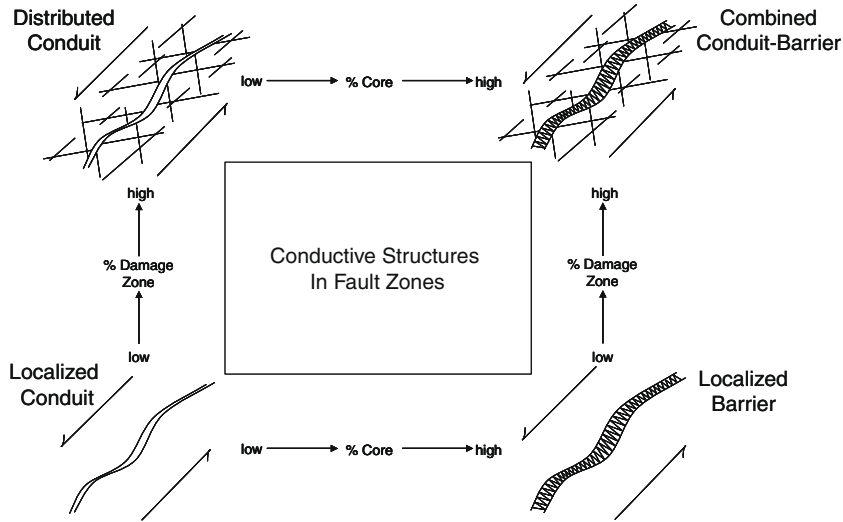
Fig. 4. Conceptual scheme for conductivity structures in "zones" modified according to Caine et al. 1996.
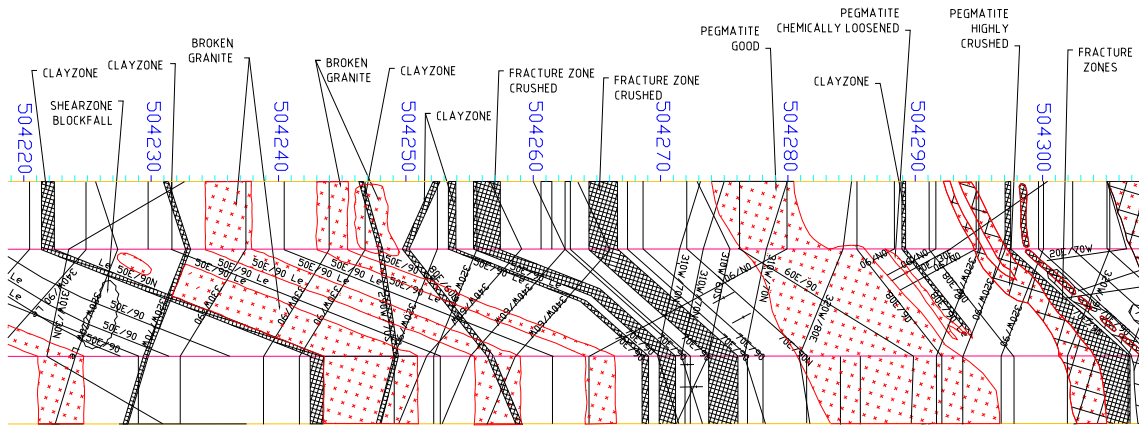

Fig. 5. Example of the illustrated mapping from the southern part of the Namntall Tunnel showing the typical large number of zones and dikes in this area. (Stuge and Lindström, 2007).
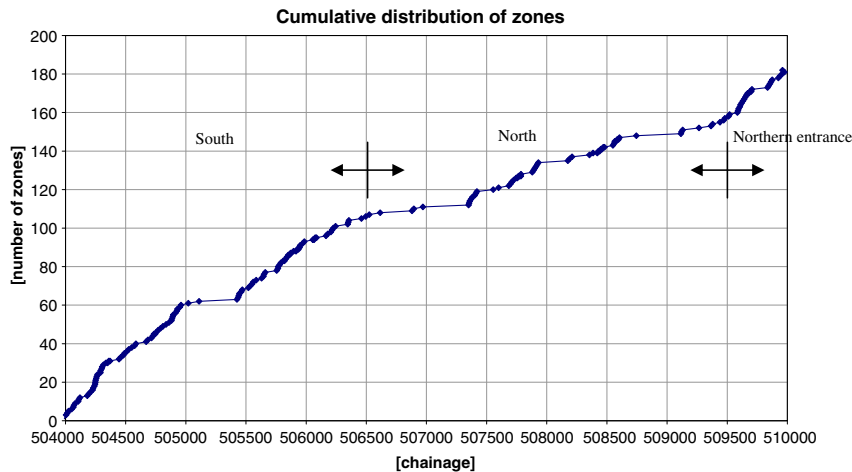

Fig. 6. The cumulative distributions of zones over the tunnel length.

2.3.2. Block size

"The joints intersecting a rock mass divide the rock into blocks with sizes ranging from sugar cube of cm^3 in fragmented or crushed rock to several m^3 in massive rock. The sizes are a result of the joint spacings, the number of joint sets, and the size and persistence of the joints" (Palmström, 2005). Goodman (1993) states that "Joints are extremely important in some rock masses. Even though the rock substance itself may be strong or impermeable, or

both, the system of joints may creates significant weakness and fluid conductivity." The block size is a parameter that has a considerable impact on the properties of the rock, both in relation to the required rock support but also to the hydrogeological conditions (other parameters may also have an impact, e.g. condition and joint geometry). In this case study, the joint density is used to (partly) explain the difference in hydrogeological conditions along the tunnel length.

The use of the volumetric joint count, a parameter in the RMi system, as a rock engineering tool has been presented by Palmström (1995). The volumetric joint count, J_v, is defined as the number of joints that intersect a rock mass volume of 1 m³ and is mapped by the geologists on site. From this value the block volume, V_b, can be estimated, Palmström (2005). From the block size an equivalent joint spacing can be calculated as a normative measure of the actual mapped joint spacing.

In order to show statistically the different joint densities along the tunnel the J_v value and the equivalent joint spacing were set at intervals (range of values), Table 1. These are roughly defined using the rock mass rating system (spacing of discontinuities), Bieniawski, 1989. For the different intervals each tunnel metre of a specific interval was added along the tunnel length (starting from the south). At any point along the tunnel the sum of each curve is equal to the tunnel length at that point (starting from the south) e.g. at chainage 506 + 000 the tunnel length is 2,015 m and the cumulative length of each curve is: $s < 0.2$ m and 321 m; $0.2 < s < 0.6$ 1389 m; $0.6 < s < 2$ 305 m $s > 2$ m 0 m, the sum is 321 + 1389 + 305 + 0 = 2015 m, which is equal to the tunnel length at that point. In much the same manner as for the number of zones, the inclination of the curves is indicative of the concentration of a specific block size in the area. The cumulative frequency of different joint spacings is presented in Fig. 7, where the frequency distribution is shown along the tunnel length.

As can be seen, Fig. 7, there is a difference between the northern and southern parts of the tunnel. It should also be stated that the zones are not represented in the volumetric joint count. However, the density of the jointing is not statistically independent of the density of the zones, more a natural explanation of why the rock mass is more densely jointed.

The median value for the southern part is 8 joints/m³, up to chainage 506 + 500. For the northern part it is 5 joints/m³ and for the northern entrance 10 joints/m³.
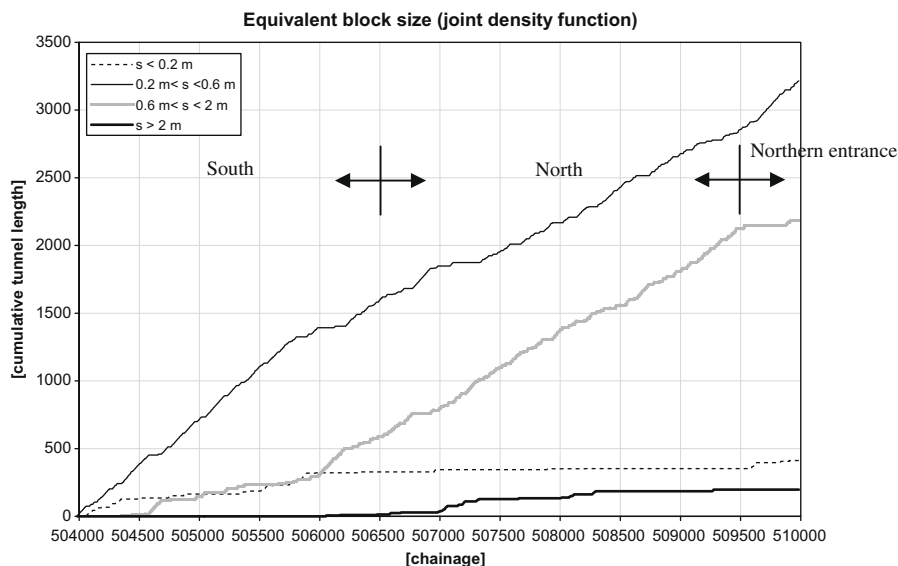
2.3.3. Joint filling

Joint filling may have an impact on the hydrogeological conditions and the grouting performance. Clay or other soft fillings may limit the water pressure test measurement and the thicker the filling the higher the probability that a conductive "barrier" structure, Fig. 4, has been encountered. For otherwise similar conditions the joint filling could be an important measure/indicator for the definition of the hydrogeological conditions. This is also true for the grouting conditions. Joint filling could limit the water pressure test result and the grout take although a soft filling could potentially move in the fractures under the higher pressure during grouting (compared to the water pressure test) and open or close flow paths. Another potentially difficult condition could be a partial clay filling, which indicates that the flow paths within a joint could be very complicated.

The joint filling was mapped along the tunnel length for each joint set. The registered value was related to the need for rock support, which means that for each mapped area the different joint systems could potentially have different joint fillings and the filling for the joint system (s) considered to be most important for tunnel

Table 1
Volumetric joint count and equivalent joint spacing used in the distribution.

J_v interval	Equivalent joint spacing, s (m)
$J_v > 16$	$s < 0.2$
$16 \geqslant J_v > 5$	$0.2 \geqslant s > 0.6$
$5 \geqslant J_v > 2$	$0.6 \geqslant s > 2$
$2 \geqslant J_v$	$2 \geqslant s$

Table 2
Joint filling mapped as Ja and divided into groups.

J_a	Wall contact	Description
1–2	Contact between joint walls	Clean joints
3–4	Contact between joint walls	Coating or thin filling of clay, chlorite, calcite, silt etc.
5–6	Some or no wall contact	Hard cohesive materials of clay, chlorite etc.
>6	Some or no wall contact	Soft cohesive materials or swelling clays.

Fig. 7. The cumulative distributions of equivalent block size along the tunnel length.

stability were noted in the classification system. Since the Q-system was used the J_a value was registered as a measure of joint filling. In this paper the J_a was divided into four groups according to Table 2. With this grouping of data the cumulative distribution for each group can be presented, Fig. 8. Each curve represents the total number of metres encountered in each group, starting from the southern tunnel entrance. The inclination of each curve represents the concentration of J_a in a particular area.

2.4. Quantification of the hydrogeological conditions

The hydrogeological conditions have been evaluated throughout the project with water pressure tests (WPT) in probe and grout holes. These were performed at the tunnel face in holes approximately 24 m long for the whole tunnel length with an overlap of about 5 m. The number of probe holes was generally between 10 and 20, arranged around the tunnel perimeter. The variations in number and length of the holes as such originated from the changes in grouting methodology that emerged from increased knowledge of the *in situ* hydrogeological conditions. The water pressure test was performed once for each hole, generally with a tested length 1 m shorter than the hole length (i.e. approx. 23 m).

The ground water level was estimated to follow the ground surface and the ground water pressure was assumed as the hydrostatic pressure at the tunnel level. The water pressure test was performed from the tunnel jumbo with a pressure of 0.5 MPa over the groundwater pressure. The digital water flow equipment had a measurement range of 2–38 l/min. The read-out range limited the water pressure test to between about 0.2 and 4 Lugeon, l/min - m MPa, (the values are for a test length of 20 m and 0.5 MPa pressure over the ground water pressure).

In order to achieve stationary conditions each test should be performed for some time but as the water pressure tests were performed as part of the production process, the measurements were generally performed in less than 5 min. However, the measured flow values are reported as stable, indicating that the results should be considered to be reasonably accurate (Fransson, 1999) in order to show statistically the difference in hydrogeological condition along the tunnel.

For each grouting fan the water pressure test (WPT) measurements were noted per hole. For each fan the largest measurement were grouped as an A, B or C fan using the definition in Table 3. The definition was based on the contractor's experience that a tight

Table 3
Definition of water pressure test interval and grout/water pressure test class A, B or C.

| Water pressure test interval	Defined class
WPT $\leqslant$ 0.5 Lugeon	A
0.5 < WPT $\leqslant$ 2 Lugeon	B
2 Lugeon < WPT	C

rock mass would have small WPT results (lower than 0.5 Lugeon) whereas a conductive rock mass would have a significantly higher WPT (more than 2 Lugeon). It was also considered that the limit was related to the highest WPT in each fan. The highest WPT in a fan is also a clearly defined limit to which the contractor easily relates.

The cumulative distribution of water pressure test classes along the tunnel is shown in Fig. 9. For each WPT class, A, B or C, the number of fans has been added along the tunnel length starting from the south. The inclination of each curve shows the concentration of each WPT class in the respective area. A steep curve indicates a higher concentration of the WPT class. The measurements show that the rock mass between chainages 506 + 850 and 509 + 500 is dominated by the A class (WPT for a fan is $\leqslant$ 0.5 Lu). Furthermore, the area between chainages 505 + 000 and 505 + 450 is dominated by the A class, which is interesting considering the geological conditions presented in Figs. 6 and 7. It seems that there is a correlation (not surprisingly) between the number of zones and the water pressure test measurement.

2.5. Summary of the geological and hydrogeological conditions

The geological conditions along the length of the tunnel have been seen to vary considerably, Figs. 6–9. However, for the different areas there are similarities in the geological data. Within these areas or geological domains the statistics are relatively congruent and these are summarized in Table 4. As can be seen, the data are significantly different for the different domains.

The geological domains can be expected to influence the grouting process and consequently the results of the grouting. A high concentration of zones and a combination of infilling and a high degree of jointing could be expected to be indicative of difficult grouting conditions. It is therefore reasonable to expect that for the southern part, where almost every grouting round crosses a zone, the grouting would be affected the most.
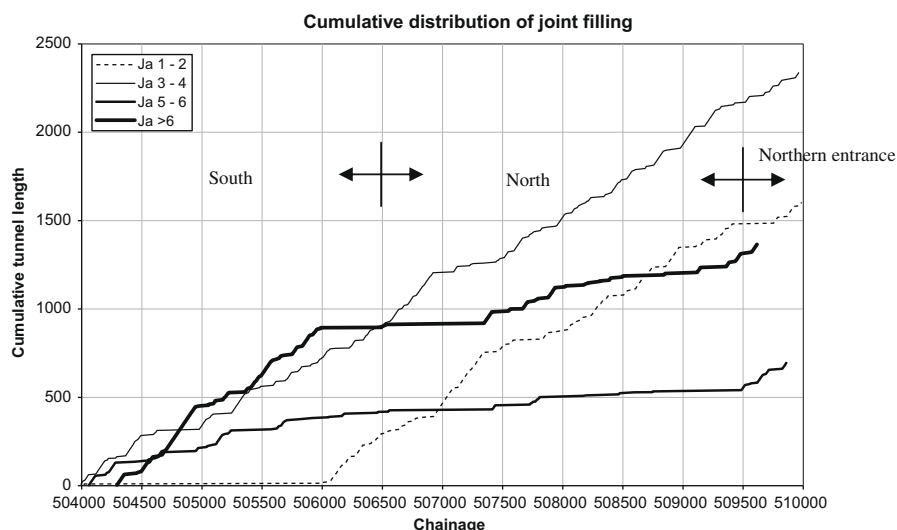
Fig. 8. The cumulative distributions of joint fillings, J_a. The most prominent figure is the curve representing clean joints. Note that there are almost no clean joints up to section 506 + 000.

Cumulative distribution of largest water pressure test (WPT) per grouting fan along the tunnel
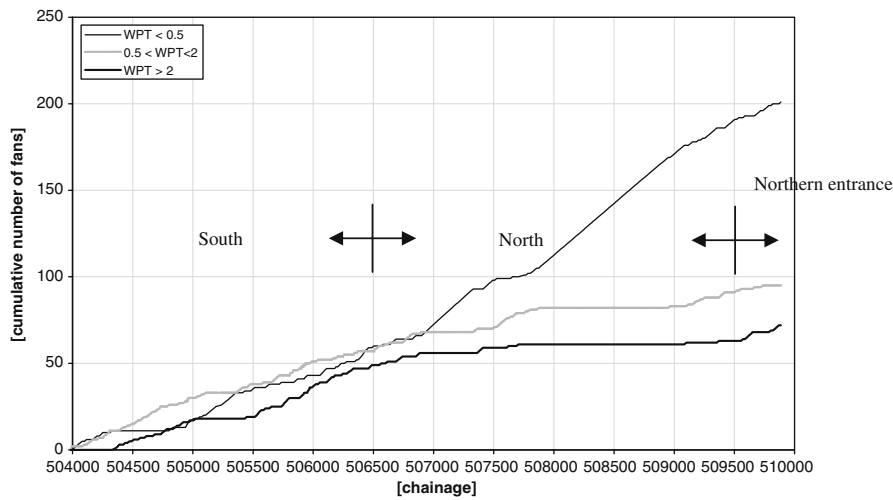

Fig. 9. The cumulative distributions of water pressure test measurements for the Namntall Tunnel. The water pressure tests are grouped according to the largest measurement in each fan (section).

Table 4
Geological domains encountered in the Namntall Tunnel.

	South (503 + 985 to 506 + 500)	North (506 + 500 to 509 + 500)	Northern entrance (509 + 500 to 509 + 986)
Distribution of zones	1 zone per 23 m	1 zone per 62 m	1 zone per 20 m
Block size	Median value 8 joints/m³	Median value 5 joints/m³	Median value 10 joints/m³
Joint filling	Dominated by hard and soft cohesive materials, some or no wall contact.	Dominated by clean joints and coating or thin filling of clay etc., contact between joint walls.	Dominated coating or thin filling of clay etc., contact between joint walls.
WPT class distribution	About equal distribution of A (36%), B (36%) and C (29%).	Dominated by A (74%), B (18%), C (8%).	About equal distribution of A (43%) and C (39%), B (17%).

3. Grout data

3.1. Grouting operation

The grouting procedure was defined with the assumption that a certain water pressure test class or grouting class (A, B or C) would need a similar grout effort regardless of where the grout fan was situated. Originally, there were only a few probe/grout holes in the A fans although the number of holes was changed after an initial period to 10 holes placed around the tunnel periphery. There were around 20 grout holes for the B and C fans. The standard grouting procedure can be summarized as a conventional Scandinavian practise of tunnel grouting sequence with a gradual decrease in w/c with increased volume and a gradual increase in pressure. The stop criteria were related to volume and pressure although the volume stop criterion was seldom used. In grouting class C, control holes were drilled after grouting. Grouting was performed with a fine-grained microcement where 95% of the grains were below 30 μm. A plasticizer was used to decrease the viscosity and the yield limit of the grout, Stille and Andersson 2008.

Different numbers of holes were used in the different water pressure test classes although the distribution of all holes is comparable between different classes given the fact that the same general grouting procedure was used. Even though zero or close to zero WPT was measured, grouting generally commenced with w/c r 1.0 or 0.8 and was pressurized up to the stipulated pressure.

3.2. Grout take

The total grout take for each fan can be plotted against the tunnel chainage, Fig. 10. The total grout take is the sum of each grout hole and it should be noted that an A fan has a minimum theoretical volume of 600 l, whereas for a B or C fan it is 1200 l. In the figure, however, the total grout take seems to indicate that there are some recognizable areas with more conductive rock. As an example, the geological conditions at about 507 + 400 and 507 + 750 could be studied to verify the correlation with the grout take.

The total grout take can also be plotted against the largest measured WPT for each fan to study the variation in data, Fig. 11. The X-axis has a logarithmic scale to improve the resolution for lower water pressure test values. The following observations are made:

- Lower water pressure test limit. For the grout in question there seems to be a limit to where no or almost no grout take over hole filling is noted. The limit in this project is about 0.2–0.3 Lugeon.
- Large cone of variation. For larger water pressure tests there seems to be a cone of variation where there is an almost equal probability of the final total grout take.
- General trend. The overall view is that for larger water pressure test there is a larger grout take.

The grout take versus the water pressure test in Fig. 11 has been grouped in the geological domains. There seems to be a larger variation in the data for the south compared to the north and northern entrance parts. Another observation would be that although the maximum values are lower for both the north and the northern entrance part, the variation seems greater for the north. A possible explanation for the variation (or the probability of having a certain value) is the joint filling that is found in the grouting class C rock, Figs. 8 and 9. The soft cohesive filling ($J_v > 6$) seems to influence the grout takes for both limits (minimum and maximum). Whilst the
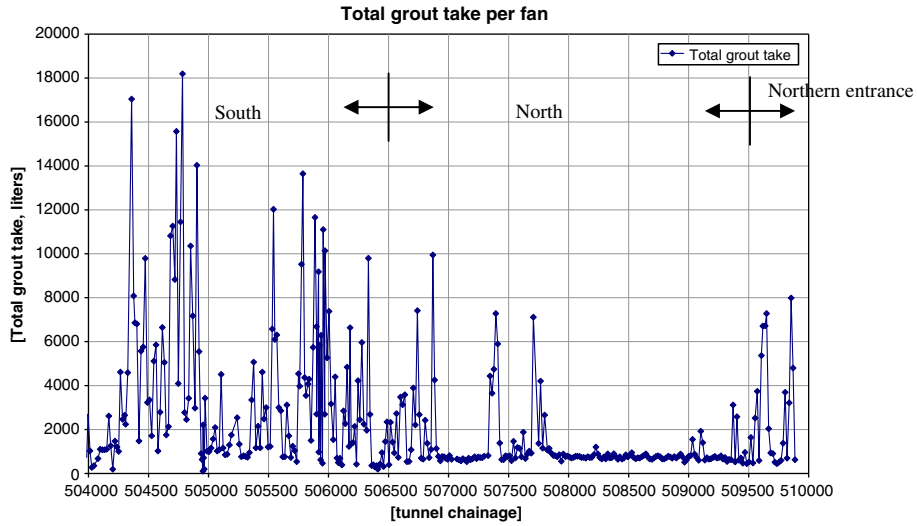
Fig. 10. The total grout take plotted against the location, tunnel chainage, for each fan.
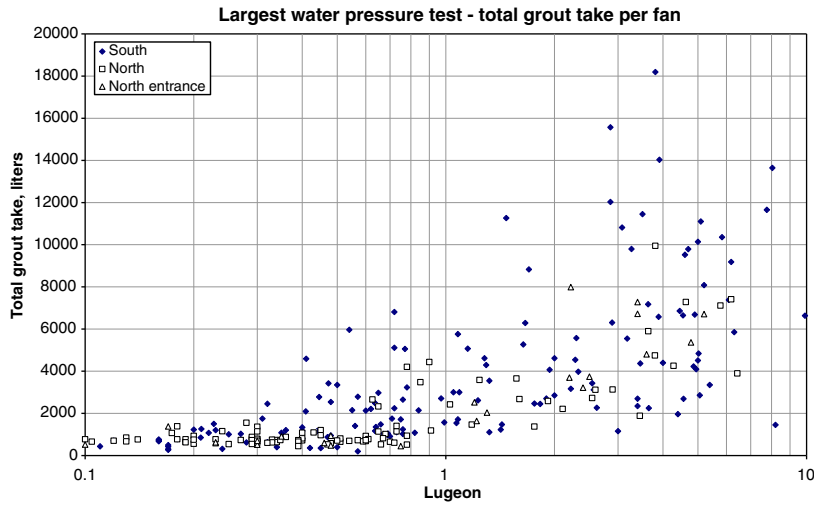

Fig. 11. Grout take plotted against the largest water pressure test for each fan.
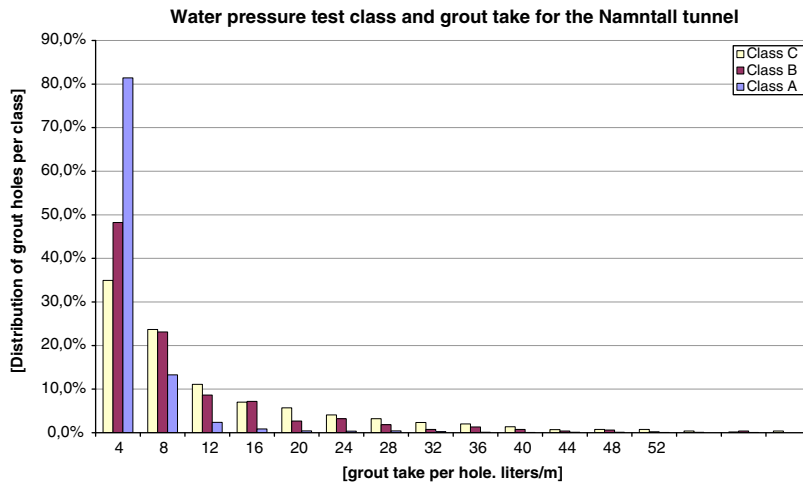

Fig. 12. Histogram for the grout take for grout classes A–C. The figure shows the relationship between water pressure test class and grout take distribution.

different workforces may influence the data between north and south somewhat, the majority of the grouting class C rock was gro-uted by a workforce working on both the southern and northern parts.

By arranging the grout data into the different water pressure test classes (or grouting classes) the distribution of grout take can be studied for each subgroup. The grout take per metre of borehole is studied to limit influences from different hole lengths, number of holes etc. The data is presented in a histogram, where all three classes are represented, Fig. 12. The Y-axis shows the percentage of holes and the X-axis shows the grout take. For example, about 14% of the grouting class A holes have a grout take between 4 and 8 l/m. Furthermore, Fig. 12 shows that there is an overall relationship between the grout take and the water pressure test in a fan. It also shows that there is a considerable number of holes in each fan that have a grout take approximately equal to the hole volume (3.2 l/m), although there is a significant difference between classes A and C.

4. Conclusion

4.1. Evaluation of geological and hydrogeological factors influencing grouting

The geological conditions are clearly influenced by the deep failure lines and the following intrusions of metabasites, pegmatites and granites. By overlaying the different figures (Figs. 6–10) there is a correlation between the geological conditions, the water pressure test and the grout take. The most prominent correlation seems to be between the density of zones (Fig. 6) and the water pressure test distribution/grout take (Figs. 9 and 10). The need for and the effect on the grouting work is thus influenced most by the density of zones whereas other factors, such as fracture frequency and joint filling, are correlated to the density of zones and are thus of a secondary nature in this case. However, all these geological factors should be studied if the large-scale distributions of the water pressure tests in the rock mass are to be explained.

It is also evident that in the northern part the grout take seems smaller, often no larger than the hole filling. It is possible that the *in situ* stress, which is greater in these areas, contributes to the tightness of the fractures.

4.2. A statistical evaluation between WPT-values and grout take

The water pressure test classification used in the project is based on the highest measured value for each fan. The statistical relationship of grout take for individual holes is quite weak although the overall relationship shows that there is a correlation between the water pressure test class and grout take. It is also clear that there is a larger variation in the southern part of the tunnel compared to the north and the northern entrance parts, which can be attributed to the different geological conditions, mainly the zone characteristics.

There seems to be a limit under which the grout take can only be expected to be roughly equal to the hole filling (Fig. 11). This means that a WPT class based on such a value could indicate a rock mass where there is no real use or need for grouting. However, this value would need to be co-ordinated with the water discharge requirements and the grout properties.

It is clear that a similar classification can be used for other projects and that such a classification can be used as a prognosis tool.

4.3. Results in relation to water ingress measurements

During the excavation of the tunnels the ingress of water into the tunnel was measured, Fig. 13. The measurements were made at concrete dams that prevented the water passing along the tunnel. These were set at each cross tunnel, approximately every 500 m. As can be seen in the figure, the ingress is clearly different between the south and the north parts of the tunnel.

The south part of the tunnel has a water pressure test class distribution that is dominated by the B and C classes compared to the north part, which is dominated by the A class, Fig. 14. The total grout take distribution also reflects this condition.

Although the grouting is much more intensive on the southern side the resulting water ingress is higher than on the northern side. This implies that considering the difference in rock cover (2–5 times) and the difference in discharge (2–4 times) and assuming a direct relationship between the discharge, hydraulic conductivity and the pressure head (rock cover), the difference in conductivity after grouting can be concluded to be a factor of 4–20 times worse than for the northern part in a more or less class A rock mass. This is indicative of the grouting difficulties that were encountered in the southern tunnel part.

4.4. Final remarks

The geological model for the zones can explain some of the difficulties encountered during the grouting work. The nature of the zones, including the surrounding area (damage or transition zone), indicates a more or less continuous influence throughout the southern part of the tunnel, including a major part with no or some
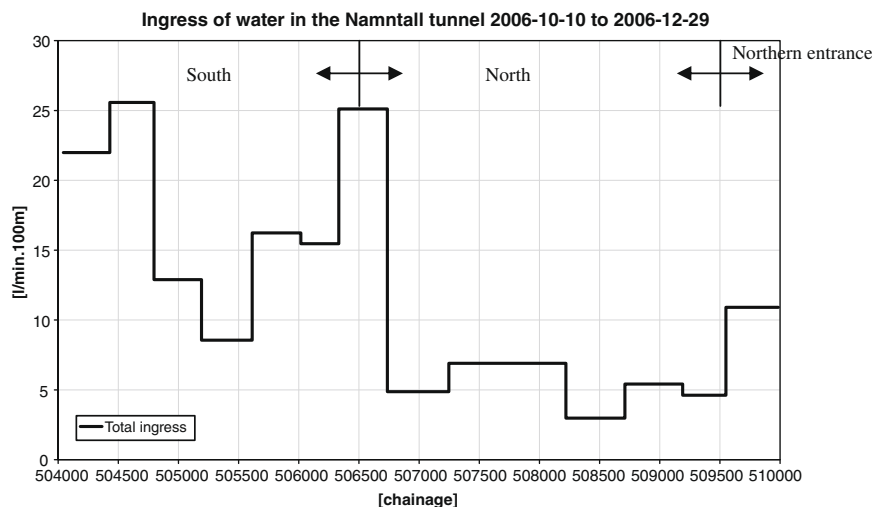

Fig. 13. Total ingress of water in the Namntall Tunnel, including track and service tunnels. The measurement took place on October 10, 2006 and December 29, 2006.
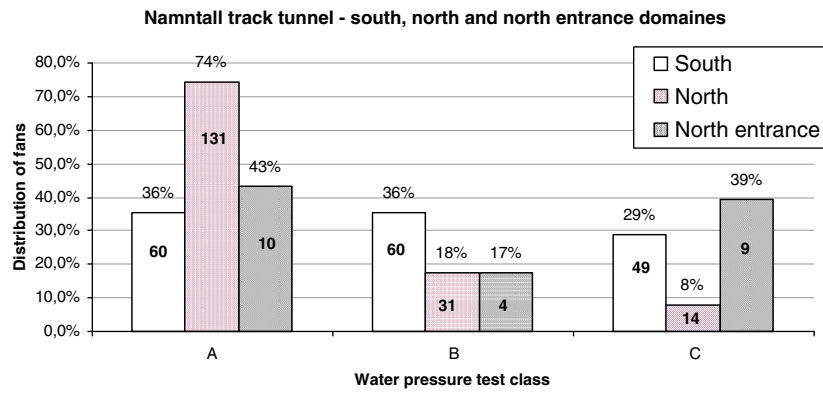
Namntall track tunnel - south, north and north entrance domaines

Fig. 14. Distribution of water pressure test classes for the south, north and northern entrance regimes.
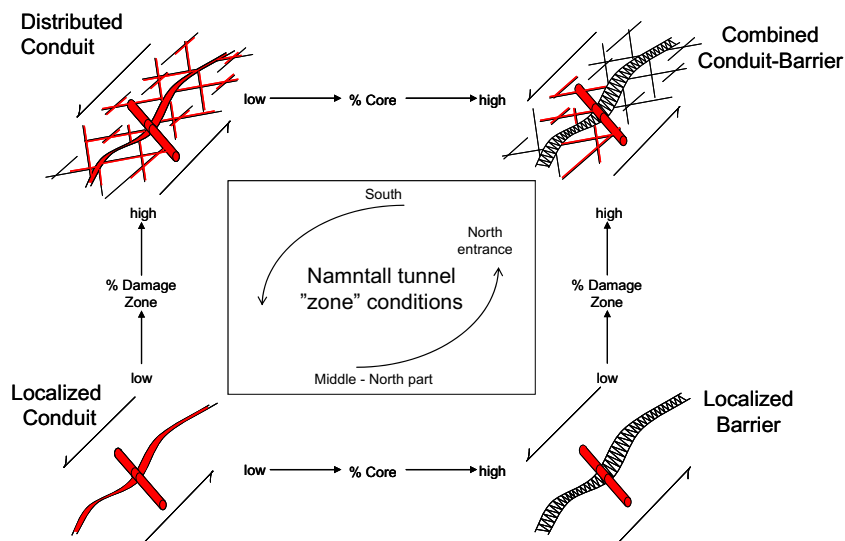

Fig. 15. Conceptual model for the zones and grouting 'performance' in the Namntall Tunnel (modified according to Caine et al. 1996). The red colour indicates grout.

wall contact with soft cohesive infilling. This means that a conceptual model for the zones in this area would fall into a group with a barrier (often a clay-filled core) and a damage zone with conductive rock. For the northern part of the tunnel with the majority of the tunnel length in the host rock, the existing zones and the grout take in this area indicate smaller damage zones, possibly with cleaner joints, even though infilling in the core probably still acts as a barrier.

The degree of difficulty to grout a specific area is shown conceptually in Fig. 15. The localized conduits or fractures are generally easy to grout whereas the localized barriers may be tight. However, if the gouge material is conductive the grouting will be difficult. The distributed conduit is generally easier to grout although the quality of the work may be hampered by capacity problems inherent to the grouting process. A combined conduit barrier can be expected to be the most difficult to grout as the fracture hydraulic network is very complicated. It thereby follows that characterization of the zones at an early stage could be very useful.

The grout take and the resulting water discharge indicate that a different approach to the grouting process could be suggested. Based on the large grout takes and the corresponding low grout pressures that were common in the grouting class C rock, use of two grout rounds is recommended. Analysis of fracture characteristics (Gustafson et al., 2005) indicates that in the southern part micro-cements or other small aperture grouting agents could be used to increase penetrability and reduce water discharge. However, it was also noted that the bottleneck in the grouting process was the grout mix capacities. The standard capacity for ordinary grout platforms was simply not sufficient to grout under higher pressure for a longer period of time in order to reach a stipulated penetration length (Gustafson and Stille, 2005) for smaller fractures.

The contractor, who is the first to witness the geological conditions, must be aware of the consequences of poor agreement between tender and reality. It is of great importance that the deviations are brought up immediately since these will always have technical and financial consequences.

It is a clear conclusion that a geological description (and a prognosis) that focuses on the grouting is required to prepare those involved better for the extent and level of activity that may be required in order to satisfy the environmental requirements of society. This report shows that it is possible to make such a prognosis through the relationships presented.

References

Barton, N., 2002. Some new Q-value correlation to assist in site characterisation and tunnel design. International Journal of Rock Mechanics and Mining Sciences 39, 185–216.
Bieniawski, Z.T., 1989. Engineering Rock Mass Classifications. Wiley, New York.

Botniabanan, A.B., 2003. Adapted from the Tender Documents Rev.E, Project E3541 Offersjön-Bjällstaån.

Botniananan, A.B., 2003. Exploratory Drillings, Tender Documents Rev.E, Project E3541 Offersjön-Bjällstaån.

Butrón, C., 2009. Drip Sealing of Tunnels in Chrystalline Rock: Pre-Excavation Design and Evaluation. Lic. Thesis, Chalmers University, Sweden.

Caine, J.S., Evans, J.P., Forster, C.B., 1996. Fault zone architecture and permeability structure. Geology (11), 1025–1028.

Fransson, Å., 1999. Grouting Predictions Based on Hydraulic Tests of Short Duration. Lic. Thesis, Chalmers University, Sweden.

Goodman, R.E., 1993. Rock in engineering construction. Engineering Geology. Wiley, New York. 385 p.

Gustafson, G., Fransson, Å., 2005. The use of the pareto distribution for fracture transmissivity assessment. Hydrogeology Journal. doi:10.1007/s10040-005-0440-y.

Gustafson, G., Stille, H., 2005. Stop Criteria for Cement Grouting. Felsbau 3/2005, 62–68.

Hässler, L., 2007. Personal Communication. Golder Associates AB.

Lindström, L., 2008. Site Geologist, Personal Communication. Vattenfall Power Consultants AB.

Lundqvist, T., Gee, D., Kumpalainen, R., Karis, L., Kresten, P., 1990. Beskrivning till Berggrundskartan Över Västernorrlands län 18, 18–44. pp. 322–327.

Moye, D.G., 1967. Diamond drilling for foundation exploration. Civil Engineering Transactions (April), 95–100.

Munier, R., Stenberg, L., Stanfors, R., Milnes, A.G., Hermanson, J., Triumf, C-A., 2003. Geological Site Descriptive Model. SKB Report, R-03-07.

Palmström, A., 1995. RMi – A Rock Mass Characterization System for Rock Engineering Purposes. PhD Thesis, Oslo University, Norway, 400 p.

Palmström, A., 2005. Measurements of and correlations between block size and rock quality designation (RQD). Tunnels and Underground Space Technology 20, 362–377.

Stille, B., Andersson, F., 2008. Pre-grouting – Application of Grouting Research in the Field. SveBeFo Report 79.

Stuge, B., Lindström, L., 2007. Mapping from the Namntall Tunnel. As Built Drawing.

Björn Stille
Håkan Stille
Gunnar Gustafson
Shinji Kobayashi

Experience with the real time grouting control method

Erfahrungen mit einer Echtzeit Kontrollmethode für das Injizieren

A new concept of "real time grouting control method" is described by which grout penetration and grouting control are made applicable in real time by applying theories for grout spread. The stop criterion with this method can be related to achieved grout spread, and grouting may be considered complete when the grout penetration for the smallest fracture to be sealed is above a predetermined target value, or before the grout penetration for the largest fracture aperture reaches a certain maximum limiting value. It might also be possible by online monitoring of the process to predict the course of the grout spread and flow and to analyse the risk of uplift and jacking. Four tunnel projects in Sweden are presented in the paper. These references indicate that the real time grouting control method may be applicable to real grouting design and control.

Nachfolgend wird ein neues Konzept einer „Echtzeit Kontrollmethode für Injektionen" beschrieben, das für das Eindringen von Injektionsgut im Fels und für die Prozesskontrolle neuartige theoretische Überlegungen zur Ausbreitung des Injektionsguts im Untergrund ansetzt. Das Abbruchkriterium kann mit dieser Methode auf die erreichte Ausbreitung bezogen werden. Die Injektion kann danach dann als abgeschlossen angesehen werden, wenn die Verfüllung der kleinsten zu behandelnden Kluft ein vorgegebenes Maß überschritten hat oder bevor die Verfüllung der größten zu behandelnden Kluft einen vorgegebenen Maximalwert erreicht. Mit dieser Methode kann bis zu einem gewissen Grad auch der Verlauf, die Rate und die Ausbreitung von Injektionsgut vorhergesagt werden. Weiterhin kann analysiert werden, wann das Risiko von örtlichen oder generellen Hebungen eintritt. Vier Schwedische Tunnelprojekte dienen in diesem Beitrag als Beispiele der Anwendung dieser Kontrollmethode. Diese Referenzen sollen auch zeigen, dass die Methode praxistauglich ist.

1 Introduction
1.1 Background

The objective of grouting of tunnels and dam foundations is to reduce water flow into the tunnel or under the dam. This is achieved by filling up the water bearing fractures to a certain depth, creating a watertight zone. The conductivity of the grouted zone is related to the type of cement used and the thickness of the zone is related to the grout spread. Grout spread is normally in the order of 3 to 15 m.

The spread of grout is governed by a number of complex relations. Up to 1990, the understanding was more or less based on empirical knowledge as described in [1]. A deeper theoretical understanding of the mechanism as manifested in [2], [3] [4] [5] has had an impact on the development of both new stop criteria and new grouting materials.

Research during recent years has given us a better understanding of the water-bearing structures of the rock mass as well as analytical solutions for grout spread [6]. In [7] the concept of analysis of grout spread in real time was discussed for the first time but was then based on numerical calculations. The analytical solutions of the governing differential equations have implied the possibility of developing tools for analysing grout spread in real time. The principle was first described in [8] and was later further developed in [9] [10].

1.2 Grouting control with the real time grouting control method

Modern grouting equipment has a computerised logging tool which continuously records different grouting para-

1 Einführung
1.1 Grundlagen

Das Ziel von Injektionen in Tunneln und unter Staudämmen ist es, jeweils das Zusitzen von Wasser aus dem Gebirge oder die Unterströmung der Bauwerke zu verringern. Dies wird durch die Verfüllung wasserführender Klüfte bis in eine bestimmte Tiefe erreicht, womit jeweils eine Art Dichtschirm hergestellt wird. Die erreichte Undurchlässigkeit hängt vom verwendeten Zement und von der Reichweite der Injektion ab. Diese Reichweite liegt normalerweise zwischen 3 und 15 m.

Die Ausbreitung des Injektionsguts folgt einer Reihe komplexer Zusammenhänge. Bis 1990 beruhte das Verständnis dazu mehr oder weniger auf Erfahrung, wie in [1] beschrieben. Ein vertieftes theoretisches Verständnis der Mechanismen, wie in [2] [3] [4] [5] dargelegt, beeinflusste seither sowohl die Entwicklung neuer Abbruchkriterien als auch neuer Injektionsmittel.

Die Forschung der letzten Jahre führte dabei einerseits zu einem besseren Verständnis der wasserführenden Strukturen im Fels, andererseits zu analytischen Lösungen, was die Injektionsgutausbreitung anbelangt [6]. Das Konzept der online Analyse der Ausbreitung von Injektionsgut wurde erstmals in [7] erörtert, war aber damals auf numerische Berechnungen abgestellt. Die analytischen Lösungen der relevanten Differentialgleichungen lieferten später die Möglichkeit, Injektionsgutausbreitung in Echt-
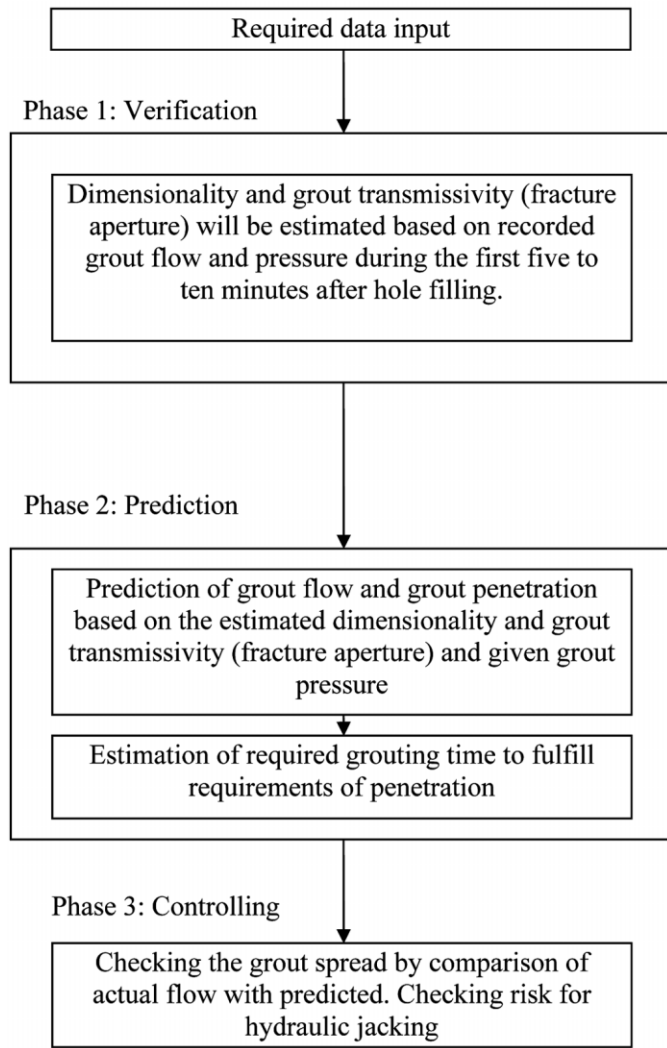
Fig. 1. *Grouting control procedures using the real time grouting control method*
Bild 1. *Kontrollmaßnahmen zur Steuerung der Injektion in Echtzeit*

Table 1. Data required for the real time grouting control method
Tabelle 1. Erforderliche Daten für die Echtzeit-Injektionskontrollmethode

Hydro geological design data	Smallest aperture size that has to be sealed – Minimum penetration distance Largest aperture size – Maximum penetration distance
Grout material properties	Yield value Viscosity Grout mix penetrability (minimum aperture size)
Other data	Groundwater pressure Hole filling volume

meters such as grouting time, grouting pressure, grout flow and grouted volume. By online monitoring of grouting it is possible – using the theories mentioned above – to predict the course of the grout flow and penetration and also analyse the risk of uplift and jacking. Used as a stop criterion, it can be related to desirable grout penetration instead of relying on maximum volume or minimum flow.

Grouting is completed when the grout penetration of the smallest fracture to be sealed is above a certain minimum value (target value) or before the grout penetration for the largest fracture aperture reaches a certain maximum value (limiting value). The concept and procedures for this real time grouting control method system are shown in Figure 1

When used as a stop criterion, the minimum penetration length and/or maximum penetration length will be required as input data. The grout material properties must also be known. In addition, other data such as groundwater pressure and hole filling volume are required. Table 1 shows the data required for the grouting control system.

zeit zu verfolgen. Die Grundlage dafür wurde erstmals in [8] beschrieben und später in [9] [10] weiterentwickelt.

1.2 Steuerung des Injektionsvorgangs mit der Echtzeit Kontrollmethode

Modernes Injektionsgerät ist in der Regel mit einer entsprechenden Datenerfassung für die Injektionsparameter Zeit, Injektions(pumpen)druck, Injektionsrate und Volumen ausgerüstet. Durch eine Echtzeit Auswertung dieser Daten gelingt es – auf der Grundlage der oben erwähnten Theorien – das Eindringen des Injektionsguts und die Risiken von Dilatation bzw. örtlicher oder genereller Hebung vorauszusagen. Wenn man diese Methode als Abbruchkriterium benutzt, wird sie sich auf diese Weise auf Reichweite statt wie bisher auf maximales Volumen oder minimale Rate stützen.

Die Injektion kann danach dann als abgeschlossen angesehen werden, wenn die Verfüllung der kleinsten zu behandelnden Kluft ein vorgegebenes Maß überschritten hat oder bevor die Verfüllung der größten zu behandelnden Kluft einen vorgegebenen Maximalwert erreicht. Das Konzept und die Verfahrensschritte zu diesem System sind in Bild 1 dargestellt.

Wenn man das System als Abbruchkriterium verwendet, müssen die minimale und/oder die maximale Reichweite als Eingabewerte gegeben sein. Die (rheologischen) Eigenschaften des Injektionsguts müssen ebenfalls bekannt sein. Außerdem sind Daten wie etwa der Grundwasser(gegen)druck oder das Bohrlochvolumen erforderlich. Tabelle 1 zeigt im Überblick, welche Eingabedaten für das System erforderlich sind.

2 Das Eindringen von Injektionsgut als Binghamsche Flüssigkeit unter konstantem Druck
2.1 Grundlegende Gleichungen

Zementsuspensionen als Injektionsgut können als Bingham-Fluide mit einer charakteristischen Fließgrenze τ_0 und einer plastischen Viskosität μ_g beschrieben werden. Um analytische Lösungen für das Eindringen des Injektionsguts zu erhalten, werden die charakteristische Injektionszeit t_0, die relative Injektionszeit t_D und die relative (Injektions)Reichweite I_D definiert [8], und zwar wie folgt:

2 Grout penetration of a Bingham fluid at constant pressure
2.1 Basic equations

Cement grouts can be described as Bingham fluids characterized by a yield strength τ_0 and a plastic viscosity μ_g. In order to obtain analytical solutions for grout penetration, the characteristic grouting time t_0, the relative grouting time t_D, and the relative grout penetration I_D are defined according to [8] as:

$$t_0 = \frac{6\Delta p \cdot \mu_g}{\tau_0^2} \tag{1}$$

$$t_D = \frac{t}{t_0} \tag{2}$$

$$I_D = \frac{I}{I_{max}} \tag{3}$$

The maximum penetration can be calculated, see for example [7], based on a simple force balance when grouting has come to a stop as:

$$I_{max} = \left(\frac{\Delta p}{2\tau_0}\right) \cdot b \tag{4}$$

The relative penetration I_D as a function of the relative grouting time t_D for both the 1D and the 2D cases is calculated in [8] as shown in Figure 2. The relative borehole radius expressed by the ratio between the maximum penetration and the radius of the injection borehole r_b ($\gamma = I_{max}/r_b$) will also to some degree influence the relative penetration for the 2D case. The normal range of the ratio will be in the order of 300 to 1,000.

2.2 Injected volume and grout flow

The injected volume and grout flow for both 1D and 2D cases are also derived by [8] according to the following equations.

For the 1D case, the volume injected into the channel at width w and aperture b is calculated as:

$$V = I \cdot w \cdot b = I_D \cdot I_{max} \cdot w \cdot b = I_D \cdot \left(\frac{\Delta p}{2\tau_0}\right) \cdot w \cdot b^2 \tag{5}$$

This is calculated for several fractures as:

$$V_{tot} = I_D \cdot \left(\frac{\Delta p}{2\tau_0}\right) \cdot \sum wb^2 = I_D \cdot V_{max,1D} \tag{6}$$

The grout flow can be calculated as:

$$Q = \frac{dV_{tot}}{dt} = \frac{dI_D}{dt_D} \cdot \frac{1}{t_0} \cdot \left(\frac{\Delta p}{2\tau_0}\right) \cdot \sum wb^2 = \frac{dI_D}{dt_D} \cdot \frac{V_{max,1D}}{t_0} \tag{7}$$

For the 2D case, the volume injected into a circular fracture with aperture b is calculated as:

$$V = \pi \cdot I^2 \cdot b = \pi \cdot \left(I_D \cdot I_{max}\right)^2 \cdot b = \pi \cdot I_D^2 \cdot \left(\frac{\Delta p}{2\tau_0}\right) \cdot b^3 \tag{8}$$
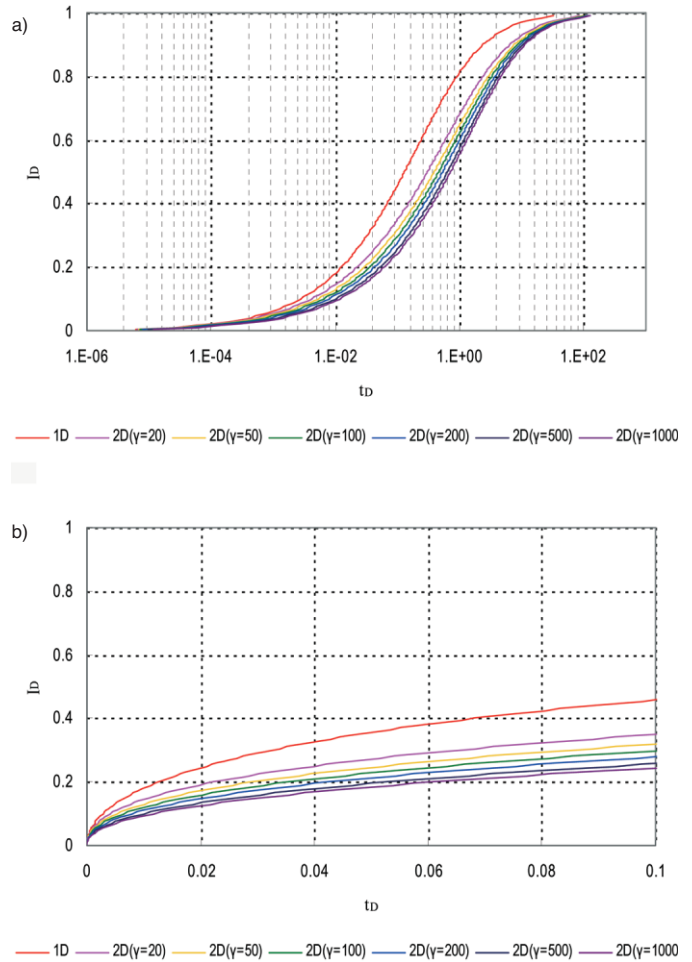

a)

b)

Fig. 2. The relative penetration as a function of the relative grouting time in the a) logarithmic X axis and b) in the normal X axis [8]
Bild 2. Die relative Reichweite als Funktion der relativen Injektionszeit auf einer (a) logarithmisch skalierten X-Achse und einer (b) normal skalierten X-Achse [8]

$$t_0 = \frac{6\Delta p \cdot \mu_g}{\tau_0^2} \tag{1}$$

$$t_D = \frac{t}{t_0} \tag{2}$$

$$I_D = \frac{I}{I_{max}} \tag{3}$$

Die maximale Reichweite der Injektion kann aufgrund einer einfachen Gleichgewichtsbedingung zum Zeitpunkt der Stagnation berechnet werden (ein Beispiel wird dazu in [7] gegeben):

$$I_{max} = \left(\frac{\Delta p}{2\tau_0}\right) \cdot b \tag{4}$$

Die relative Reichweite I_D als Funktion der relativen Injektionszeit t_D wird in [8] sowohl für den eindimensionalen (1D) als auch für den zweidimensionalen (2D) Fall der Ausbreitung berechnet (Bild 2).

This is calculated for several fractures as:

$$V_{tot} = \pi \cdot I_D^2 \cdot \left(\frac{\Delta p}{2\tau_0} \right) \cdot \sum b^3 = I_D^2 \cdot V_{max,2D} \qquad (9)$$

The grout flow can be calculated as:

$$Q = \frac{dV_{tot}}{dt} = 2\pi \cdot I_D \cdot \frac{dI_D}{dt_D} \cdot \frac{1}{t_0} \cdot \left(\frac{\Delta p}{2\tau_0} \right)^2 \cdot \sum b^3 = I_D \cdot \frac{dI_D}{dt_D} \cdot \frac{V_{max,2D}}{t_0} \qquad (10)$$

2.3 Analysis of dimensionality

In order to analyse the flow dimensionality of the fracture, Qt/V is suggested as an index in [8]. Figure 3 shows the plots of Qt/V as a function of t_D. A significant and characteristic difference can be seen between 1D and 2D cases. It could be pointed out that the normal interval is $0 < t_D < 0.1$ as shown in Figure 2a. Here the control parameter is approximately constant. Since t_D is proportional to the real grouting time, Qt/V can be plotted against the real time. As the diagram shows, the parameter is roughly constant at 0.85 for the 2D flow case and 0.45 for the 1D case in a broad interval covering the normal I_D interval for cement grouting.

2.4 Approximations for analytical grout penetration

The relationships between the relative penetration and the relative time for both 1D and 2D cases have to be approximated in order to develop a handy solution. The following relationships have an acceptably small error:

$$I_D = \sqrt{\theta^2 + 4\theta} - \theta \qquad (11)$$

$$\theta_{1D} = \frac{t_D}{2(0.6 + t_D)} \qquad (12)$$

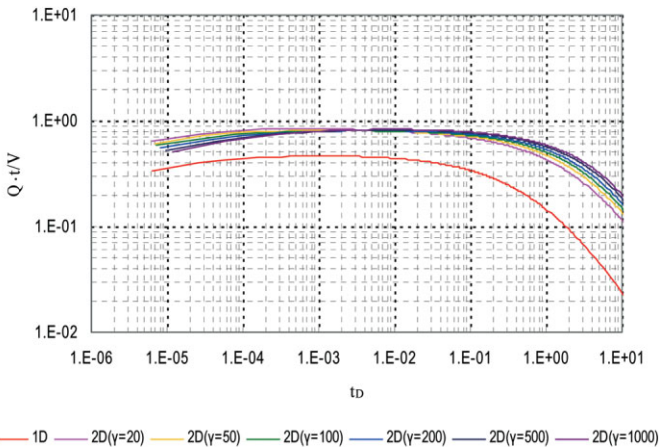$$\theta_{2D} = \frac{t_D}{2(3 + t_D + 0.23 \ln(t_D))} \qquad (13)$$

Fig. 3. The index for analysing the dimensionality, Q·t/V for 1D and 2D cases [8]
Bild 3. Der Index zur Analyse der Dimensionalität (der Strömung in Klüften) Q·t/V für 1D und 2D Fälle [8]

Der relative Bohrlochradius r_b (ausgedrückt als Verhältnis zwischen diesem Radius und der Reichweite der Injektion $\gamma = I_{max}/r_b$) wird zu einem gewissen Maß die relative Ausbreitung im zweidimensionalen Fall beeinflussen. Die übliche Bandbreite für dieses Verhältnis reicht von 300 bis 1.000.

2.2 Injiziertes Volumen und Injektionsrate

Das Volumen an verpresstem Injektionsgut und die Injektionsrate sowohl für 1D und 2D Fälle werden in [8] nach den folgenden Gleichungen hergeleitet.

Für den 1D Fall errechnet sich das in den Strömungskanal mit der Weite w und der Öffnung b verpresste Injektionsvolumen als:

$$V = I \cdot w \cdot b = I_D \cdot I_{max} \cdot w \cdot b = I_D \cdot \left(\frac{\Delta p}{2\tau_0} \right) \cdot w \cdot b^2 \qquad (5)$$

Für mehrere solcher linearer Strukturen lautet die Formel:

$$V_{tot} = I_D \cdot \left(\frac{\Delta p}{2\tau_0} \right) \cdot \sum wb^2 = I_D \cdot V_{max,1D} \qquad (6)$$

Die Injektionsrate schreibt sich:

$$Q = \frac{dV_{tot}}{dt} = \frac{dI_D}{dt_D} \cdot \frac{1}{t_0} \cdot \left(\frac{\Delta p}{2\tau_0} \right) \cdot \sum wb^2 = \frac{dI_D}{dt_D} \cdot \frac{V_{max,1D}}{t_0} \qquad (7)$$

Für den 2D Fall errechnet sich das Injektionsvolumen einer kreisförmigen Rissform mit der Öffnungsweite b mit:

$$V = \pi \cdot I^2 \cdot b = \pi \cdot \left(I_D \cdot I_{max} \right)^2 \cdot b = \pi \cdot I_D^2 \cdot \left(\frac{\Delta p}{2\tau_0} \right) \cdot b^3 \qquad (8)$$

Für mehrere solcher kreisförmiger Strukturen lautet die Formel:

$$V_{tot} = \pi \cdot I_D^2 \cdot \left(\frac{\Delta p}{2\tau_0} \right) \cdot \sum b^3 = I_D^2 \cdot V_{max,2D} \qquad (9)$$

Die Injektionsrate schreibt sich für das kreisförmige 2D Modell:

$$Q = \frac{dV_{tot}}{dt} = 2\pi \cdot I_D \cdot \frac{dI_D}{dt_D} \cdot \frac{1}{t_0} \cdot \left(\frac{\Delta p}{2\tau_0} \right)^2 \cdot \sum b^3 = I_D \cdot \frac{dI_D}{dt_D} \cdot \frac{V_{max,2D}}{t_0} \qquad (10)$$

2.3 Die Analyse der Dimensionalität

Um die „Dimension" des Strömungsregimes in einer Rissstruktur zu analysieren, wird das Verhältnis Rate zu Volumen Q*t/V in [8] als Index herangezogen. Bild 3 zeigt den Verlauf entsprechender Kurven als Funktion Q*t/V und der Zeit t_D. Dabei kann eine deutliche und charakteristische Differenz zwischen 1D und 2D Situationen festgestellt werden. Man könnte meinen, dass das "Norminterval" für t_D $0 < t_D < 0,1$ ist, wie in Bild 2a dargestellt. Dort ist der Kontrollparameter ungefähr konstant. Nachdem t_D proportional zur realen Injektionszeit ist, kann Q*t/V ebenfalls gegen die reale Zeit aufgetragen werden. Wie das betreffende Diagramm zeigt, liegt der entsprechende Para-

In reality, the grouting pressure is not constant because grouting normally starts at a low grouting pressure, which is then increased to the maximum. The grout is characterized in terms of rheology such as yield strength and plastic viscosity. In order to take changes in grouting pressure or time-dependent grout properties into account, a stepwise procedure can be used by using a fictitious time interval [10].

In normal grouting work, it is quite common to change the grout mix from thin to thick during grouting. However, since obtaining the theoretical solution for changing grout mixes is not a straightforward matter, only the lower and upper boundaries for penetration length after the grout mix has been changed from thin grout (Grout A) to thick grout (Grout B) can be calculated as proposed in [9].

3 Application of the real time grouting control method
3.1 Required data input

In the following section, actual grouting logs recorded from the grouting field experiment at the 450 m level in the Äspö HRL, and shown in Figure 4, are used to explain the grouting control method. To complete the required data and make up an example, the following values are assumed:
– Hydro-geological design data:
  • Smallest aperture size 0.05 mm, minimum required penetration length 7.5 m,
  • Largest aperture size 0.10 mm, maximum required penetration length 25 m,
– Grout properties:
  • Yield value τ_0 0.296 · $e^{0.0004t}$ Pa,
  • Viscosity (μ_g) 0.0056 · $e^{0.0004t}$ Pas,
– Groundwater pressure 3.36 MPa,
– Hole filling volume 70 l.

3.2 Phase 1 – verification
3.2.1 Determination of dimensionality

After the grout hole has been filled (8 minutes), the corrected time can be calculated on the basis of the grouting pressure and the grout properties. By using the corrected time, the recorded grout flow and the grouted volume, the dimensionality of the flow in the fracture can be calculated during the grouting procedure. As examples, the indexes for determination of the dimensionality after 15 min. (grouting time 7 minutes) are shown in to Figure 5. Although a spread of calculated values is found due to the fluctuation of the grouting pressure, it is likely that the flow dimension of grouting No. 2 is 2D. The average value for the index parameter is $Qt/V_{average} = 0.82$.

3.2.2 Estimation of grout transmissivity (fracture apertures)

As stated in Section 2.2, the theoretical grout volume can be calculated for both the 1D and 2D cases with equations 6 and 9. In both cases it has to be born in mind that grout may enter several fractures, shown by the term Σwb^2 for the 1D case and Σb^3 for the 2D case. Both terms are a function of the fracture aperture. However the generally Pareto distributed transmissivity [11] of the fractures

meter für den 2D Fall in etwa konstant bei 0,85 und für die 1D Situation (lineare Ausbreitung) über eine weite Bandbreite des „normalen" I_D Intervalls für Zementinjektionen bei 0,45.

2.4 Analytische Näherungslösung für die Ausbreitung von Injektionsgut

Die rechnerische Beziehung zwischen relativer Ausbreitung und relativer Zeit für beide Fälle (1D und 2D) müssen einer Näherungslösung zugeführt werden, um eine feldtaugliche Handhabung zu erreichen. Die im Folgenden dafür gewählten Gleichungen weisen dazu eine nur geringe, und daher annehmbare Ungenauigkeit auf:

$$I_D = \sqrt{\theta^2 + 4\theta} - \theta \tag{11}$$

$$\theta_{1D} = \frac{t_D}{2(0.6 + t_D)} \tag{12}$$

$$\theta_{2D} = \frac{t_D}{2(3 + t_D + 0,23\ln(t_D))} \tag{13}$$

Bei der realen Durchführung zeigt sich, dass der Injektionsdruck nicht wirklich konstant ist. Er beginnt relativ niedrig und wird dann in der Regel bis zu einem Maximum gesteigert. Die Injektionsmischung andererseits ist durch ihre rheologischen Parameter (Fließgrenze und plastische Viskosität) charakterisiert. Um nun die realen Änderungen von Injektionsdruck und zeitabhängige Parameter-Änderungen des Injektionsguts zu berücksichtigen, wird ein schrittweises Vorgehen mit dem Ansatz eines fiktiven Zeitintervalls [10] vorgenommen.

Bei üblichen Injektionsarbeiten ist es durchaus die Regel, dass von dünnen Mischungen zu Beginn im weiteren Verlauf der Arbeiten auf dickere Mischungen übergegangen wird. Nachdem aber die theoretischen Kriterien für diesen Wechsel nicht eindeutig sind, können nur die innere und äußere Grenze der Reichweite (nach Änderung der Konsistenz der Mischung von Mischung A auf Mischung B) tatsächlich – wie in [9] vorgeschlagen – berechnet werden.

3 Anwendung der Echtzeit Injektions Kontrollmethode
3.1 Erforderliche Eingabedaten

Im folgenden Abschnitte werden Felddaten, wie sie bei der Ausführung der experimentellen Injektionsarbeiten auf Niveau –450 m in der Äspö HRL aufgezeichnet wurden, zur Darstellung der Anwendung der Methode verwendet (Bild 4). Um die erforderlichen Daten für die Darstellung des Beispiels zu ergänzen, wurden noch folgende Annahmen getroffen:
– Hydrogeologischen Entwurfsdaten:
  • Kleinste Kluftweite 0,05 mm, geringste erforderliche Reichweite 7,5 m,
  • Größte Kluftöffnung 0,1 mm, größte erforderliche Reichweite 25 m,
– Eigenschaften des Injektionsguts:
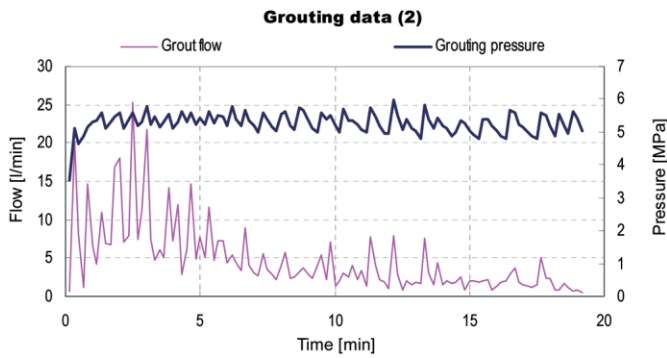 • Fließgrenze τ_0 0,296·$e^{0.0004t}$ Pa,

Fig. 4. *Recorded grout flow and grouting pressure*
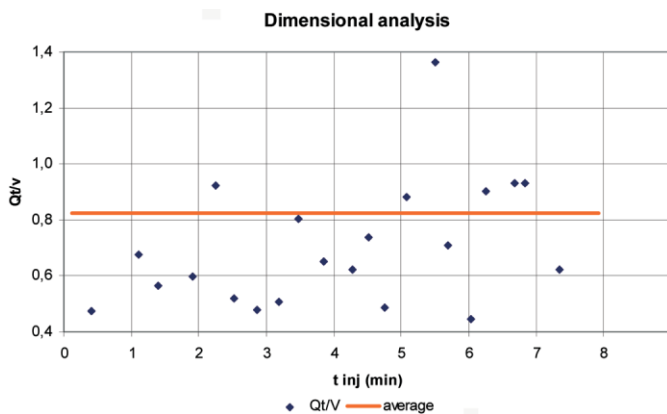Bild 4. *Gemessene Injektionsraten und Injektionsdrücke*

Fig. 5. *Index for analysing the dimensionality, Qt/V*
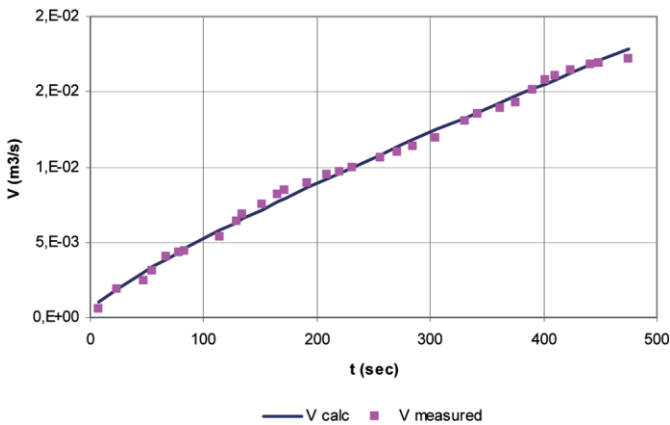Bild 5. *Index zur Analyse der Dimensionalität, Qt/V*

Fig. 6. *Comparison of calculated and measured grout volumes*
Bild 6. *Vergleich gerechneter und gemessener Injektionsgut-volumina*

means that the largest fracture dominates the water inflow and the penetration of the grout. Taking the cube root of Σb^3 will therefore give a reasonable approximate value of the largest aperture for the 2D case. Figure 6 shows a comparison of calculated and measured injected volumes after the borehole had been filled with grout. The parameter $\Sigma b^3 = 5.5 \cdot 10^{-13}$ m^3 was determined by minimizing the sum of squared differences between them. Assuming that the whole transmissivity corresponds to one fracture gives b = 82 μm. This value is roughly the same as given as max-

- Viskosität μ_g 0,0056·$e^{0.0004t}$ Pas,
– Grundwasserdruck 3,36 Mpa,
– Bohrloch-Füllvolumen 70 l.

3.2 Phase 1 – Prüfung der Annahmen
3.2.1 Bestimmung der Strömungsdimension

Nachdem das Bohrloch gefüllt wurde (8 min), kann die korrigierte Zeit aufgrund des Injektionsdrucks und der rheologischen Eigenschaften der Mischung berechnet werden. Unter Ansatz der korrigierten Zeit, der gemessenen Rate und des verpressten Volumens kann in der Folge die Dimension der Strömung in der Kluft errechnet werden. Als Beispiele dafür werden in Bild 5 die dafür errechneten Indizes für die Dimension nach 15 min (Injektionszeit 7 min) ermittelt und gezeigt. Und obwohl eine gewisse Fluktuation des Injektionsdrucks diese berechneten Werte etwas streut, ist es wahrscheinlich, dass die Strömungsdimension der Injektion Nr. 2 auch 2,0 beträgt bzw. eine reine 2D Situation ergibt. Der durchschnittliche Wert für den Index-Parameter Q*t/V$_{average}$ beträgt 0,82.

3.2.2 Abschätzung der auf das Injektionsgut bezogenen Transmissivität (Kluftweiten)

Wie bereits in Abschnitt 2.2 erwähnt, kann das theoretische Injektionsvolumen aufgrund der Gleichungen (6) und (9) für 1D und 2D Situationen berechnet werden. Für beide muss allerdings eingeschränkt werden, dass Injektionsgut in mehrere Klüfte gleichzeitig eindringen kann, wie im Term Σwb^2 für den 1D Fall und mit Σb^3 für den 2D Fall beschrieben. Allerdings bedeutet nach der allgemeinen Pareto-Verteilung der Klufttransmissivitäten [11], dass die weiteste Kluft sowohl die Wasser- als auch die Strömung von Injektionsgut dominiert. Wenn man dafür allerdings die dritte Wurzel aus der Summe aller b^3 ansetzt, wird man einen vernünftigen Näherungswert für die größte Kluft im 2D Fall erhalten. Bild 6 zeigt einen Vergleich zwischen gerechneten und gemessenen Injektionsvolumina (nach Bohrlochfüllung). Der Ausdruck für $\Sigma b^3 = 5,5 \cdot 10^{-13}$ m^3 wurde dabei über das Minimum der quadratischen Abweichung ermittelt. Unter der Annahme, dass die gesamte Transmissivität einer einzelnen Kluft zugeordnet würde, erhält man für diese Weite den Wert b = 82 μm. Dieser Wert korrespondiert – der Größenordnung nach – gut mit dem als Maximum vorgegebenen. Für den 1D Fall muss allerdings die Breitenabmessung eines eventuellen Kanals abgeschätzt werden.

3.3 Phase 2 – Prognose
3.3.1 Berechnung von Reichweite und Injektionsrate

Wenn die Strömungsdimension in der Kluft einmal bestimmt ist, können aufgrund der Kluftweite die Reichweite und Injektionsrate errechnet werden. Bild 7 zeigt die Reichweite der Injektion nach 15 min, zusammen mit der korrespondierenden Rate.

3.3.2 Abschätzung der erforderlichen Injektionszeit (als Abbruchkriterium)

Die Injektion kann nach 15 min noch nicht als abgeschlossen betrachtet werden, weil die Verfüllung der
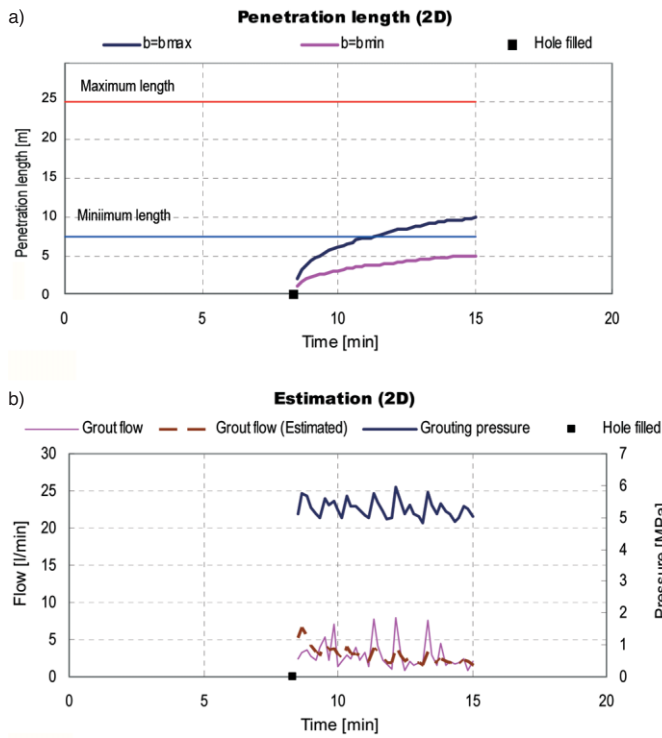
a)

b)

Fig. 7. Estimations for the 2D case up to 15 min, a) penetration distance b) grout flow
Bild 7. Abschätzung für den 2D Fall von (a) Reichweite und (b) Injektionsrate in den ersten 15 min

a)

b)

Fig. 8. Predictions over a period of 30 minutes for the 2D case using the increased grouting pressure, a) grout flow, b) penetration distance
Bild 8. Prognosen über eine Injektionsperiode von 30 min für den 2D Fall unter Anwendung erhöhter Drücke (a) Injektionsrate (b) Reichweite

imum aperture. For the 1D case, the width of the channel must also be estimated.

3.3 Phase 2 – prediction
3.3.1 Calculation of penetration length and grout flow

Once the dimensionality of the fracture has been determined, the theoretical penetration length and grout flow can be calculated based on the fracture aperture. Figure 7 shows the penetration length after 15 min and the grout flow.

3.3.2 Estimation of required grouting time stop criteria

Grouting cannot be considered complete at t = 15 min., as the grout penetration in the smallest fracture aperture to be sealed has not yet reached the target value and the grout penetration in the largest fracture is not above the limit value. It appears as though the grout penetration of the minimum fracture aperture will not reach above the required minimum value. Nor will the grout penetration for the maximum fracture aperture reach above the required maximum value for a reasonably long time to come. In this case, the grouting design should be changed by, for example, using a higher grouting pressure or a grout material with a lower viscosity.

It is possible to predict the grouting by using the estimated fracture apertures (grouted fracture "volume") Σwb^2 for the 1D case and Σb^3 for the 2D case at a certain point. However, the grouting pressure must of course be assumed in order to predict the grout flow and the grout
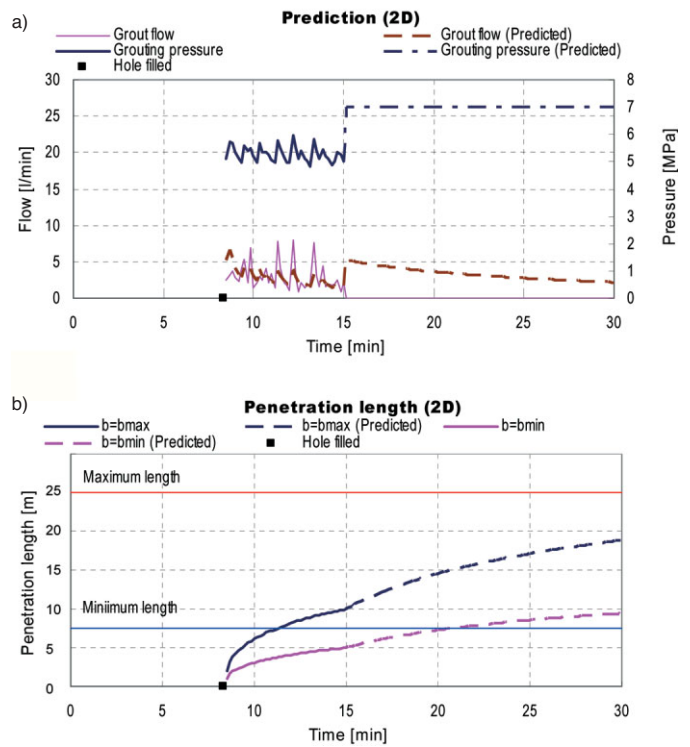
kleinsten Kluft den Zielwert noch nicht erreicht und die Verfüllung der weitesten Kluft den vorgegebenen Grenzwert noch nicht überschritten hat. Aus den gegebenen Daten muss hier allerdings vermutet werden, dass das erstere auch gar nicht eintreten wird. Noch wird die Verfüllung der größten Kluft innerhalb vernünftiger Behandlungszeit den erforderlichen Maximalwert überschreiten. In einem solchen Fall sollte das Injektionskonzept angepasst werden, etwa durch Wahl eines höheren Injektionsdrucks oder einer Mischung mit niedrigerer Viskosität.

Ab einem gewissen Punkt in der Behandlung kann damit der Injektionsvorgang aufgrund der geschätzten Öffnungsweiten (injiziertes Rissvolumen Σwb^2 für den 1D Fall und Σb^3 für den 2D Fall) prognostiziert werden. Jedoch muss dafür immer noch der relevante Injektionsdruck angenommen werden, um die Rate und Reichweite ermitteln zu können. Die Reichweite kann dabei durch einen höheren Druck vergrößert werden. In dem Fall sollte eine Berechnung für einen (Referenz)Druck von 7 bar vorgenommen werden, wie in Bild 8 gezeigt. Die Rechnung dort zeigt, dass die gewünschte Reichweite infolge erhöhten Injektionsdrucks nach 22 min eintreten wird. Dies wird daher das neue Abbruchkriterium der Behandlung in diesem Fall sein.

3.4 Phase 3 – Überwachung

Es ist bekannt, dass Injektionen im Gebirge Spannungen verursachen. Dabei muss jedoch in der Regel das Risiko unkontrollierter Verformung vermieden werden, und dies hängt mit Injektionsdruck und Volumen zusammen [12].

penetration. The penetration could be improved by increasing the grout pressure. In this case, a calculation has also been made for a pressure of 7 MPa as shown in Figure 8. The calculation gives the result that the required penetration will be achieved after about 22 minutes with increased grouting pressure. This will be the stop criterion for the grouting.

3.4 Phase 3 – controlling

Grouting will induce stresses in the rock mass. The risk of uncontrolled deformations has to be avoided and depends on pressure and volume [12]. Studies carried out by [13] showed that the risk of hydraulic uplift was better analysed by introducing grout penetration instead of volume. Since the penetration distance will be calculated during the grouting process in the real time grouting control method, it may be possible to check the risk of uplift in real time. Comparison between predicted and measured grout flow or estimation of grout transmissivity (fracture aperture) will also give a direct possibility to notice hydraulic jacking. Some examples will be shown in chapter 4.

The term uplift in this context corresponds to the ultimate bearing capacity of rock mass. Hydraulic jacking may occur at lower level [14]. It is important to point out that there are also other cases such as leakage of grout to the face or jacking the face, which also have to be considered. Such risks can be controlled by reviewing the flow-pressure data. The largest risk of uplift is connected with the greatest penetration. Therefore the penetration for the largest fracture aperture should be used in the calculations. In [13] the allowable lifting force is calculated with an assumption of a circular open fracture of the lifted rock mass geometry. Corresponding analysis has been carried for the 1D cases in [10].

4. Experience from different case histories
4.1 Case histories

The theory of grout penetration and grout flow has been tested on four projects in order to demonstrate the applicability of the theory of dimensionality, estimation of fracture apertures and theoretical grout flow. Only

Studien zu diesem Thema, ausgeführt in [13] zeigen, dass das Risiko von Hebungen besser über die Kontrolle der Reichweite zu erkennen waren als über das Injektionsvolumen. Nachdem die Reichweite nach der vorgestellten Methode hier in Echtzeit erfolgt, könnte es damit möglich werden, auch das Hebungsrisiko ebenfalls in Echtzeit zu prüfen. Der Vergleich zwischen prognostizierter Rate und die zu Injektionsgut relativierte Transmissivität (Kluftweiten) wird ebenfalls eine direkte Möglichkeit eröffnen, hydraulische ausgelöste Bewegung zu erkennen. Einige Beispiele werden dazu in Kapitel 4 gegeben

Der Ausdruck „Hebung" korrespondiert in diesem Zusammenhang mit der Bruchfestigkeit des Gebirges. Hydraulische Kluftdilatation und lokale Verschiebungen können jedoch bereits früher eintreten [14]. Es ist außerdem wichtig, hier darauf hinzuweisen, dass auch Austritte von Injektionsgut an der Ortsbrust oder Verformung derselben durch den Injektionsdruck interpretiert werden müssen. Solche zusätzliche Risiken können über die Beobachtung der Injektionsraten- und Druckdaten kontrolliert werden. Das größte Hebungsrisiko ist dabei mit der größten Reichweite verbunden. Deshalb sollte auch den entsprechenden Berechnungen die Reichweite in der weitesten Kluft zugrunde gelegt werden. In [13] wird die zulässige Hebungskraft über eine Kreisfläche unter dem Gewicht der relevanten Gebirgsgeometrie angesetzt. Entsprechende Analysen für 1D Geometrien wurden in [10] ausgeführt.

4. Erfahrungen von verschiedenen Injektionsprojekten
4.1 Fallstudien

Die hier vorgestellte Theorie der Bestimmung von Injektionsreichweite und Injektionsrate wurde an vier Projekten getestet, um die Anwendbarkeit der Theorie der Strömungsdimensionalität, der Abschätzung von Kluftweiten und der theoretischen Injektionsrate zu demonstrieren. In diesem Aufsatz werden nur relevante beispielhafte Daten und Rechengänge vorgetragen.

Die Fallstudien betreffen das Äspö Hard Rock Laboratory auf Sohle –450 m, die Northern Link Road Projekte in Stockholm und von Botniabanan sowie ein Eisenbahnprojekt in Mittelschweden. Die Daten von Äspö

Table 2. Case history summary
Tabelle 2. Fallbeispiele

Case history	Geology	Depth (data from:)	Ingress (after grouting)	Comments
Äspö	Äspö diorite, very competent	450 m	<4.5 l/min.100 m	Swedish nuclear repository research center, very good quality data [10]
Northern Link NL101	Granite, Gneiss,	10–20 m	~2 l/min.100 m	Road tunnel system, Swedish road competent administration, Long (20 m), planar and smooth fractures, bedding planes [15]
Northern Link NL34	Sedimentary gneiss, fractured	20 m	~4 l/min.100 m*	Road tunnel system, Swedish road administration, fractured rock, zones [16]
Botniabanan (E3541)	Meta greywacke, partly very fractured	80 m	~20 l/min.100 m	Rail road tunnel system, Swedish rail road administration, partly very fractured, high frequency of zones [18]

*Estimated value, project is under construction.

relevant sample data and calculations are shown in this paper.

The case histories are from Äspö Hard Rock Laboratory at the 450 m level, the Northern Link Road projects in Stockholm and from Botniabanan, a railway project in the middle of Sweden. The data from the Äspö Hard Rock Laboratory have been showed in paragraph 3 to demonstrate the application of the theory, which was performed in a very controlled environment under the supervision of SKB (Swedish Nuclear Fuel and Waste Management Co). Short summaries of the project data are shown in Table 2.

4.2 Method of analysis

The method requires logging and processing of data for each individual grout hole. This starts with the evaluation of dimensionality after about 5 to 10 min when the hole is filled. At this point an initial sum of fracture apertures is calculated. From this a theoretical flow is derived which may then be compared to the actual conditions.

4.3 Examples of applications

The data from [10] [15] [16] are shown in Figures 9 to 14. In these records it is shown that the data from the grouting hole can be used to calculate a theoretical grout flow that follows actual data fairly well. Some cases, which show hydraulic jacking, are also given.

4.3.1 Dimensionality

The dimensionality shows the dominating grout flow paths within the rock mass. Since the calculated product of $Q*t/V$ is influenced by the oscillating pump pressure, the dimensionality shows a corresponding fluctuation. In the calculations made by [16], the dimensionality is calculated with a corrected time for the 1 and 2D flow case. A correction is made for each flow case and each results in separate different dimensionality data. In Figure 9, dimensionality data are shown for a 2D and a 1D case but with both possible sets presented. As can be seen, either set gives the same interpretation of 2D flow.

In some cases (Figure 9c), the data indicate that the dimensionality can vary [10] [16] and can change from 2D to 1D and back again during the course of grouting a hole. This is not surprising however considering the heterogeneity of the rock mass and the fact that grouting is performed sequentially and each grout hole will interfere with the grouting performed previously. One should also consider the experience from exploratory water tests that indicate either erosion of fractures or clogging [1] [17]. Other explanations could be elastic deformations in the rock mass [4] or block movements within the rock mass. For these cases, the calculated theoretical flow can be adjusted after the dimensionality for a fairly good fit.

4.3.2 Prediction of grout flow

After the dimensionality of the hole has been evaluated, the sum of fracture apertures and theoretical flow can be calculated. The calculated flow in Figure 10 is related to
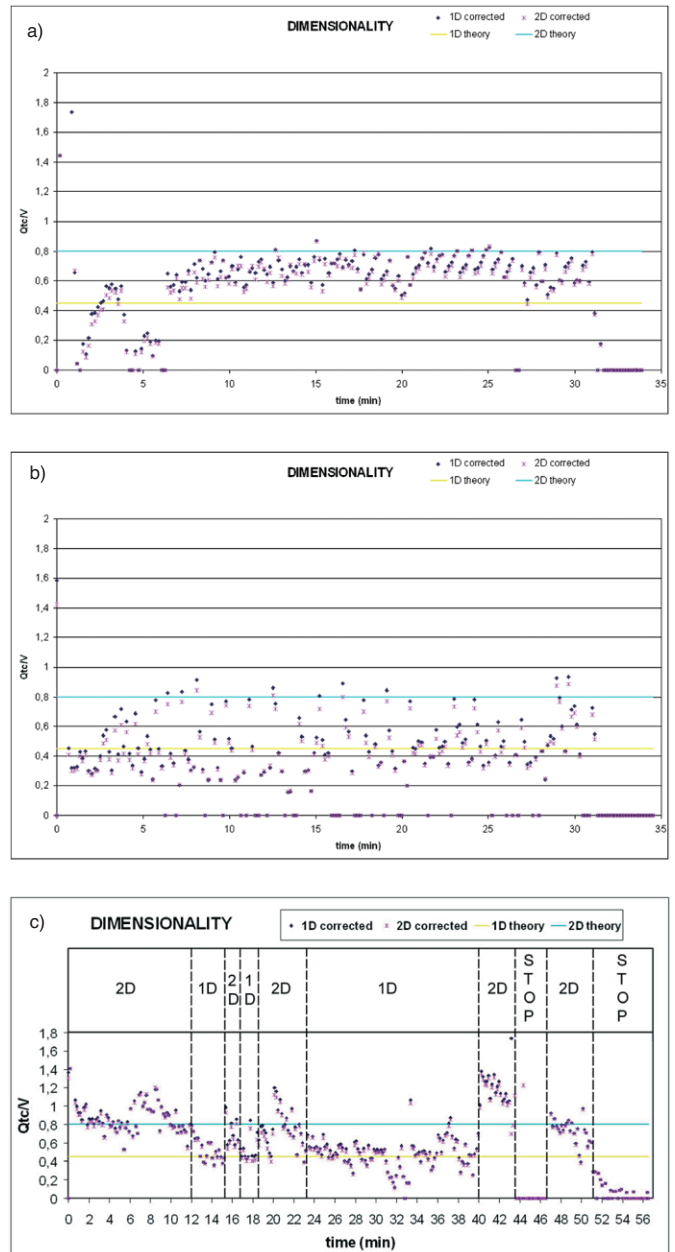

Fig. 9. Dimensionality: a) 2D flow (hole 31, fan 6); b) 1D flow (hole 1, fan 7); c) varying flow 2D to 1D to 2D (hole 22, tunnel 301, section 1547)
Bild 9. Dimensionalität: (a) 2D Fließen (Bohrloch 31, Schirm 6); (b) 1D Fließen (Bohrloch 1, Schirm 7); (c) unterschiedliche Rate 2D zu 1D zu 2D (Bohrloch 22, Tunnel 301, Abschnitt 1547)

Hard Rock Laboratory wurden bereits in Abschnitt 3 vorgestellt, um dort die Anwendung der Theorie zu präsentieren, weil diese unter sehr kontrollierten Bedingungen und unter der Aufsicht der SKB (Swedish Nuclear Fuel and Waste Management Co) erfolgten. Eine kurze Zusammenfassung der charakteristischen Daten dazu kann man der Tabelle 2 entnehmen.

4.2 Methodik der Analysen

Die Methodik verlangt die Analyse aller relevanten Daten von jedem behandelten Bohrloch. Dieser Vorgang beginnt mit der Auswertung zur Dimensionalität der Strömungsre-

Fig. 11. Possible uplift or jacking of the rock mass, hole 2, section 267, 2D flow, NL101
Bild 11. Mögliche lokale oder generelle Hebung des Gebirges, Bohrloch 2, Abschnitt 267, 2D Fließen, NL101
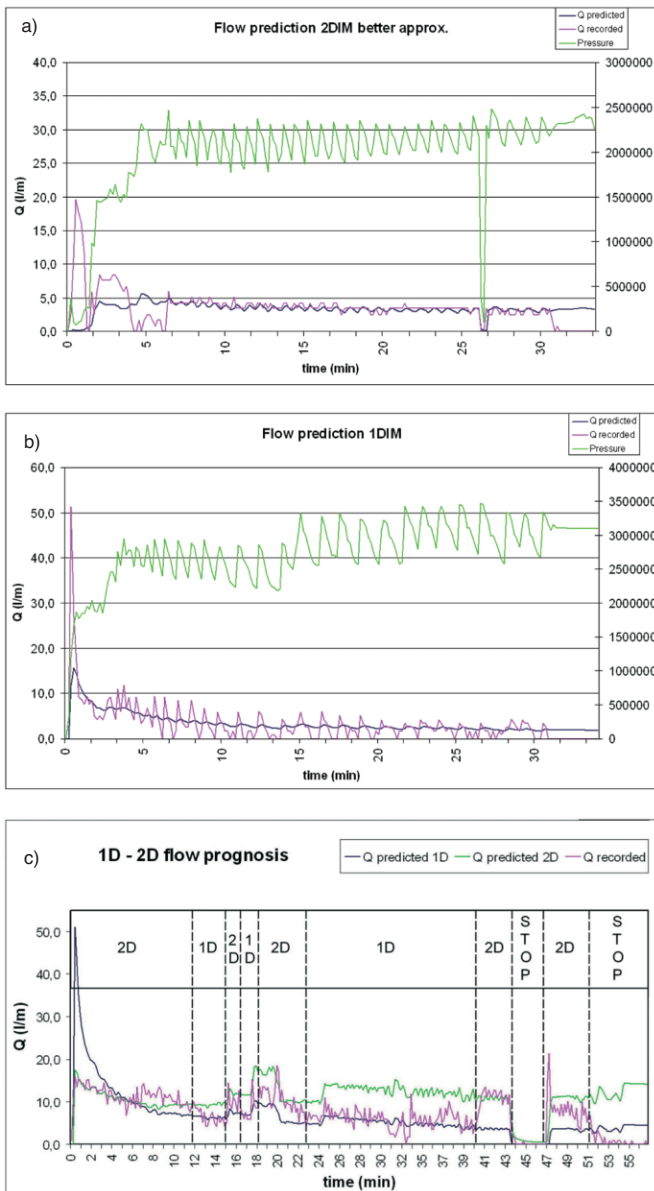
Fig. 10. Comparison between measured and predicted flow: a) 2D flow (hole 31, fan 6); b) 1D flow (hole 1, fan 7); c) varying flow (hole 22, tunnel 301, section 1547)
Bild 10. Vergleich zwischen gemessenen und prognostizierten Raten (a) 2D Fließen (Bohrloch 31, Schirm 6); (b) 1D Fließen (Bohrloch 1, Schirm 7); (c) unterschiedliche Rate (Bohrloch 22, Tunnel 301, Abschnitt 1547)

the dimensionalities in Figure 9. The calculation of the theoretical flow follows the pressure curve and the resulting theoretical flow curve can be compared to the actual recorded values. In the figure, the nominal Q-predicted is used as the theoretical flow.

As can be seen in Figure 10c where both 1D predicted flow (pink) and 2D predicted flow (green) are shown, the recorded grout flow follows the respective theoretical curve according to the varying dimensionality.

4.3.3 Jacking

Sometimes, other anomalies have been recorded during grouting. These include uplift or jacking of the ground for shallow grouting operations (Figures 11 and 12). Other
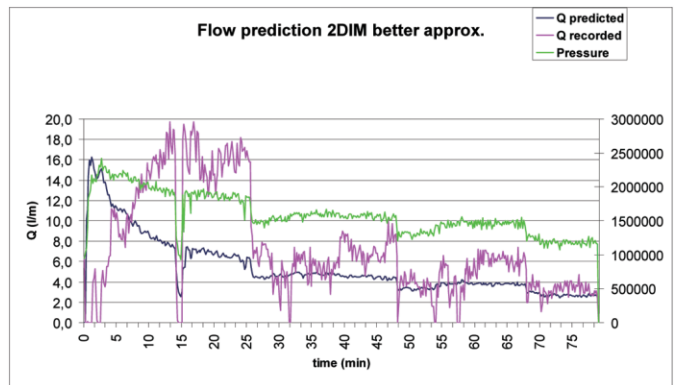
gime 5 bis 10 min nach erfolgreicher Bohrlochfüllung. Zu diesem Zeitpunkt wird eine erste Summe aller Kluftweiten errechnet. Daraus folgt die theoretische Ermittlung einer entsprechenden Rate, welche sodann mit der tatsächlichen verglichen wird.

4.3 Beispiele von Anwendungen

Die Daten für [10] [15] [16] sind in den Bildern 9 bis 14 zusammengefasst. In diesen Aufzeichnungen wird gezeigt, dass es sehr gut gelingt, die Berechnungen zur theoretischen Rate aus den individuellen Bohrlochdaten mit den tatsächlich registrierten Werten in Übereinstimmung zu bringen. Einige Fälle, in denen hydraulische Verformung vorkommt, werden ebenfalls gezeigt.

4.3.1 Strömungsdimensionalität

Mit dem Index für die Dimensionalität gelingt es, die dominante Geometrie der Strömungswege im Fels abzubilden. Weil aber das errechnete Produkt aus Q*t/V durch den oszillierenden Pumpendruck beeinflusst wird, zeigt auch die Dimensionalität entsprechende Fluktuation. In den Berechnungen in [16] wird die Dimensionalität der Strömung mit einer korrigierten Zeit für 1D und 2D Fälle gerechnet. Eine solche Korrektur wird für jeden der betrachteten Fälle des Fließens gemacht, und jeder dieser Fälle mündet daher in einen jeweils anderen Dimensionalitätsindex. In Bild 9 werden Daten für die Dimensionalität jeweils für einen 2D und einen 1D Fall gezeigt, jedoch jeweils auch mit beiden möglichen Datensätzen. Wie man sehen kann, ergibt jeder der Sätze dieselbe Interpretation einer zweidimensionalen (2D) Ausbreitung.

In einigen Fällen sieht man (Bild 9c), dass sich die Dimension der Strömung verändern kann [10] [16] und sich während des Verlaufs der Injektion in einem Bohrloch (Passe) etwa von einem 2D Regime zu einer 1D Strömung und wieder zurück wandeln kann. Das überrascht allerdings dann nicht, wenn man die Heterogenität des Gebirges in Betracht nimmt und die Tatsache berücksichtigt, dass Injizieren ein sequenzieller Vorgang ist, bei dem aufeinanderfolgende Bohrlöcher mit der jeweils vorangegangenen Behandlung interferieren können. Darüber hi-
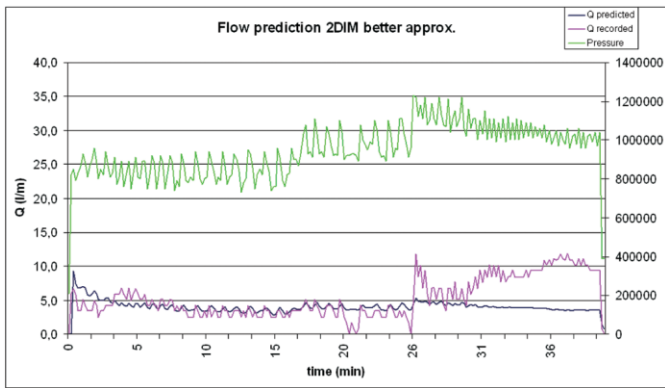
Fig. 12. Possible uplift or jacking of the rock mass, hole 16, fan, 2D flow
Bild 12. Mögliche lokale oder generelle Hebung des Gebirges, Bohrloch 16, Schirm, 2D Fließen

Fig. 13. Possible jacking influencing a local area of the rock mass, 2D flow
Bild 13. Mögliche lokale Hebung mit Einfluss auf ein nur beschränktes Umfeld, 2D Fließen

anomalies seem to influence smaller areas of the rock mass (Figure 13).

An example of probable jacking with an increasing grout flow for an almost constant pressure comes from the NL101. As can be seen in Figure 11, the pressures are subsequently lowered resulting in an immediate reduction in grout flow but the subsequent trend is that the flow increases. This indicates a probable jacking or uplift of the rock mass (the rock cover was about 10 m during this grouting round).

A similar case from NL33, 34 is shown in Figure 12 where after 26 minutes of grouting the pressure is increased, resulting in an immediate increase in flow. After this possibly local jacking, the flow goes down followed by a continuous increase in flow until the grouting is aborted after about 40 minutes in spite of the fact that the pressure was reduced.

In Figure 13, the grout pressure is increased with a small amount giving a non-proportional increase in grout flow. Later on grout flow diminishes, indicating that the action in the rock mass is more localised, including possible rock movements in the fracture zone opening one fracture and closing others.

Another example of rock movements, under about 80 m of rock cover, comes from the E3541 (Figure 14). In this example, the grout pressure suddenly drops and the grout flow increases. The rock mass in this area was locally heavily fractured, which can also be concluded from grout flow (20 l/min) before jacking. Prediction and recorded grout flow curve are quite close up to about 15 min after the start of grouting. The sudden increase in grout flow is clearly not proportional to the theoretical curve. The reason was possible jacking or face instability resulting in the large grout flow (up to 60 l/min). After this, grouting was stopped and a thicker grout was used.

5 Conclusion

In the paper the concept of "real time grouting control method" is described for the calculation of grout penetration and the control of grouting in real time by applying new theories for grout spread. The stop criterion is related to the achieved grout spread, and grouting is considered completed when the grout penetration for the smallest
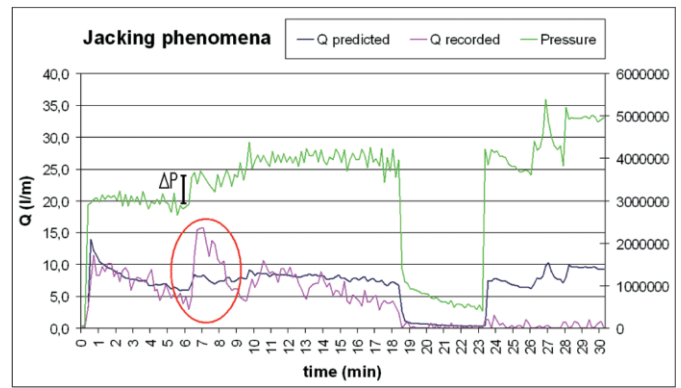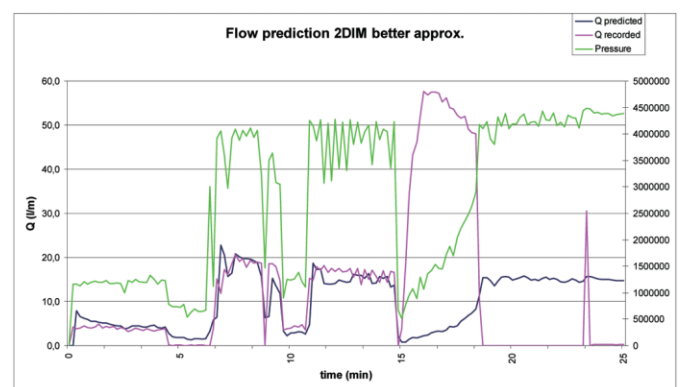

Fig. 14. Possible jacking or face instability resulting in large grout flows from E3541, hole 18, section 517790; modified after [18]
Bild 14. Mögliche örtliche Verformung oder instabile Ortsbrust mit infolge großer Injektionsraten aus E3541, Bohrloch 18, Abschnitt 517790, modifiziert nach [8]

naus ist auch die bekannte Erfahrung aus Wasserabpressversuchen gültig, dass Kluftfüllungen erodieren oder durch Suffusion zu Verstopfung neigen können [1] [17]. Weitere andere Erklärungen können in elastischer Verformung des Gebirges [4] oder in Blockbewegungen innerhalb des Felsverbands gefunden werden. In solchen Fällen kann die theoretisch errechnete Rate über die Dimensionalität zu einer zufriedenstellenden Übereinstimmung gebracht werden.

4.3.2 Prognose der Injektionsrate

Nachdem die Dimensionalität des Bohrlochs (der Passe) auf diese Art ausgewertet ist, können die Summe der Kluftweiten und der theoretische Fluss an Injektionsgut berechnet werden. Die so in Bild 10 errechneten Raten stehen in Beziehung zu den Indizes der Dimension des jeweiligen Strömungsregimes in Bild 9. Die Berechnung der theoretischen Rate folgt der Druckkurve, und die sich daraus ergebende Ratenkurve kann gut mit den Feldaufzeichnungen verglichen werden. In der erwähnten Abbildung wird die nominell prognostizierte Rate als Wert für die theoretische Rate verwendet.

fracture to be sealed is above a predetermined target value, or before the grout penetration for the largest fracture reaches a certain maximum limiting value.

Online monitoring allows the prediction of the course and the spread of the grout flow and also analysis of the risk of uplift and jacking. The most significant action resulting from the examples presented would have been the indication when to abort grouting or lower the grout pressures. Data from four tunnel projects in Sweden prove with their trends that calculated flow dimensionality, the calculated fracture apertures and the calculated grout flows were quite close to those measured. This indicates that the real time grouting control method is reasonably applicable to grouting design and control.

References

[1] *Houlsby, A.C.*: Construction and design of cement grouting. New York: John Wiley & Sons, 1990.

[2] *Lombardi, G.*: The Role of Cohesion in Grouting. ICOLD, 1985.

[3] *Hässler, L., Stille, H. and Håkansson, U.*: Simulation of grouting in jointed rock. Proc. 6th International Congress on Rock Mechanics, Vol. 2, pp 943–946. Montreal, 1988.

[4] *Gustafson, G. and Stille, H.*: Prediction of groutability from grout properties and hydro geological data. Tunnelling and Underground Space Technology 11 (1996), No. 3, pp 325–332.

[5] *Eriksson, M., Stille, H. and Andersson, J.*: Numerical calculations for prediction of grout spread with account for filtration and varying aperture. Tunnelling and Underground Space Technology 15 (2000), No. 4, pp 353–364.

[6] *Gustafson, G. and Claesson, J.*: Steering Parameters for Rock Grouting, Submitted to Journal of Rock Mechanics and Mining Science. 2005.

[7] *Hässler, L.*: Grouting of rock – Simulation and classification. PhD Thesis, Royal Institute of Technology, Stockholm., 1991.

[8] *Gustafson, G. and Stille, H.*: Stop criteria for cement grouting, Felsbau 23 (2005), No. 3, pp 62–68.

[9] *Kobayashi, S. and Stille, H.*: Design for rock grouting based on analysis of grout penetration. Verification using Äspö HRL data and parameter analysis. R-07-13, Swedish Nuclear Fuel and Waste Management Company. Stockholm, 2007.

[10] *Kobayashi, S., Stille, H., Gustafson, G. and Stille, B.*: Real Time grouting Control Method, Development and application using Äspö HRL data. R-08-133, Swedish Nuclear Fuel and Waste Management Company. Stockholm, 2008.

[11] *Gustafson, G. and Fransson, Å.*: The use of the Pareto distribution for fracture transmissivity assessment. Hydrogeology Journal (2005) No. 14, pp. 15–20.

[12] *Lombardi, G. and Deere, D.*: Grouting design and control using the GIN principle. Water Power and Dam Construction, June 1993, pp. 15–22.

[13] *Brantberger, M., Stille, H. and Eriksson, M.*: Controlling the grout spread in tunnel grouting – Analyses and developments of the GIN-method Tunneling and Underground Space Technology 15 (2000), No. 4, pp 343–352.

[14] *Gothäll, R. and Stille, H.*: Fracture dilation during grouting, Tunnelling and Underground Space Technology 24 (2009), pp 126–135.

[15] *Bohlin, M. and Urtel, K.*: Utvärdering av injekteringsutförände – Fallstudie av NL101 och Hornsberg, Stockholm. Master Thesis, Division of Soil and Rock Mechanics, Royal Institute of Technology, 2008.

Wie aus Bild 10c ersichtlich (prognostizierte Rate für 1D Fließen in rosa und prognostizierte Rate für 2D Fließen in grün) folgt der gemessene Verlauf der Rate über die Zeit tatsächlich dem theoretische prognostizierten Verlauf entsprechend der jeweils sich ändernden Strömungsdimension.

4.3.3 Lokales Anheben und Rissdilatation

Gelegentlich wurden auch andere Anomalien zum Verlauf der Injektionen berichtet. Diese beziehen sich auf Hebungen oder Verschiebungen des Untergrunds im Falle seichter Einsätze unter Gelände (Bilder 11 und 12). Andere Anomalien scheinen sich auf nur kleinere Bereiche des Untergrunds zu beziehen (Bild 13).

Ein Beispiel für mögliches örtliches Anheben des Gebirges gefolgt von einem fast gleichbleibenden Injektionsdruck kann in NL101 beobachtet werden. Wie aus Bild 11 ersichtlich, wurden die Drücke in der Folge gesenkt, was zwar zu einer sofortigen Reduktion der Rate führte, aber sich später dieser Trend wieder umkehrte und die Rate wieder anstieg. Dies ist ein Hinweis auf wahrscheinliches örtliches Anheben oder eine generelle Hebung des Felsverbands (die Felsüberlagerung betrug über dieser Injektionsanwendung etwa 10 m).

Ein ähnlicher Fall ergab sich in NL33 und 34 und ist in Bild 12 dargestellt. Dort wurde der Druck nach 26 min gesteigert, was auch zu einer spontanen Steigerung der Rate führte. Nach diesem möglicherweise örtlich begrenzten Anheben geht dort die Rate wieder zurück, wird aber gefolgt von einem neuerlichen stetigen Anstieg, bis die Injektion nach 40 min abgebrochen wurde, obwohl der Druck abfiel.

In Bild 13 wurde der Injektionsdruck um nur ein kleines Inkrement erhöht, was dort zu einem überproportionalen Anstieg der Rate führte. Später reduzierte sich die Rate – was auf eine eher örtlich begrenzte Reaktion im Gebirge schließen lässt; einschließlich möglicher Bewegungen in einer Bruchzone, wo möglicherweise eine Kluft geöffnet und andere wieder geschlossen wurden.

Ein weiteres Beispiel von Bewegungen im Fels (unter 80 m Überlagerung) stellt E3541 dar (Bild 14). In diesem Beispiel fällt der Injektionsdruck plötzlich ab, und die Rate steigt an. Das Gebirge war in diesem Bereich stark geklüftet, was auch aus den Raten (20 l/min) vor der Verformung geschlossen werden kann. Prognose und tatsächliche Ausführung der Raten über die Zeit sind dabei bis 15 min nach Injektionsbeginn fast deckungsgleich. Der dann erfolgende plötzliche Anstieg der Rate ist aber deutlich abweichend vom theoretischen Verlauf. Die mögliche Begründung dafür lag in lokaler Hebung oder Instabilität der Ortsbrust mit einem damit verbundenen Ansteigen der Rate auf bis zu 60 l/min. Danach wurde die Injektion gestoppt und eine dickere Mischung zum Einsatz gebracht.

5 Schlussfolgerung

In dieser Präsentation wird das Konzept einer „Echtzeit Injektions Kontrollmethode" vorgestellt, mit der die Ermittlung der Reichweite und eine Echtzeit Prozesskontrolle – unter Anwendung neuartiger Theorien zur Injektionsgutausbreitung – möglich werden. Das Abbruchkriterium

[16] *Bruno, A.*: Grouting operation monitoring and analysis of the "Real Time Grouting Control" method. Master Thesis at KTH and Politecnico di Torino, 2009.

[17] *Eriksson, M. and Stille, H.* Cementinjektering i hårt berg (Grouting with cement based grout in hard jointed rock). SveBeFo, Stockholm, 2005.

[18] *Stille, B. and Anderson, F.*: Injektering – tillämpning av injekteringsforskning i fält. Pre-grouting – application of grouting research in the field. Stockholm, SveBeFo rapport 79, 2008.

ist auf die erzielte Ausbreitung abgestellt, und der Vorgang ist dann als abgeschlossen betrachtet, wenn die Verfüllung der kleinsten zu behandelnden Kluft ein bestimmtes vorgegebenes Maß überschritten hat oder bevor die Verfüllung der größten zu behandelnden Kluft einen vorgegebenen Maximalwert erreicht.

Die online Beobachtung des Prozesses erlaubt die Prognose des Verlaufs und der Injektionsgutausbreitung bzw. die Analyse der Risiken von generellen oder lokalen Hebungen. Das wesentlichste Ergebnis aus den vorgestellten Beispielen ist die neuartige Möglichkeit zu erkennen, wann die Injektion abgebrochen, oder der Injektionsdruck gesenkt werden muss. Die Daten von vier Tunnelprojekten in Schweden bestätigen dabei tendenziell, dass die errechneten Strömungsdimensionen, die errechneten Kluftöffnungsweiten und die errechneten Injektionsraten den jeweils gemessenen Werten sehr nahe kamen. Dies weist darauf hin, dass diese Echtzeit Injektions Kontrollmethode zur Anwendung für Injektionsplanungen und der Kontrolle von Ausführungen durchaus anwendbar ist.
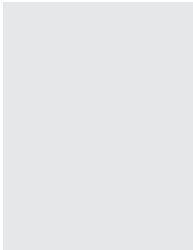
Björn Stille, M.Sc. Civil Engineering
Vattenfall Power Consultants AB
Jämtlandsgatan 99
PO Box 527
SE-162 16 Stockholm
Sweden
Bjorn.stille@vattenfall.com

Professor Gunnar Gustafson
Chalmers University of Technology
GEO Division
S-412 96 Göteborg
Sweden
gunnar.gustafson@chalmers.se

Professor Håkan Stille
KTH Royal Institute of Technology
Soil and Rock Mechanics
SE-100 44 Stockholm
Sweden
hakan.stille@byv.kth.se
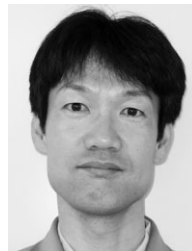
Shinji Kobayashi, M.Sc.
Shimizu Corporation
Shibaura 1-2-3, Minato-Ku
105-8007 Tokyo
Japan
shinji.kobayashi@shimz.co.jp

Distribution of rock mass hydraulic conductivity and its application on rock engineering problems.

Björn Stille[a,b] M.Sc. Civil Engineering

Corresponding author: +46-(0)72 71 650 66, bjorn.stille@sweco.se

[a]Sweco Civil AB, P.O.Box 34044, SE-100 26 Stockholm, Sweden

[b]Division of GeoEngineering, Chalmers University of Technology, SE-412 96 Göteborg, Sweden

Håkan Stille[c] Prof.

[c]Royal Institute of technology, division of soil and rock mechanics, SE-100 44 Stockholm, Sweden

Abstract

The engineering works of tunnel construction include technical/economic and environmental considerations. The groundwater situation is often considered by the environmental court rulings and put requirements and restrictions on the design and the execution of the works. As the groundwater is influenced by the seepage into a tunnel the relevant value of mean hydraulic conductivity is investigated through probe drilling and tests. However, there is a large variation in measured data and little guidance for interpretation. This paper propose a method to describe the distribution of transmissivity data and an analyze method to scale the test measurements to a relevant scale or length. Four cases are presented where the water pressure tests performed in the grout holes are analyzed and the lognormal distribution parameters are identified. Two of the cases are analyzed with the proposed method to study the scale effects. The results illustrate the consequence on the geometrical mean values for different test interval lengths. For one grout fan, of about 20 grout holes, water pressure tests were performed with both 3 m and 20 m interval lengths in the same hole. These tests are compared to the theoretical result with good match up.

The seepage through the rock mass is discussed as well as recommendations of relevant flow regimes depending on the engineering problem. The different mean values that can be used are also discussed in relation to the flow regimes.

Keywords: grouting, hydraulic conductivity, distribution, scale, mean values, groundwater flow.

1. Introduction

As a part of the engineering works for tunnel construction, the environmental impacts of the tunnel need to be considered. These are usually both of temporary and permanent nature, where vibrations from drilling and blasting (including sound and air-pressure waves) are typical temporary effects and lowering of the groundwater table, settlements etc. are considered permanent or semi-permanent effects. One important aspect for tunnel construction under Scandinavian conditions is sealing of the (usually) hard crystalline rock to avoid lowering of the groundwater table and environmental damages. In parallel with the environmental issue of groundwater control are the economic aspects of grout time, overly large grout penetration and grout take. The key issue related to both

environment and economy will be to predict the water seepage into the tunnel and to seal the tunnel to a sufficient level.

Several studies on geohydrological conditions, water seepage and grouting have been carried out e.g by Gustafson (2009) who summarizes some of the works performed at the Äspö hard rock laboratory for the Swedish nuclear waste repository research. The studies at Äspö show that there is a scale effect between shorter water pressure test intervals and pressure tests for longer intervals and complete holes. Gustafson also discusses which mean value of the hydraulic conductivity, k [m/s] (arithmetic, geometrical and 3D or harmonic) that should be used when calculating water seepage into a tunnel and shows that these values tend to converge towards the arithmetic mean for longer distances. The geometrical mean of the hydraulic conductivity are however often used for water seepage calculations. Furthermore these are often based on the relatively short (3 m) interval test lengths. The Transmissivity, T m^2/s, is sometimes used as an alternative to hydraulic conductivity and is the conductivity times the length of the tested borehole section. The transmissivity is thus scale dependent.

The most common sources of geohydrological information for Scandinavian tunneling projects with regards to hydraulic properties comes from water pressure tests in 3 to 9 m lengths (Axelsson et al 2007). Sometimes performed as double packer tests (the tested part of the bore hole is closed off by two packers) but often from single packer tests (where one packer is used to measure every 3 m and the results are subtracted from the previous measurement to produce the result for a specific part of the bore hole). During construction, and as a part of the grouting works, water pressure tests are sometimes performed, as was the case for the Namntall tunnel as described by Stille&Gustafson (2010). The accuracy of such 'during construction' methods varies depending on the equipment and at the Namntall project it was concluded that results below 0,2 and over 4 Lugeons (liter/min.m.MPa) were unreliable (corresponding to a transmissivity of T = $7,4 \cdot 10^{-7}$ and $1,5 \cdot 10^{-5} \ m^2/s$).

The main focus for this paper are the statistical distribution of the water pressure tests and the transmissivity calculated from these tests, the theory and method for scaling the distribution to the appropriate level and finally to analyze the size of the probability that the rock mass has an mean hydraulic conductivity lower than a set value. Three important issues need to be considered.

1. The distribution of hydraulic conductivity in the rock mass.
2. The influence of the scale
3. Water seepage flow regimes and appropriate mean values for the seepage calculations

The paper has the following disposition:

In section 2 is the effective hydraulic conductivity and mean values discussed.

In section 3 is a statistical analysis performed on four cases with water pressure test data to predict the transmissivity distribution on a tunnel. The studied cases are described in appendix A and the statistical distribution is described in appendix B.

In section 4 is the influence of scale (section length) studied on the mean properties of the lognormal distribution shown with data from the water pressure tests. The theory for scaling data is shown in appendix C.

Section 5 concludes the paper and includes a discussion on the water seepage analysis is discussed demonstrating the need for an observational approach regarding the grouting process and the water seepage into tunnels.

2. Effective hydraulic conductivity and mean values

The starting point for most analytical solutions of water seepage is based on Darcy´s law where the water flow, q, is calculated with a gradient, i, and a material property, k, hydraulic conductivity.

$$q = KA \cdot i$$

The hydraulic conductivity, K, is defined as the rate of volume flow across a unit area ($m^3 \cdot m^{-2} \cdot s^{-1}$) and is a property for a porous media with a unit [m/s]. The water flow through a rock mass however, occurs in the rock fractures. The flow property of a fracture is often described with the transmissivity, which can be estimated from hydraulic water pressure tests or inflow tests with the well-known Moye´s equation, Moye (1967):

$$T = \frac{q}{2\pi dH}\left(1 + ln\left(\frac{L}{2R_w}\right)\right)$$

There are a number of equations similar to Moye´s where the factor within the parenthesis is evaluated differently. The difference is depending on the assumptions of the effect of point or linear sources or the influence of 3d conditions for the tested length as is discussed by for example Barker (1988) and Ylinen (1994). However, the choice of equation may indicate that there may be a non-negligible model error in the calculation of the transmissivity and hydraulic conductivity. The difference for a tested interval length of 3 - 9 m water pressure test is about 25% - 20% between Ylinen (smaller) and Moye (larger value), as is discussed in Sturk et al (2013).

The transmissivity is related to the hydraulic conductivity with the equation:

$$T = K \cdot L$$

The transmissivity has a relationship to the width of the fracture through the well-known cubic law Snow (1968), de Marsily (1986).

$$T = \frac{\rho \cdot g \cdot b^3}{12 \cdot \mu}$$

The equation is based on the assumption of water flow through a plane with parallel walls separated by the fracture width b. The width b is in this context referred as the hydraulic fracture width, b_{hyd}, which is generally smaller than the mean fracture width (Hakami, 1995 and Tsuji et al, 2012). The transmissivity for each individual fracture can be summed up for a total transmissivity over an interval.

The gradient, or driving force behind the water flow through the rock mass depend on the length of the flow path and the pressure difference. If the tunnel or dam is grouted the gradient is often assumed to act over the thickness of the grouted zone or around it.

As has been shown in numerous papers are the transmissivities or hydraulic conductivities in a rock mass neither uniform nor isotropic but vary considerably from rock volume to rock volume. The measurements show that the rock mass transmissivities can be described statistically. It is therefore interesting to study the distribution and the influence of studied rock volume, Holmen (1997), with respect to size and mean values. From an engineering point of view the calculation of water inflow to a tunnel or under a dam should be done with as much precision as possible to define the requirements on the grouting works but also with regards to the environmental court rulings. This in turn requires either the use of relevant mean values or the whole statistically described distribution.

When evaluating the mean hydraulic properties of the rock mass, Gustafson (2009) suggest, based on the Äspö hard rock laboratory data see Rhen et al (1997) for example, that three different levels could be considered.

1. Small scale – fractures (size: individual fractures)
2. Mid-scale – stochastic continuum where the interval transmissivities can be described as lognormal distributed. (size: 3-30 m)
3. Large scale –homogenous medium (size: 500 – 1000 m)

Gustafson indicate in the division of different scales that the statistical models for estimating the distribution of the hydraulic properties are different. For the small scale the individual fracture transmissivity can be calculated and used as an estimate for water seepage. The fracture distribution is often described as Power law or Pareto distributed. For the mid-scale several fractures intersect the test section or the tunnel and fracture independence cannot be assumed. Instead the interval transmissivities are a better description of the hydraulic properties of this scale. The interval transmissivities for the mid-scale are in this investigation and in several reports e.g. de Marsily (1986) described as lognormal distributed. For the large scale the rock mass can, for some cases, be described as a homogenous porous medium according to Gustafson (2009). For such a large scale the properties of the whole rock mass is estimated as a constant corresponding to the arithmetic mean value.

The division into these three scales is not without discussion and differing opinions. The large scale (500 – 1000m) is in Gustafson (2009) referred to as the REV (representative elementary volume) for which the rock mass can be described as a homogenous medium. However, several papers e.g. Wang et al (2002) show that the REV is considerably smaller down to about 10 m, Table 1.
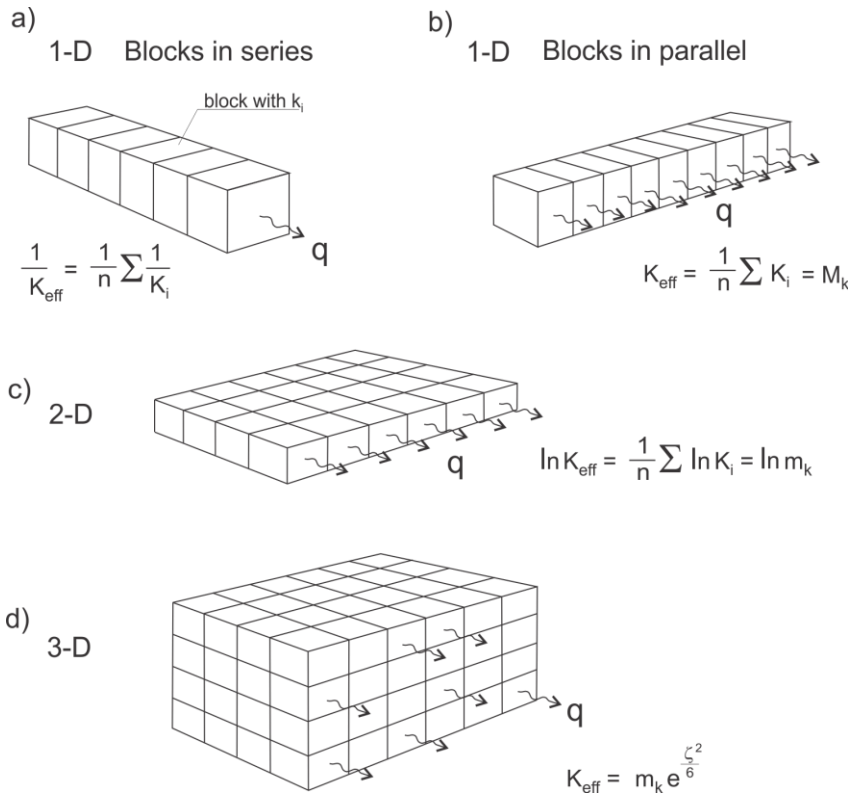
Table 1.   **REV Paper review summary.**

Paper	REV	Study	Comments
Numerical estimation and prediction of stress dependant permeability tensor for fractured rock masses [1]	13x13 m; 14x14 m	Numerical model with mean fracture aperture 4 mm (frac set 1) and 2 mm (frac set 2)	The REV is in this paper more of a function of fracture length and spacing related to the side length of the model. It is not a REV for a transmissivity distribution in the rock mass.
Evaluation of the representative elementary volume (REV) of a fractured geothermal sandstone reservoir [2]	10x10 m	Numerical model with constant fracture aperture, 200 μm. Fracture length mean 1,7 m and standard deviation 0,6 m	The REV in this paper is the volume where the assumed fracture length variation no longer influences the hydraulic conductivity. It is not a REV for a transmissivity distribution in the rock mass.
Estimation of REV size and three-dimensional hydraulic conductivity tensor for a fractured rock mass through a single well packer tests and discrete fracture fluid flow modeling[3]	15x15x15 m	Numerical 3D model seemingly considering variation in interval transmissivities. Fracture length mean variation 0,98 to 2,5 m and standard deviation 2,27 to 4,12 m	The real variation in interval transmissivities is not used, the data show a variation of about 400x but the analyzed variation seems to be truncated. The REV shows the influence of the variation of fracture length and not for a transmissivity distribution in the rock mass.
REV and its properties on fracture system and mechanical properties, and an orthotropic constitutive model for a jointed rock mass in a dam site in China [4]	25x25x25 m	Numerical 3D model studying REV for mechanical properties considering fracture length variation 2,82 to 4,2 m with a standard variation 1 ,32 to 2,73 m	The analysis is performed without including the long fracture set (mean 22 m). It seems reasonable that the existence of such a long fracture may influence the behavior of the model. The analysis is not relevant for transmissivity variations in a rock mass.

[1] He et al 2012, [2] Müller et al 2009, [3] Wang et al 2002, [4] Wu & Kulatilake 2012

These papers present different conclusions but they do not seem to disapprove the hypothesis by Gustafson (2009) that the large scale behavior (with mean properties as governing parameters) would be about 500 – 1000 m. This literature review is not conclusive and there certainly exist other papers with perhaps more relevant analysis of REV:s that may show other conclusions.

Holmen (1997) defined the effective hydraulic conductivity for a rock volume as a representative mean value depending on the flow regime and the statistical distribution of the hydraulic conductivity. The flow regime in turn depends on the heterogeneity of the rock mass. The different flow regimes are shown in Figure 1, and the effective hydraulic conductivity is defined by the harmonic-, arithmetic- and geometric mean values, with special consideration for the 3D flow case. The harmonic mean is relevant for a flow through a series of blocks, the arithmetic mean for parallel blocks, the geometric mean for a plane of blocks and the 3D-value for a volume of blocks. The 3D value is calculated according to "Matherons conjecture" for 3 dimensions. What type of flow that is relevant for the engineering problem should be evaluated from situation to situation and should consider the geometry, rock quality, rock cover, flow path and the size of each block. The use of the different mean values could also be used for an estimate of upper and lower boundaries of the hydraulic conductivity where for example the arithmetic mean could be considered as an upper boundary and the geometric mean the lower boundary. The spatial correlation should also be considered whereas the blocks in the model are considered as independent with individual hydraulic conductivity. The influence of heterogonous conditions (such as fracture zones) could influence and change the relevant model and therefore the relevant mean for the engineering problem.

a)
1-D   Blocks in series

block with k_i

$$\frac{1}{K_{eff}} = \frac{1}{n}\sum\frac{1}{K_i}$$

q

b)
1-D   Blocks in parallel

q

$$K_{eff} = \frac{1}{n}\sum K_i = M_k$$

c)
2-D

q

$$\ln K_{eff} = \frac{1}{n}\sum \ln K_i = \ln m_k$$

d)
3-D

q

$$K_{eff} = m_k e^{\frac{\xi^2}{6}}$$

Figure 1.   **Flow regimes and corresponding effective hydraulic conductivity (K_{eff}). n is the number of blocks and K_i is the hydraulic conductivity of each block, M_k is the arithmetic mean value and the m_k is the median value and ξ^2 is the variance of $\ln K_i$. Holmen (1997).**

The distribution of block hydraulic conductivities is important in principle since it influences the effective hydraulic conductivity of the flow regimes. The identification of relevant statistical distribution for section transmissivities was performed by for example De Marsily (1986), identifying the lognormal distribution as relevant for most data. The distribution and the up scaling of measured data to relevant block volumes were previously discussed by Holmen (1997).

3. Evaluation of lognormal distribution parameters of section transmissivity for different cases

The evaluation lognormal distribution parameters have been performed for four cases, Appendix A. For these cases the water pressure test results from the tunneling operation are analyzed and the lognormal distribution, Appendix B, is fitted to the measured data. The lognormal distribution have a mean value of μ (=E(X)) and a variance of σ^2. A property of the lognormal distribution is that the log values of the stochastic variate (transmissivity) is normal distributed with a mean value of λ (=E(lnX)) and a variance = ξ^2.

The water pressure tests (WPT) presented in this analysis are performed in the grout holes over the whole bore hole length for a limited time, 3 – 5 min, with a pressure of 0,5 MPa above the groundwater pressure. The transmissivities are calculated from the WPT tests and are presented as CDF's "Grouthole test results" in the figures.

The transmissivity values from the water pressure tests are fitted to a lognormal distribution. The lognormal distribution has the property that the log values of the stochastic variate (X) are normal

distributed with E(lnX)= λ and a Variance = ξ^2. The case records are presented with the statistical values of the normal distribution of ln(X) and the mean transmissivity value, T_μ, and the standard deviation T_σ (Figure 2, Figure 3, Figure 4 and Figure 5). The application of the lognormal distribution and the identification of the mean value and the standard deviation should be performed for the range of reliable data. The easiest way to perform such a curve fitting is to manually change the λ and the ξ values until a good fit is achieved.

Presented data

The transmissivity results (over a section length of 20 m) and the transmissivity data are presented in the figures. The largest discrepancies are both for small and high values, as expected due to larger measurements errors.
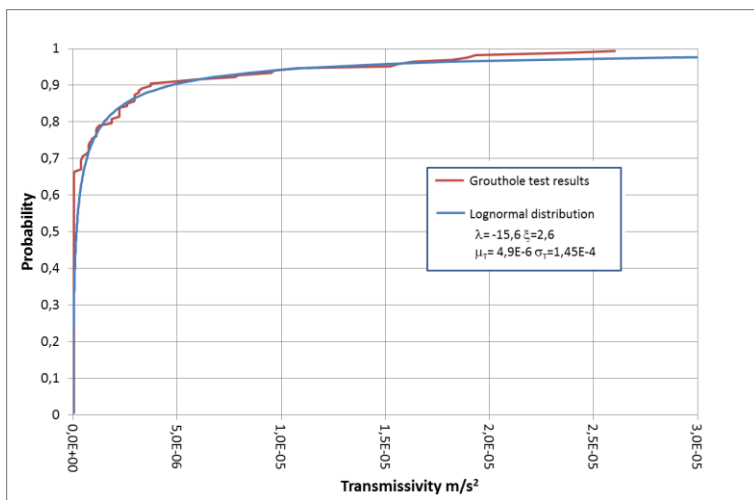
The Bangårds tunnel on the Cityline

Figure 2.   Transmissivity distribution for the Bangårdstunnel.
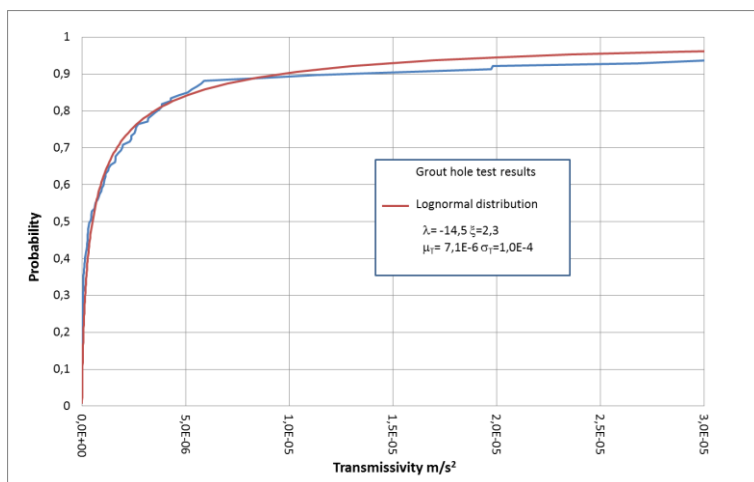
The Odenplan Station on the Cityline

Figure 3.   Transmissivity distribution for the Odenplan Station
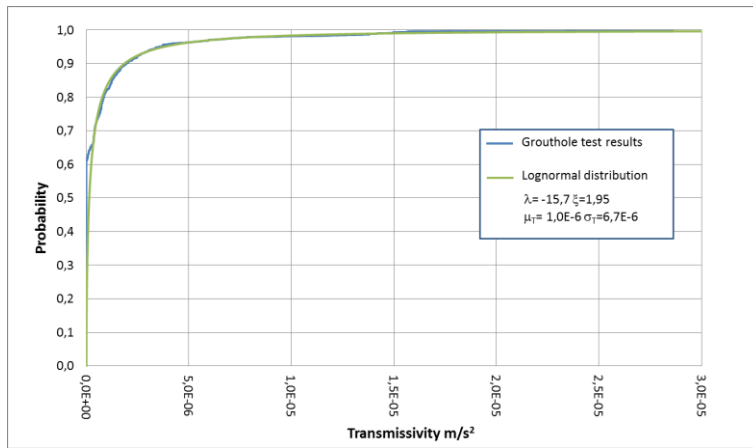
7

The Namntall tunnel – north

Figure 4   **Transmissivity distribution of the Namntall tunnel north part.**
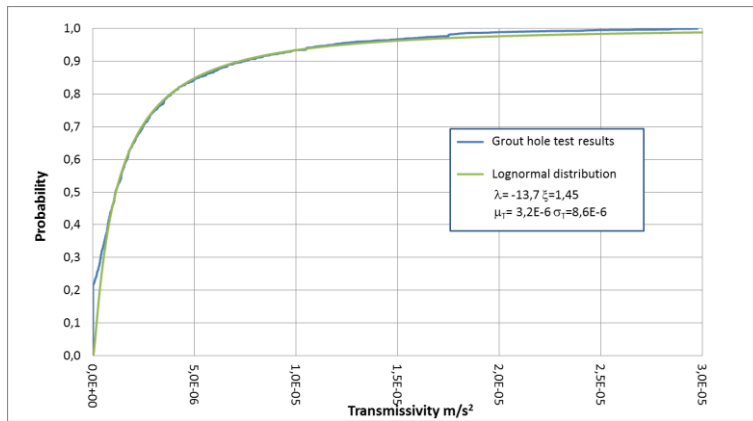
The Namntall tunnel – south

Figure 5   **Transmissivity distribution of the Namntall tunnel south part.**

The fit is very good which confirms the use of the lognormal distribution to describe the variation of section transmissivity.

4. Influence of scale

Theories:

The theory for the lognormal distribution is presented in appendix B and the method to scale up the standard deviation and thus the geometric mean in appendix C. The Mean values of a distribution can be arithmetic, geometrical (for a lognormal distribution equals the median), "3-D" or harmonic. One of the properties of a lognormal distribution is that the mean values can be added for two lognormal distributions. This means that it is possible to scale the data to a size that is relevant for the engineering problem. If the transmissivity data is measured over a length, L_{base}, and the transmissivity is investigated for a length, L, then the mean values can be calculated from:

$$n = L/L_{base}$$

The arithmetic mean value and the standard deviation will then become:

$$T_a = \mu_{T,L} = n \cdot \mu_{L_{base}}$$

$$\sigma_{T,L} = \sqrt{n} \cdot \sigma_{L_{base}}$$

The geometrical mean value of the transmissivity distribution can be calculated for different lengths, L, as:

$$T_g = \frac{\mu_{T,L}}{\sqrt{1 + \left(\frac{\sigma_{T,L}}{\mu_{T,L}}\right)^2}}$$

In this case the hydraulic conductivity is a useful value since it normalizes the values of T and makes them comparable for different scales. The hydraulic conductivity can be described as K = T/L and the mean value is calculated as:

$$\mu_K = \frac{1}{L} \cdot \frac{L}{L_{base}} \mu_{T,L_{base}} = \frac{\mu_{T,L_{base}}}{L_{base}}$$

The arithmetic mean is evidently independent of an increase in scale. However, the standard deviation is dependent on the length, L, according to:

$$\sigma_K = \frac{1}{L} \cdot \sqrt{\frac{L}{L_{base}}} \cdot \sigma_{T,L_{base}} = \frac{\sigma_{T,L_{base}}}{\sqrt{L \cdot L_{base}}}$$

The geometrical mean of the hydraulic conductivity for a length L can therefore be calculated with:

$$K_g = \frac{\mu_{K,L}}{\sqrt{1 + \left(\frac{\sigma_{K,L}}{\mu_{K,L}}\right)^2}}$$

According to the definition for a lognormal variate X the variance of the normalized function is $\xi^2 = Var(lnX)$ and can be expressed for the length, L, as:

$$\xi^2 = ln\left(1 + \frac{\sigma_{T,L_{base}}{}^2}{\mu_{T,L_{base}}{}^2}\frac{L_{base}}{L}\right)$$

From the so called "Matherons conjecture" the relative hydraulic conductivity, K_D, can be described depending on the flow dimension as:

$$K_D = K_g \cdot e^{\left[\xi^2\left(\frac{1}{2}-\frac{1}{D}\right)\right]} \text{ where } D = flow\ dimension$$

The statistics are based on the prerequisite that the data are statistically independent. The correlation distance for section transmissivity probably depends on the actual rock mass characteristics, for fractures in a hard crystalline host rock the correlation distance has been estimated by Butron (2012) to 2-8 m. The scale of fluctuation indicates that the measured data can be expected to be more or less independent.

These equations show that the differences between the arithmetic mean and the geometrical mean value will be smaller for an increase in scale. It should be noted that this is the statistical relation, there is also an uncertain amount of correlation between the measurements which could influence the results see for example Gustafson (2009).

For most problems in tunneling situations the length of a grouting fan is an engineering applicable scale, however an extrapolation for the whole tunnel may be required to evaluate tunnel seepage. The relationship between the statistical parameters and the hydraulic conductivity for different section lengths can be calculated by adding the transmissivities and dividing μ_T/L which will produce the arithmetic mean, K_a. The arithmetic mean, K_a, is independent of scale while the standard deviation will decrease with scale. Since the geometrical mean, K_g, depends on the standard deviation it will imply that the geometrical mean and K_{3d} will increase with scale and approach the arithmetic mean for very large scales.

The calculation presented in Figure 6 and Figure 7 is based on data from the Bangårdstunnel and Station Odenplan on the Cityline, Table 2. The measured section intervals range from 3 m to around 20 m long for these tunnels (water pressure tests before grouting).

Table 2.   Statistical data for the Cityline Bangårdstunnel (Station City) and the Cityline Station Odenplan.

Bangårdstunneln	3 m	20 m
σ [m/s]	$1,9\cdot10^{-5}$	$7,2\cdot10^{-6}$
ξ [-]	2,9	2,6
K_a [m/s]	---	$2,5\cdot10^{-7}$
K_g [m/s]	---	$8,4\cdot10^{-9}$
Station Odenplan		
σ [m/s]	$9,7\cdot10^{-6}$	$5\cdot10^{-6}$
ξ [-]	2,6	2,3
K_a [m/s]	$3,3\cdot10^{-7}$	$3,55\cdot10^{-7}$
K_g [m/s]	$1,1\cdot10^{-8}$	$2,5\cdot10^{-8}$
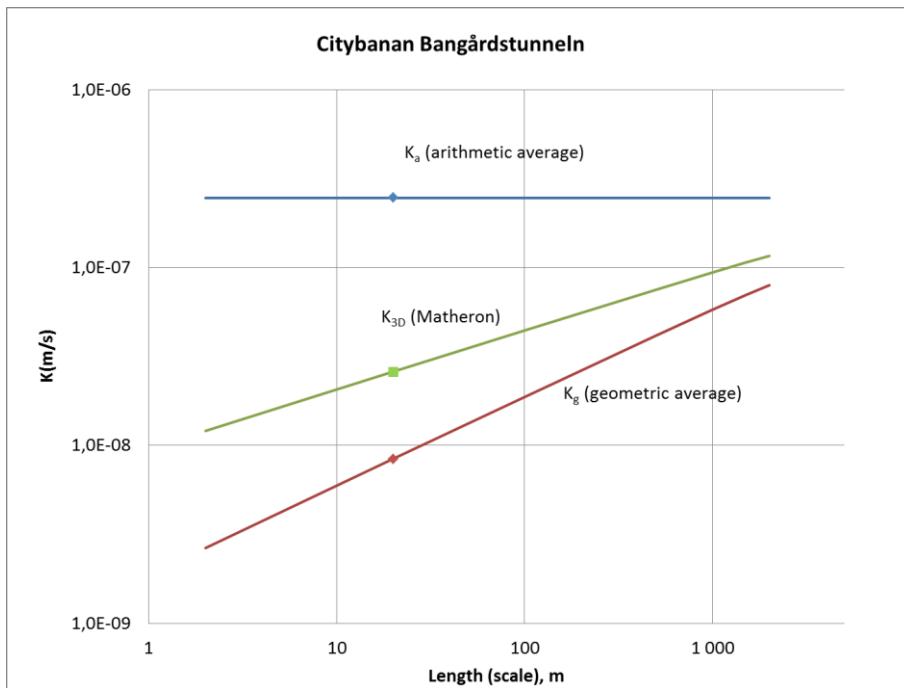
Figure 6   Statistical relation between the arithmetic, geometrical and 3D(Matheron) hydraulic conductivity mean values for the Cityline Bangårdstunnel (station City) for different lengths (X-axis). The calculation is based on the measured 20 m grout hole data.

At the Station Odenplan the water pressure tests were carried out for both 3 m and 20 m sections in the same bore holes. It can be shown that the arithmetic mean value for the 20 m sections is about equal to the 3 m sections. However, the standard deviation decreased from $9,7\cdot10^{-6}$ to $5\cdot10^{-6}$, which confirm the general findings that the geometrical mean should increase with scale, Figure 7 and Table 2.
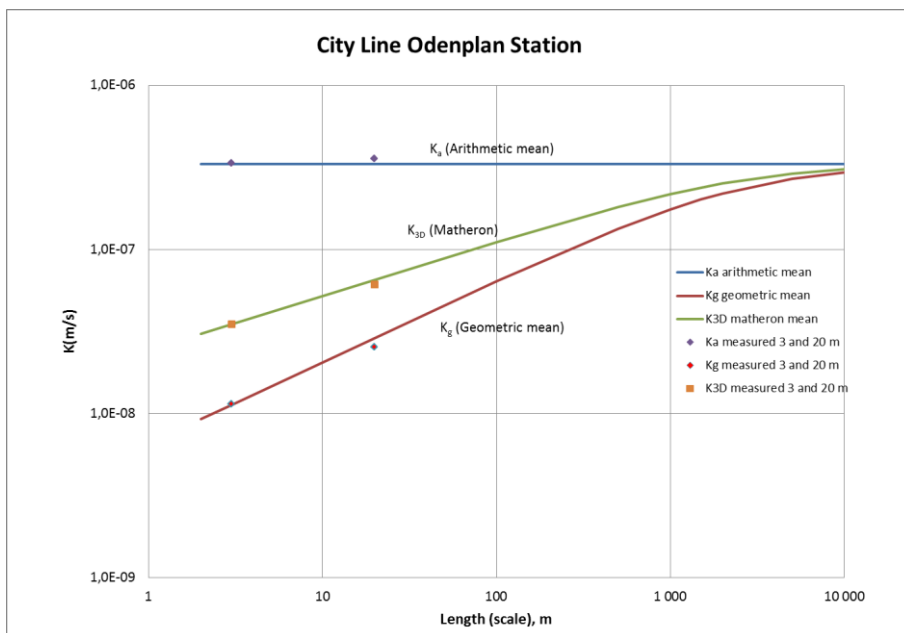
Figure 7   Statistical relation between the arithmetic, geometrical and 3D(Matheron) hydraulic conductivity mean values for the Cityline Odenplan Station for different lengths (X-axis). The calculation is based on 3 m data from the grout holes.

11

When evaluating geohydrological data it seems that considerable care should be taken when analyzing mean values. Both the variation and the section length have to be considered. It is clear that if the transmissivity is evaluated from 3 m interval water pressure tests, the scale effect on the mean values shall be considered.

By studying the density function for the different scales some light is cast upon the properties of the hydraulic conductivity distribution. The density function can be plotted to illustrate the variation in likelihood of encountering a specific value, Figure 8. In the figure, the calculated density functions are presented for the intervals 20 m, 100 m, 500 m, 1000 m and 5000 m. These represent the scales from a grout hole length (20 m) to the whole tunnel.
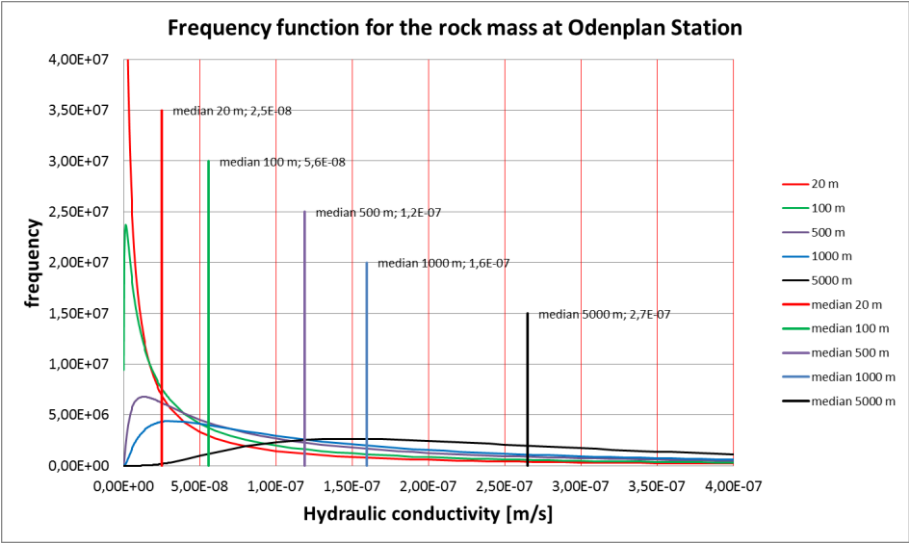

Figure 8   **Density function for different scales (intervals) of hydraulic conductivity at Station Odenplan.**

The results are quite interesting in that they illustrate the variation and high probability that a very low value is encountered for the 20 m interval (median) whereas for the larger intervals the probability to have a certain value is more evenly distributed over the measured spectrum. The median represent the probability that for a stochastic tunnel or part of a tunnel, there is a 50% chance that the hydraulic conductivity is lower than or equal to the median.

It can be shown that for a lognormal distribution the probability that the variable X is smaller than b is:

$$P(X < b) = \Phi\left(\frac{lnb - \lambda}{\xi}\right)$$

The probability that the hydraulic conductivity will be larger than a certain figure is a relevant question for seepage analysis. The statistical data can be used to calculate this probability for the different scales. As an example, the probability of twice the mean value is shown, Table 3.

.

Table 3. Data from Station Odenplan and calculation of probability that K< K$_{limit}$ (μ_K ;2·μ_K) for different lengths. Based on calculations from the 20 m grout hole data.

Length	μ_K	σ_K	CV (σ/μ)	Median $\mu / \sqrt{1 + (CV)^2}$	λ	ξ	Φ P(K< μ_K)	Φ P(K< 2μ_K)
3 m	3.55·10^{-7}	1.3·10^{-5}	36.4	9.8·10^{-9}	-18.45	2.68	0.91	0.95
20 m	3.55·10^{-7}	5.0·10^{-6}	14.1	2.5·10^{-8}	-17.50	2.3	0.88	0.93
100 m	3.55·10^{-7}	2.2·10^{-6}	6.3	5.6·10^{-8}	-16.70	1.92	0.83	0.91
500 m	3.55·10^{-7}	1.0·10^{-6}	2.8	1.2·10^{-7}	-15.95	1.48	0.77	0.89
1000 m	3.55·10^{-7}	7.1·10^{-7}	2.0	1.6·10^{-7}	-15.65	1.27	0.74	0.88
5000 m	3.55·10^{-7}	3.2·10^{-7}	0.9	2.7·10^{-7}	-15.14	0.76	0.65	0.9

5. Discussion and conclusion

The Rock engineering problems is in this paper related to the water inflow to a tunnel or under a dam. The flow can be modelled with different mean values depending on the relevant flow regimes in Figure 1. For an ungrouted tunnel it is suggested that the effective hydraulic conductivity is represented by a mean value ranging from the 3D-mean (model d) to the Arithmetic mean (model b) with a scale (block size) depending on the depth of the tunnel but not less than 20 m. In the case of a grouted tunnel the grouting will significantly change the hydraulic conductivity close to the tunnel and the pressure gradient will act across the grouted zone. The water flow for a grouted tunnel will be parallel (model b) and the effective hydraulic conductivity would be represented by the arithmetic mean (model b) after grouting. The scale is recommended to be equal to the grout hole length i.e. around 20 m.

For water flow under dams along a horizontal layer a 2D flow (model c) could represent the effective hydraulic conductivity. However, this would depend on the thickness of the layer. For other cases or thicker layers, the 3D flow (model d) could represent the effective hydraulic conductivity. Grouting is often performed as a grout curtain in which case the flow through the grout curtain would be represented by a parallel flow (model b) and the arithmetic mean value would be the effective hydraulic conductivity of the grout curtain. An appropriate scale would be the layer thickness.

For a closed repository at greater depth the flow through the rock mass would be represented by the 3D effective hydraulic conductivity (according to model d) with a block scale of 50 to 100 m.

The mean values can be analyzed and scaled according to the presented theory. The lognormal distribution seems to fit the transmissivity data. It is important to take the accuracy of the measuring system into consideration when evaluating the data. In this study there seem to be an interval between $7.4 \cdot 10^{-7}$ and $1.5 \cdot 10^{-5}$ m^2/s, which is more reliable. When analyzing the scale effects, an increase in scale reduces the variance and the geometrical mean increases. For tunnels over 500 m in length the difference between the mean and arithmetic values seems to be relatively small. This would also support the general description of the REV size being 500 to 1000 m according to Gustafson (2009). Considering the general trend in the statistical data, it would seem reasonable that arithmetic mean values should be used for calculating seepage into most tunnels longer than 100 to 1000 m. However, the requirement is that the data is from the same hydrogeological domain. The variation in data should be considered, especially for cases with a limited number of tests. By applying the statistical data the variation can be used to describe a likely interval of mean hydraulic conductivity that can be used as an upper and lower boundary for calculating seepage.

The geometrical mean values represent the 50% value of the rock mass hydraulic conductivities. This means that there is a 50% chance that the actual mean value is higher than the geometrical mean. In the case of the arithmetic mean value the chance that the actual mean is higher than the arithmetic would be about 10%. There seem to be little difference between the probability that mean value is larger than the arithmetic mean or twice this value. This is a function of the relative low probability to encounter the higher values in the distribution.

It seems reasonable that the boundaries of the mean hydraulic conductivity values are the arithmetic mean (upper boundary) and the geometrical mean of the tunnel (lower boundary). For the grout results the expected mean hydraulic conductivity after grouting should be related to the geological conditions that are encountered.

It can be concluded that there are significant uncertainties when analyzing geohydrological data especially during the investigation phase (generally few holes over long distances).

The probability that the hydraulic conductivity is accurately predicted is relatively low, 50 – 90% depending on what mean values are used. This calls for a design approach that can be adjusted for actual conditions equivalent to an observational method where the inflow and the grouting works are followed up. It is recommended that the initial part of the tunnel is followed more closely since any changes to the design or grout operation have greater impact at an early stage.

Appendices

A. Case Study

The Bangårds tunnel and The Station Odenplan on the Cityline

The Cityline project, a 6 kilometer-long commuter train tunnel through the central part of Stockholm with two new stations, Odenplan and Stockholm City is currently under construction. The production cost is calculated to be 16.8 billion SEK (2007) and is scheduled to be finished in 2017. The purpose of constructing this line is to free two railway tracks through Stockholm of the commuter traffic. After completion of the project the railway capacity through Stockholm will be approximately doubled.

In the early spring of 2010, a grouting trial test was carried out in the Bangård tunnel, an access tunnel toward the Stockholm City Station, Tsuji et al (2012). The grouting works were performed as continuous pre-grouting to limit the risk of lowering the ground water table thereby possibly disturbing and damaging adjacent functions such as existing subway, media tunnels and basements of commercial buildings. In the trial test a total of 14 grouting fans were analyzed over a tunnel length of 250 m. Generally the fans consisted of 22 grout holes of 21 m length. The main purpose of the field test was to verify and evaluate the grouting works and to explore the possibilities to revise the current grouting procedures for the future works in Cityline. The tunnel was excavated in gneiss or gneissic granite of generally good quality.

The Station Odenplan is the northern part of the Cityline project, which connects the northern tracks at Tomteboda with the new station at Odenplan. The tunnel is constructed by drilling and blasting and the studied sections was excavated during the winter 2010. The grouting is performed as continuous pregrouting as for the Bangårdstunnel. Water pressure test protocols have been studied for 7 fans as a primary source for evaluation. These include test results over the hole length (20 m) as well as for 3 m intervals. The predominant rock type is gneiss with stretches of gneiss/granite of

generally good quality, however for one of the fans a weakness zone was encountered with significantly increased transmissivities.

The Namntall tunnel

The 6 km Namntall Tunnel is a part of the Botniabanan project linking Örnsköldsvik and Kramfors. The tunnel was constructed as part of a design and build contract consisting of a single-track rail tunnel (65 m2) and a parallel service tunnel (35 m2). The client, Botniabanan AB (BBAB), is a partnership (90/10) between Trafikverket, former Banverket (Swedish Rail Administration), and the municipal authorities in the area. The tunnels were excavated using the drill and blast method between 2004 and 2007.

For the most part the Namntall Tunnel, with a rock cover of between 20 and 150 m, was excavated in a greywacke and through a major intrusion of granite. The tunnels were excavated by means of drilling and blasting and with, for Scandinavian conditions, a normal grouting routine, including probe drilling, water pressure tests (Moye, 1967), evaluation of the grout class, drilling of grout holes, cement grouting, drilling of control holes (water pressure tests) and supplementary drilling/grouting. The grouting is performed to reduce the water discharge into the tunnel as defined in the contract.

The tunnel conditions were significantly heterogeneous to be able to divide the tunnel in a northern (3 km) and a southern (2,5 km) part and are described in Stille&Gustafson (2010).

B. The lognormal distribution

The lognormal distribution can be studied in most statistical text books and is defined through the mean value and a standard deviation.

A random variable X has a lognormal probability distribution if lnX (the natural logarithm of X) is normal distributed. For this case, the density function of X is

$$f_x(x) = \frac{1}{\sqrt{2\pi}\xi x} e^{\left[-\frac{1}{2}\left(\frac{lnx-\lambda}{\xi}\right)^2\right]} \quad 0 \le x < \infty \qquad [B.1]$$

Where λ = E(lnX) and $\xi=\sqrt{Var(lnX)}$ are the mean and standard deviation of lnX respectively. Because of its relationship with the normal distribution (through the logarithmic transformation), probabilities associated with a lognormal variate can also be determined using a table of standard normal probabilities. For example the probability that X will assume values in an interval (a,b) is

$$P(a < X \le b) = \int_a^b \frac{1}{\sqrt{2\pi}\xi x} e^{\left[-\frac{1}{2}\left(\frac{lnx-\lambda}{\xi}\right)^2\right]} dx \quad [B.2]$$

Let

$$s = \frac{lnx - \lambda}{\xi} \qquad [B.3]$$

Then $dx = x\xi ds$, and

$$P(a < X \le b) = \frac{1}{\sqrt{2\pi}} \int_{(lna-\lambda)/\xi}^{(lnb-\lambda)/\xi} e^{\left[-\frac{1}{2}s^2\right]} ds$$

$$= \Phi\left(\frac{lnb - \lambda}{\xi}\right) - \Phi\left(\frac{lna - \lambda}{\xi}\right) \qquad [B.4]$$

Here can the probability of Φ for the value of $(lnb - \lambda)/\xi$ or $(lna - \lambda)/\xi$ be determined from a table of standard normal probabilities. Note that the probability is a function of the parameters λ and ξ. These parameters are related to the mean value, μ, and standard deviation, σ, of X as follows. Let Y=lnX, which is N(λ, ξ). It follows that $X = e^Y$ and

$$\mu = E(X) = E(e^Y)$$

$$= \frac{1}{\sqrt{2\pi}\xi} \int_{-\infty}^{\infty} e^y\, e^{\left[-\frac{1}{2}\left(\frac{y-\lambda}{\xi}\right)^2\right]} dy$$

$$= \frac{1}{\sqrt{2\pi}\xi} \int_{-\infty}^{\infty} e^{\left[y-\frac{1}{2}\left(\frac{y-\lambda}{\xi}\right)^2\right]} dy$$

By completing the square and developing the expression, we get

$$\mu = \left[\frac{1}{\sqrt{2\pi}\xi} \int_{-\infty}^{\infty} e^{\left[-\frac{1}{2}\left(\frac{y-(\lambda+\xi^2)}{\xi}\right)^2 dy\right]}\right] e^{(\lambda+\frac{1}{2}\xi^2)} \qquad [B.5]$$

The quantity within the brackets can be recognized as the total unit area of the Gaussian density function $N(\lambda + \xi^2, \xi)$ and therefore are the mean value

$$\mu = e^{(\lambda+\frac{1}{2}\xi^2)} \qquad [B.6]$$

And thus

$$\lambda = ln\mu - \frac{1}{2}\xi^2 \qquad [B.7]$$

The variance can be determined in a similar way:

$$E(X^2) = \frac{1}{\sqrt{2\pi}\xi} \int_{-\infty}^{\infty} e^{2y}\, e^{\left[-\frac{1}{2}\left(\frac{y-\lambda}{\xi}\right)^2\right]} dy$$

$$= \frac{1}{\sqrt{2\pi}\xi} \int_{-\infty}^{\infty} e^{\left[-\frac{1}{2\xi^2}\{y^2 - 2(\lambda+2\xi^2)y + \lambda^2\}\right]} dy$$

By completing the square on the exponent the integral yields

$$E(X^2) = \left[\frac{1}{\sqrt{2\pi}\xi} \int_{-\infty}^{\infty} e^{\left[-\frac{1}{2}\left\{\frac{y-(\lambda+2\xi^2)}{\xi}\right\}^2 dy\right]}\right] e^{[2(\lambda+\xi^2)]} \qquad [B.8]$$

$$= e^{[2(\lambda+\xi^2)]}$$

Thus we get the variance according to

$$Var(X) = \sigma^2 = e^{[2(\lambda+\xi^2)]} - e^{\left[2\left(\lambda+\frac{1}{2}\xi^2\right)\right]}$$

$$= \mu^2\left(e^{\xi^2} - 1\right) \qquad [B.9]$$

From this we obtain

$$\xi^2 = \ln\left(1 + \frac{\sigma^2}{\mu^2}\right) \qquad [B.10]$$

The median value is often used for the central value of a lognormal variate. If x_m is the median then the probability, by definition, for the central value is 0,5.

$$P(X \le x_m) = 0,5$$

$$\Phi\left(\frac{\ln x_m - \lambda}{\xi}\right) = 0,5$$

Thus

$$\left(\frac{\ln x_m - \lambda}{\xi}\right) = \Phi^{-1}(0,5) = 0$$

And consequently is

$$\lambda = \ln x_m \leftrightarrow x_m = e^{\lambda} \qquad [B.11]$$

So we obtain the relationship between the mean and the median of a lognormal variate as

$$x_m = \frac{\mu}{\sqrt{1 + \frac{\sigma^2}{\mu^2}}} \qquad [B.12]$$

C. Mean hydraulic transmissivities

The Mean values of a distribution can be arithmetic, geometrical (for a lognormal distribution equals the median) or harmonic. One of the properties of a lognormal distribution is that the mean values can be added for two lognormal distributions. This means that it is possible to scale the data to a size that is relevant for the problem. If the transmissivity data is measured over a length, L_{base}, and the

transmissivity is investigated for a length, L, then the mean values can be calculated from the following:

$$n = {}^{L}\!/_{L_{base}} \qquad [C.1]$$

If y is a function g for a number of stochastic variates X$_i$ then the following can be expressed:

$$y = g(\dots, X_i, \dots) \qquad [C.2]$$

$$E(Y) = g(\dots, \mu_{x_i}, \dots) \qquad [C.3]$$

$$VAR(Y) = \sum \left(\frac{\partial g}{\partial x_i}\right)^2 \cdot VAR(x_i) \qquad [C.4]$$

This means that the mean value and standard deviation is:

$$T_a = \mu_{T,L} = n \cdot \mu_{L_{base}} \qquad [C.5]$$

$$\sigma_{T,L} = \sqrt{n} \cdot \sigma_{L_{base}} \qquad [C.6]$$

The geometrical mean value of the transmissivity distribution can be calculated for different lengths, L, as:

$$T_G = \frac{\mu_L}{\sqrt{1 + \left(\frac{\sigma_L}{\mu_L}\right)^2}} \qquad [C.7]$$

The hydraulic conductivity can be described as K = T/L. In this case is the hydraulic conductivity a useful value since it normalizes the values of T and makes them comparable for different scales.

If

$$Y = aX \rightarrow \begin{matrix} \mu_y = aE(X) = a\mu_x \\ \sigma_y = a\sigma_x \end{matrix} \qquad [C.8]$$

Thus

$$\begin{matrix} \mu_K = a\mu_{T,L} \\ \sigma_K = a\sigma_{T,L} \end{matrix} \qquad [C.9]$$

For $a = 1/L$ then

$$\mu_K = \frac{1}{L} \cdot \frac{L}{L_{base}} \mu_{T,L_{base}} = \frac{\mu_{T,L_{base}}}{L_{base}} \qquad [C.10]$$

Which is independent of L.

$$\sigma_K = \frac{1}{L} \cdot \sqrt{\frac{L}{L_{base}}} \cdot \sigma_{T,L_{base}} = \frac{\sigma_{T,L_{base}}}{\sqrt{L \cdot L_{base}}} \qquad [C.11]$$

For the lognormal variate X the variance is $\xi^2 = Var(lnX)$. As was shown above

$$\xi^2 = ln\left(1 + \frac{\sigma^2}{\mu^2}\right)$$

$$\xi^2 = ln\left(1 + \frac{\sigma_{T,L_{base}}{}^2}{\sqrt{L \cdot L_{base}}{}^2} \frac{L_{base}{}^2}{\mu_{T,L_{base}}{}^2}\right)$$

$$\xi^2 = ln\left(1 + \frac{\sigma_{T,L_{base}}{}^2}{\mu_{T,L_{base}}{}^2} \frac{L_{base}}{L}\right) \quad [C.12]$$

Based on stochastic theory can a probable value of the effective transmissivity be described. From the so called "Matherons conjecture" can the flow dimension relative hydraulic conductivity, K_D, be described as:

$$K_D = K_g \cdot e^{\left[\xi^2\left(\frac{1}{2} - \frac{1}{D}\right)\right]} \ where \ D = flow \ dimension \quad [C.13]$$

Gustafson (2009) shows that data from the Äspö HRL cannot be described as a 2D problem since the mean values for the whole bore holes are larger than the geometrical mean value. However it should be noted that it has been proved that the expression cannot be general in 3D, Hunt&Ewing (2009). In any case, for a 3-dimensional problem the expression becomes:

$$K_{3D} = K_g \cdot e^{\left[\frac{\sigma^2}{6}\right]} \quad [C.14]$$

Acknowledgements

References

Axelsson M. Eriksson M. Wilén P., 2007, "Dimensionering av typinjektering – koncept 1" design document 9563-13-025-001 for Cityline in Swedish.

Barker J A., 1988, "A generalized radial flow model for hydraulic tests in fractured rock", Water Resources Res 24(10): 1796-1804

De Marsily G., 1986, "Quantitative Hydrogeology: Ground Water Hydrology for Engineers", Academic Press. Inc. San Diego, USA.

Gustafson G., 2009, "Hydrogeologi för bergbyggare", in Swedish, Formas, ISBN 978-91-540-6029-0.

Hakami E., 1995, "Aperture distribution of rock fractures" Doctoral Thesis, Division of Engineering Geology Department of Civil and Environtmental Engineering, Royal Institute of Technology.

He J. Chen S-H. Shahrour I., 2012 "Numerical estimation and prediction of stress-dependent permeability tensor for fractured rock masses." International Journal of Rock Mechanics & Mining Sciences 59 (2013) 70-79.

Holmén J., 1997, "On the flow of groundwater in closed tunnels – generic hydrogeological modelling of nuclear waste repository, SFL 3-5", Doctoral thesis, Uppsala University.

Hunt A. Ewing R., 2009, "Percolation theory for flow in porous media". Springer, ISBN-13:978-3540897897.

Hämäläinen H., 2013, "Monitoring Hydraulic Conductivity with HTU at Eurajoki, Olkiluoto, Drillholes OL-KR31 and OL-KR32, in 2011" Working Report 2013-07.

Moye D.G., 1967: Diamond Drilling for Foundation Exploration. Civil Engineering Transactions, April, pp 95-100.

Müller C. Siegesmund S. Blum P., 2009 "Evaluation of the representative elemtentary volume (REV) of a fractured geothermal sandstone reservoir." Environ Earth Sci (2010) 61:1713-1724 DOI 10.1007/s12665-010-0485-7.

Rhén I. Bäckblom G. Gustafson G. Stanfors R. Wikberg P., 1997, "Äspö HRL - Geoscientific evaluation 1997/2. Results from pre-investigations and detailed site characterization. Summary report." SKB TR-97-03, Svensk Kärnbränslehantering AB.

Snow D T., 1968, "Rock fracture spacing, openings and porosity", Journal of Soil Mechanics, Foundation Division. Proc of the American Society of Civil Engineers Vol 94, 73-91

Stille B. Gustafson G., 2010 "A review of the Namntall tunnel project with regard to grouting performance", Tunneling and Underground Space Technology, 25 (4) p. 346-356.

Sturk R. Striberger J. Aurell O. Stille B., 2013 "Grouting operations in complex and heavily water bearing ground – an analysis and summary from the Hallandsås project" 7th Nordic grouting symposium (2013).

Tsuji M. Holmberg M. Stille B. Rafi J Y. Stille H., 2012, "Optimization of the grouting procedure with RTGC method. Data from a trial grouting at city line project in Stockholm." SKB R-12-16, Svensk

Kärnbränslehantering AB.

Wang M. Kulatilake P.H.S.W. Um J. Narvaiz J., 2002 "Estimation of REV size and three-dimensional hydraulic conductivity tensor for a fractureed rock mass through a single well packer test and discrete fracture fluid flow modeling", International Journal of Rock Mechanics & Mining Sciences 39 (2002) 887-904.

Wu Q. Kulatilake P.H.S.W., 2012 "REV and its properties on fracture system and mechanical properties, and an orthotropic constitutive model for a jointed rock mass in a dam and site in China" Computers and Geotechnics 43 (2012) 124-142.

Ylinen A., 1994 "N-Dimensional Flow Behaviour in the Single Borehole Pumping Test."
Helsinki: Teollisuuden Voima Oy. Working report PATU-94-54.